Towards Polypeptide based Nanoparticles

By

Jaco Jacobs (M.Sc.)

Supervisor: Dr. Andreas Heise

Co-supervisor: Nicholas Gathergood (Tallinn University of Technology)

A thesis submitted to Dublin City University

in partial fulfillment of the requirements

for the degree of

Doctor of Philosophy (PhD)

School of Chemical Sciences

July 2015

Declaration

I hereby certify that this material, which I now submit for assessment on the programme of study leading to the award of a degree of Doctor of Philosophy is entirely my own work, and that I have exercised reasonable care to ensure that the work is original, and does not to the best of my knowledge breach any law of copyright, and has not been taken from the work of others save and to the extent that such work has been cited and acknowledged within the text of my work.

Signed: (Candidate) ID No.:

Date:

Acknowledgement

Not all those who wander are lost;

I remember hearing this in a presentation regarding research and the paths taken to reach ones goal. At the end of three and a bit years I can't think of anything that rings more true as there is certainly no straight path towards a doctorate degree. In saying that, I have no complaints as I'm finishing up my thesis. I was fortunate enough to obtain a Marie Curie fellowship through some blind luck and Andreas seemingly very trustworthy of the ability of South African graduates. Also, Ireland has treated me well with a culture that is very easy to adapt to as it is so similar to being in South Africa… If Ireland had any decent weather, it would be some place.

The acknowledgements have to start with Dr Andreas Heise. I can't thank you enough for giving me the opportunity to come over and study in Ireland. Working alongside you has been a pleasure. You gave me all the freedom imaginable to do what I want, how I want while providing the necessary tools I needed. Being as approachable as you are has allowed for some interesting concepts being thrown back and forth, something I believe has led to some (hopefully) pioneering results.

In relation to this, I have to acknowledge the massive role the whole REFINE group has played in making this tenure such a worthwhile experience regarding friends made and knowledge gained. Also the European commission for the funding and opportunity to experience all that Europe has to offer academically and socially.

To PRG as a whole, this would not have been possible without you. You have all unknowingly or not left an impression with me that has gotten me to where I am now. For that I can't thank you all enough. Jin, Tushar, Mark, Zeliha, Fabrice, Anton, Timo, Saltuk and even Rob sneaking it in at the end, thank you. Without singling anyone out, please know the contributions you have made inside and outside the lab will always be valued.

DCU chemistry as a whole is a rising star and compares with the very best in Ireland. Specifically, I need to thank the technical staff for what you provide under the leadership of Veronica. Damian, Ambrose, John, Vinny, Catherine… you guys are one hell of a team and deserve all the accolades you get.

Outside the borders of Ireland, there are a few names that have to be mentioned. Firstly, Raf thanks for all the discussions and help you have shared over a pint. O'Sheas and Munster are ingrained into my blood now.

TU/e has helped me immensely in achieving the results I have. Dr. Hans Heuts for helping me get to grips with emulsion polymerizations as well as the continuous help regarding the finer details. Mohammad, you have a gift in the way you obtain Cryo images. Your curiosity regarding interesting morphologies (even when it's not your own work) is an attribute that will serve you very well. Was a pleasure working with you both!

Lastly, there are always people behind the curtains who have to deal with me and keep me sane. These include the friends I have made in Ireland and my family back in South Africa. Le Roy, Rich, Darren, Jeffrey and Emile you boys have kept me in and out of trouble… all greatly appreciated.

Ma en pa, julle konstante ondersteuning is iets wat ek darem regdeur my lewe kan saamdra. Dit was maar taai in die begin, maar julle het gehelp deur diep fondasie te lê. Baie dankie. Baie lief vir julle. Conna en Sus, julle sal my nou aanspreek as doktor. Jan en Lolla, dankie vir die tye wat ons kon saam leef! Chatham was mal. Lastly, Lara I owe you tremendous gratitude for your continuous support and love. Your unwavering belief in me is undeserved but something I cherish. *Bisous*.

Again, thanks to all. It was some journey.

Table of Contents

List of Publications

Jacobs, J.; Gathergood, N.; Heise, A., Synthesis of Polypeptide Block Copolymer Hybrids by the Combination of N-Carboxyanhydride Polymerization and RAFT. *Macromolecular Rapid Communications* **2013,** 34, (16), 1325-1329.

Jacobs, J.; Byrne, A.; Gathergood, N.; Keyes, T. E.; Heuts, J. P. A.; Heise, A., Facile Synthesis of Fluorescent Latex Nanoparticles with Selective Binding Properties Using Amphiphilic Glycosylated Polypeptide Surfactants. *Macromolecules* **2014,** 47, (21), 7303-7310.

Jacobs, J.; Gathergood, N.; Heuts, J. P. A.; Heise, A., Amphiphilic glycosylated block copolypeptides as macromolecular surfactants in the emulsion polymerization of styrene. *Polymer Chemistry* **2015,** 6, (25), 4634-4640.

Conference Presentations

Jaco Jacobs, Andreas Heise; Synthesis of hybrid polypeptide bioconjugates *via* the combination of RAFT and N-carboxy anhydride (NCA) polymerization; EPF 2013 Congress; Pisa, Italy; June 2013

List of Abbreviations

Acm	Acetamidomethyl
AIBN	2,2’-azobisisobutyronitrile
AMM	Activated monomer mechanism
ATR-FTIR	Attenuated total reflectance - Fourier transform infrared
ATRP	Atom transfer radical polymerization
BLG	γ-benzyl-L-glutamate
CRP	Controlled/Living radical polymerization
CTA	Chain transfer agent
CuAAC	Copper catalysed azide-alkyne click
Cys	Cysteine
DCM	Dichloromethane
DDI	Distilled Deionized (water)
DLS	Dynamic light scattering
DMF	Dimethylformamide
DMSO	Dimethylsulfoxide
DMTMM	4-(4,6-Dimethoxy-1,3,5-triazin-2-yl)-4-methylmorpholinium chloride
DP	Degree of polymerization
EDC	1-Ethyl-3-(3-dimethylaminopropyl)carbodiimide
EPR	Enhanced permeability and retention
FESEM	Field emission scanning electron microscopy
FITC	Fluorescein isothiocyanate
Fmoc	9-fluorenylmethoxycarbonyl
FRP	Free radical polymerization
HPLC	High Performance Liquid Chromatography
HVT	High vacuum technique

IR	Infrared spectroscopy
MALDI-ToF-MS	Matrix Assisted Laser Desorption Ionization Time of Flight Mass Spectroscopy
MALS	Multi-angle light scattering
M_n	number average molecular weight
M_w	weighted average molecular weight
MWCO	Molecular weight cut-off
NAM	Normal amine mechanism
NCA	*N*-carboxyanhydride
NMP	Nitroxide mediated polymerization
NMR	Nuclear magnetic resonance
PDI	Polydispersity Index
PBLG	Poly(γ-benzyl-L-glutamate)
PEG	Poly(ethylene glycol)
PLGA	Poly(L-glutamic acid)
PLL	Poly(L-lysine)
PS	Poly(styrene)
PS-*b*-PBLG	Polystyrene-*b*- poly(γ-benzyl-L-glutamate)
PS-*b*-PZLL	Polystyrene-*b*- poly(ε-benzyloxycarbonyl-L-lysine)
RES	Reticuloendothelial System
RAFT	Reversible addition-fragmentation chain-transfer
ROP	Ring-opening polymerization
SEC	Size exclusion chromatography
TEA	Triethylamine
TEM	Transmission electron microscopy
TFA	Trifluoroacetic acid
THF	Tetrahydrofuran

TLC	Thin layer chromatography
TMS	Tetramethylsilane
ZLL	ε-benzyloxycarbonyl-L-lysine

List of Symbols

α	conversion
Δ	Heat
$\int$	Integrated fraction
$[I]_0$	Initial initiator concentration
$[M]_0$	Initial monomer concentration
$Đ$	Dispersity
DP_n	Number average degree of polymerization
k_{deact}	Rate constant of deactivation
k_i	Rate constant of initiation
k_p	Rate constant of propagation
k_t	Rate constant of termination
k_{tr}	Rate constant of transfer
$M_{n,theo}$	Theoretical molar mass
Mr_{CTA}	Molecular weight of the CTA
$Mr_{monomer}$	Molecular weight of the monomer

Abstract

Jaco Jacobs

Towards polypeptide based nanoparticles

Research towards advanced materials is an area of high interest due to the ever growing technological demands from emerging applications in (nano)medicine, particularly the fields of biomedicine and biotechnology with applications ranging from tissue engineering, drug delivery and biodiagnostics. Polypeptides are envisioned to achieve a major impact on these areas due to the significant advances in the controlled ring-opening polymerisation of amino acid *N*-carboxyanhydrides (NCAs). This has fuelled opportunities for the design of well-defined macromolecular structures whose physical, chemical and biological properties are ruled by their controlled sequences and composition. Moreover, efficient orthogonal functionalization techniques have further expanded the scope for the design of functional polypeptides. The aim of this PhD was to expand the reach of these synthetic materials to be utilized in existing technologies as green alternatives. Specifically, we wanted to incorporate polypeptides in the synthesis of nanoparticles as fully biocompatible and biodegradable surfactants or emulsifiers. To evaluate their viability as potential stabilizers, it was necessary to develop improved modular routes towards biohybrid materials and incorporate them in latex formation. Chapter 2 describes the synthesis of polypeptide–polymer hybrids *via* the combination of radical addition-fragmentation chain transfer (RAFT) mediated polymerization and the ring-opening polymerization (ROP) of NCAs. Key to this successful approach was an end-group engineering strategy that prevented the simultaneous presence of amino and chain transfer agent groups. This resulted in the synthesis of glycosylated amphiphilic block copolymers which were found to be efficient stabilizers in the emulsion polymerization of styrene, offering a facile method for the synthesis of fluorescent glycosylated polystyrene nanoparticles (Chapter 3). Chapter 4 expands this concept towards fully amino acid and sugar based emulsifiers in the preparation of functionalized polymer colloids. In the final part of the work (Chapter 5), we report on a pioneering strategy regarding the controlled synthesis of polypeptide based nanoparticles utilizing a scalable miniemulsion process. This latter work is the culmination of the knowledge gained throughout the PhD which we feel has great potential as a next generation biodegradable carrier system.

Chapter 1

Literature introduction

Polymeric materials have been instrumental in the evolution of nanotechnology, an area which has evolved significantly due to the unique opportunities it offers to industries such as agriculture, food industry, cosmetics and medicine.[1-6] Arguably the greatest driving force for the rapid technological advances in nanotechnology is the support it receives from both the pharmaceutical and biomedical industries. Research in the in the fields of diagnostic and therapeutic medical applications has led to fast paced innovation regarding the design of functional nanoparticles with the ability to target, encapsulate, transfer and/or controllably release the active species.[7-9]

In the area of nanomedicine, polymer therapeutics is an interdisciplinary research field at the interface of polymer chemistry, medicine and cell biology/pharmaceutical sciences[10-12] Included in this collection of complex multifunctional polymer based drugs and carriers are polymeric micelles. These rely on the self-assembly of amphiphilic block copolymers into various three dimensional nanostructures such as micelles, vesicles, rods and worms.[13-16] However, compared to these nanoparticulate products, solid nanoparticles possess increased colloidal stability, better chemical resistance as well as ease of preparation. Currently, poly(lactic-co-glycolic acid) (PLGA) is one of the most promising materials utilized for the NP core due to its inherent biocompatibility and biodegradability.[17] Furthermore, PLGA has been successfully combined with poly(ethylene glycol) (PEG) for several systems where NPs are typically prepared *via* nanoprecipitation or emulsification.[18-22]

Non-degradable polystyrene and poly(methyl methacrylate) have also been successfully incorporated as the hydrophobic core in fluorescent NP systems.[23-25] Solid polymeric nanoparticles such as these are prepared by mini-, micro-, and emulsion polymerization processes resulting in nanoparticles, nanospheres or nanocapsules.[6, 26, 27] These systems are able to prepare narrowly defined NP distributions while being tolerant to a wide range of monomer using radical , anionic, polyaddition and polycondensation polymerization techniques.[22, 28]

Size, shape and surface properties should be specifically tailored towards the final application as these are critical for *in vitro* and *in vivo* applications.[29, 30] One of the main challenges in this process is an effective functionalization platform, necessary for targeting applications. Active targeting allows for the controlled accumulation of NPs at a desired site. This involves

the conjugation of targeting ligands to the exposed surface of NPs, which interact with receptors expressed on the targeted tissue. Targeting ligands, which have been successfully utilized thus far include antibodies, peptides, aptamers and carbohydrates (glycans).[31-35]

Accordingly, research regarding synthetic strategies towards multifunctional polymeric nanoparticle scaffold is of great interest. This involves exploiting and combining synthetic tools to obtain NPs with high levels of control, utilizing biocompatible and biodegradable materials as well as preparing materials which allow for commercial scalability. It was the aim of the work presented in this thesis to contribute to this field of research by designing novel functional nanoparticles and demonstrate their potential use is biomedical applications. The tools used in this process are controlled radical and N-carboxyanhydride polymerisation for the surfactant synthesis as well as emulsion polymerization for the particle synthesis. These techniques will be briefly introduced on the following pages.

1.1 Controlled Radical Polymerizations

Commercially, free radical polymerization is the preferred synthetic method for a large variety of high molecular weight polymers. This is due to its inherent compatibility with a wide range of monomers, solvents and reaction conditions, which inadvertently allows for a robust polymerization technique.[36, 37] In conventional free radical polymerization, this tolerance does, however, come at the price of limited control as far as architecture, topology and molecular weight distribution are concerned.

Due to the drawbacks of conventional free radical polymerization, a large body of work has been done over the last decade to develop techniques, which allow for the synthesis of a diverse range of macromolecules with well-defined architectures, functionalities and control over the degree of polymerization. The techniques developed are described as living/controlled radical polymerizations (LRP).[38,39] Living polymerizations are seen as systems where the polymer chain can propagate in the presence of monomer but does not undergo termination or chain transfer reactions.

The effectiveness of LRP techniques is due to their ability to combine the benefits of living anionic polymerization, i.e. designed molecular architecture, with the versatility and robustness of free radical polymerization. The key concept of LRP is the establishment of a reversible dynamic equilibrium between a low concentration of active species ($P^{\bullet}$), which are able to propagate and a high concentration of dormant species ($P-X$) (Scheme 1.1). For a system to have a "living character" it is necessary that the equilibrium lies towards the

dormant species. This minimizes the concentration of active radicals present at any one moment thereby reducing possible radical-radical reactions, which inadvertently terminate growing chains. The consequence of this is that all the chains grow simultaneously thus giving the technique its "living" character.

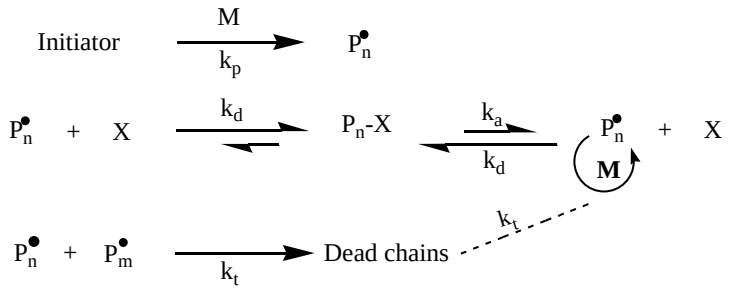

Scheme 1. 1 General mechanism for a living radical polymerization (LRP).

The most commonly used LRP techniques as noted by various LRP reviews are NMP[40, 41] (*nitroxide mediated polymerization*), ATRP[42, 43] (*atom transfer radical polymerization)* and RAFT [44,45, 46] (*reversible addition-fragmentation chain transfer*) mediated polymerization. The mechanism of NMP and ATRP differs vastly from that of RAFT mediated polymerizations as the former obtain the living character (of the system) by reversibly capping the growing radical chains with either nitroxide radicals (NMP) or via a redox process involving a metal halid salt (ATRP) to obtain the favoured dormant species (**1** and **2**) (see Scheme 1.2 and 1.3).

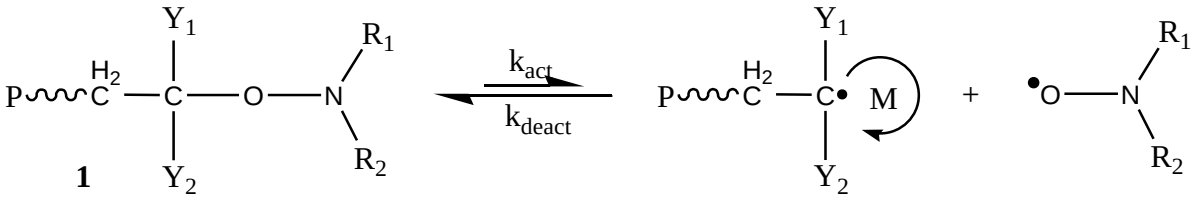

Scheme 1. 2 The general mechanism of a nitroxide mediated polymerization (NMP).

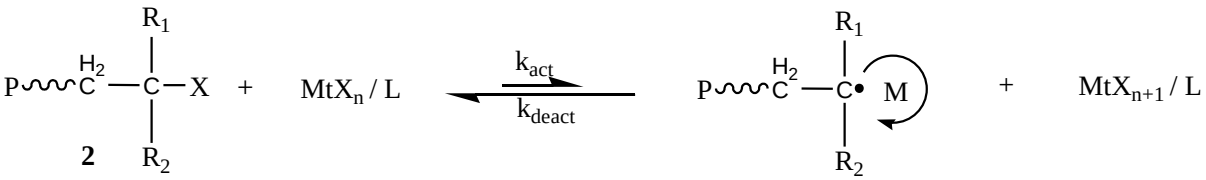

Scheme 1. 3 Mechanistic basis of atom transfer radical polymerization (ATRP).

RAFT[45, 47] mediated polymerization and a similar method, MADIX[48,49] (macromolecular design *via* interchange of xanthates) were introduced roughly at the same time in 1998 by the CSIRO group and the Rhodia research group, respectively. Both these processes have the same reversible transfer mechanism and will both be referred to by the general term of RAFT mediated polymerization.

1.1.1 RAFT mediated polymerization

RAFT is arguably the most versatile synthetic tool available for synthesizing well-defined, high molecular weight heterotelechelic polymers. It is a facile technique that can be conducted under numerous reaction conditions, is compatible with a wide range of monomers and tolerant to various functional groups.[50, 51]

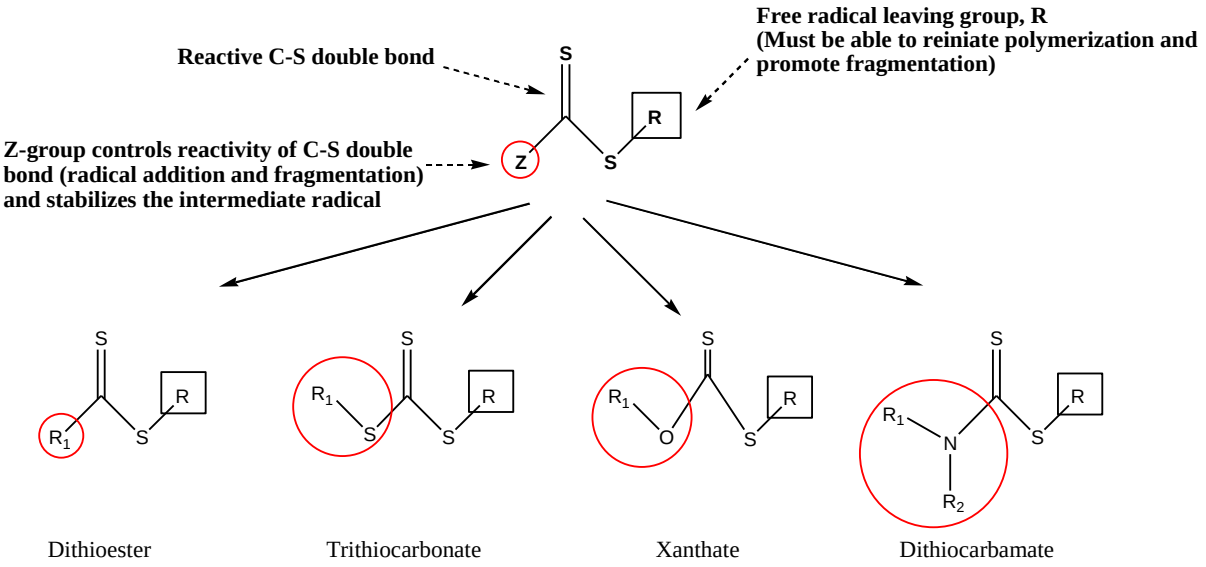

Figure 1. 1 General structures for commonly used RAFT agents.

RAFT mediated polymerization is a degenerative process which acts *via* a two-step addition-fragmentation mechanism. It has the inherent feature of being able to produce polymer with reactive/functional moieties at both the α- and ω-chain-end. This is achieved *via* the RAFT agent's R- and Z-groups (Figure 1.1), which allows for the introduction of functionalities at

these chain-ends. The R-group is found at the α-chain end while the Z-group ends up at the ω-chain end of the polymer, attached as a reactive thiocarbonyl thio moiety. It is possible to design a RAFT agent for each specific monomer, taking into account its reactivity. The R- and Z-groups, *i.e.* the re-initiating and activating groups, can mediate the polymerization to the extent of obtaining excellent control over chain-end functionalities and offering further modification possibilities.[52]

1.1.1.1 The RAFT mechanism

The fundamentals of free radical polymerization apply to the RAFT process where the rate of radical termination (R_t) is related to the square of the radical concentration ($R_t \propto [P_n\bullet]^2$) and the rate of propagation is directly proportional to the radical concentration ($R_p \propto [P_n\bullet]$). Thus to eliminate (decrease) termination and allow for a 'living' character, the radical concentration needs to be kept low. This is achieved *via* the addition of a controlling agent into the polymerization medium, which is able to create a rapid equilibrium between the active propagating radicals and the dormant polymeric thiocarbonyl thio compound (Scheme 1.4, **ii** and **iv**). This dynamic equilibrium ensures an equal probability for all the chains to grow resulting in narrowly dispersed polymers.

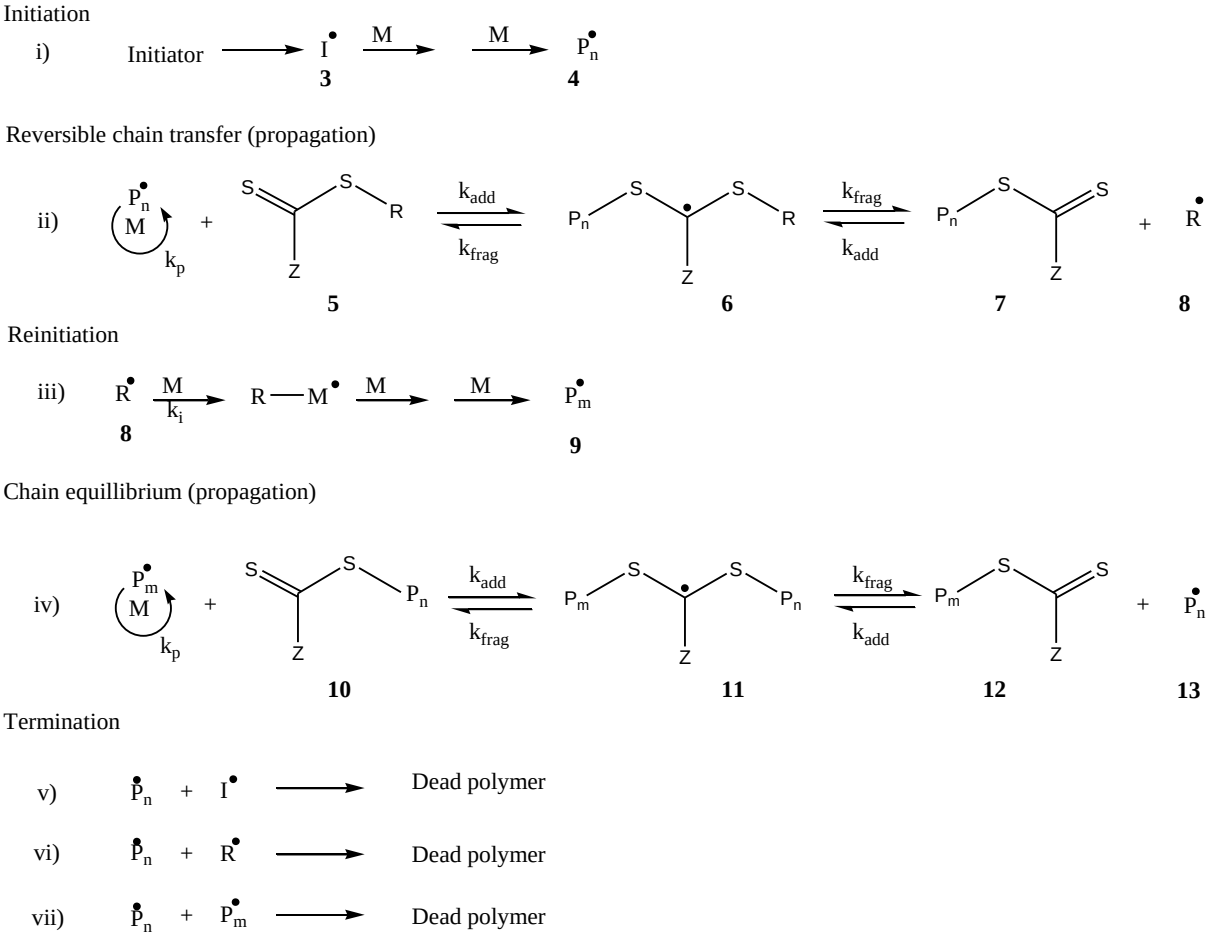

Scheme 1. 4 Mechanism of RAFT-mediated polymerization

Initiation is identical to conventional free radical polymerization where radicals (**3**) are generated by decomposition of a free radical initiator, typically an azo type molecule such as AIBN. The initial transfer reaction between the active species (**4**) and the chain transfer agent (CTA) (**5**) leads to the addition to the reactive C=S bond of the chain transfer agent to produce a carbon centered intermediate radical (**6**). This species may undergo a β-scission reaction which can either yield the reactants back, or release the R-group as a radical fragment (**8**) and leave the polymeric chain capped with the initial active species thus forming the reversible, dormant species (**7**) (this stage is commonly referred to as the pre-equilibrium, Equation ii). The released R• radical (**8**) can initiate a new chain by adding to the monomer or it can add back to the CTA producing the carbon-centered intermediate radical (**6**).

The main equilibrium (**v**) takes place solely between propagating chains (active species) and macro-CTAs (dormant species end-capped with the CTA, **10**), resulting in a rapid exchange of the CTA cap. The propagating radical chains rapidly exchange between the two dormant forms (**10**) and (**12**) and their actively propagating forms.

By using a minimal amount of initiator (only free-radical source, typically added at a concentration 0.1 to 0.2 times the RAFT agent concentration), termination reactions are minimized due to the resulting low concentration of the active species. Rapid exchange ensures that each chain has the same probability of growth, which is essential as all chains must be initiated early in the polymerization reaction for a narrow MWD.

1.1.1.2 Choice of RAFT agent

The structure of the RAFT agent is very important to the success of the RAFT process as the stability of the intermediate radical can be modified by selecting a particular Z- and to a lesser extent the R group. Subsequently, RAFT CTAs can only sufficiently control the polymerization of a certain type of monomer. In a comprehensive review by Moad *et al.*,[53] thiocarbonyl thio compounds that are used as RAFT agents in combination with certain monomer classes are reviewed and the efficient combination of CTA and monomer are given. These CTAs include dithioesters (Z = alkyl or aryl), trithiocarbonates (Z = thiol compound), dithiocarbamate (Z = dialkylamino) and xanthates (Z = alkoxy).

1.1.1.3 The R group

After the initialization step, the subsequently formed oligomeric radicals react with the RAFT agent to form the intermediate radical (**6**). The R-group (leaving group) re-initiates the polymerization which, ideally with fast consumption of the RAFT agent and subsequent fragmentation, will result in most of the chains being initiated at the commencement of polymerization. The R-group should fragment at least as quickly as the polymer chains from the stabilized radical intermediate. This rapid interchange in the chain transfer step ensures that the concentration of growing radical chains is kept lower than that of the stabilized radical intermediates, thereby limiting termination reactions.

The R-group is expected to have less effect on the kinetics of the reaction after initiation, as, after the addition of only one or two monomer units, the R-group does no longer influence the reactivity of the propagating polymer radical.

1.1.1.4 The Z group

The role of the Z-group is to control the stability of the intermediate radical by activating or deactivating the C=S double bond and thereby affecting the reactivity towards the incoming radical. The interplay between the reactivity of the incoming radical and the leaving ability of the R-group directly affects the concentration of the intermediate radicals and thus the extent to which these are involved in termination reactions.

Furthermore, the nature of the monomer has a great influence as these can be classified into two groups which effectively rate the activity of the monomer, *i.e*. "more activated" monomers (MAMs) such as such as styrene, methyl acrylate and methyl methacrylate compared to the "less activated" monomers (LAMs) which would then include vinyl acetate, *N*-vinylpyrrolidone, and *N*-vinylcarbazole. Generally RAFT agents suitable for the one type of monomer are ineffective for the other type as it results in retardation and/or inhibition during the polymerization process (Fig 1.2).[54]

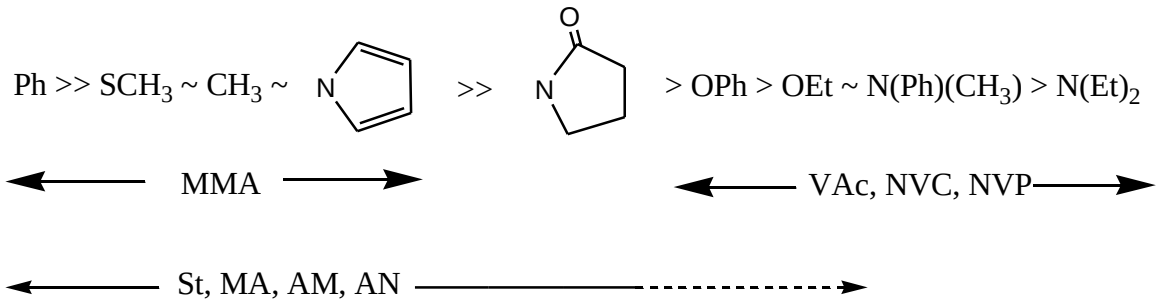

Figure 1. 2 Guidelines for selection of RAFT agents for various polymerizations. The addition rates decrease and fragmentation rates increase from left to right.[36]

Thus, it is essential to select an appropriate RAFT agent. Poor transfer efficiency,[55] slow reinitiating rate[56] and a slow rate of fragmentation[57] have been proposed as the main causes of lack of control when doing RAFT mediated polymerizations.

1.2 Polypeptides *via* living ring-opening polymerizations of *N*-carboxyanhydrides

Peptides and proteins play significant roles in our everyday lives. They are built from α-amino acids, connected *via* amide bonds. Unfortunately, the synthesis of natural polypeptides (proteins) with well-defined amino acid sequences, are severely limited to low molecular weight polypeptides of minimal quantities. This is due to the synthesis method namely *via* solid-phase peptide synthesis (SPPS) *i.e*. a one-by-one amino acid addition *via* a solid-phase support.[58, 59]

In contrast, the ring opening polymerization of *N*-Carboxyanhydrides (ROP NCAs) is a method, which allows for the synthesis of high molecular weight polypeptides with specific architectures in a highly controlled manner.[60-62] This permits for the synthesis of structurally simplistic mimics when compared to their natural counterparts as they lack specific amino acid sequences, but still have the ability to form stable secondary structures (α-helices and β sheets) in solution *via* hydrogen bonding as well as hydrophobic, electrostatic and dipolar interactions.[63-65]

The necessity for structural control over the synthetic polypeptides is evident in the importance it plays for proteins. It is the structural homogeneity in the sequences (primary structure) of these α-amino acids, which eventually determines their secondary structure and essentially needs to be a reproducible process when produced synthetically. Thankfully, significant advances in the controlled ROP of NCAs has fuelled opportunities for the design of well-defined macromolecular structures such as block[66-68], graft[69], star (co)polymers[70-73] and polymer brushes[74-76] which shows parallels to the development in controlled radical polymerizations. These materials have shown their potential in an array of areas, non-more so than the biomedical fields with applications in tissue engineering, drug delivery and therapeutics.[77]

1.2.1 NCA ROP Mechanisms

The ROP of NCAs has two likely mechanisms agreed upon by various authors, dependent on the type of initiator used.[60, 61, 63] The normal amine mechanism (NAM) entails that the initiator is a nucleophile with a mobile hydrogen atom. These include (primary and secondary) amines, alcohols and water, where the nucleophilic attack of the initiatior results in a carbamic acid intermediate which, after decarboxylation results in a terminal amino group. It is the formed primary amine that continues the propagation and allows for the formation of the eventual polypeptide (Scheme 1.5). Low dispersities can be engineered *via* the correct choice of initiator as seen with primary amines, where the latter's reactivity exceeds that of the ω-amines of the propagating chains, resulting in the situation where $k_i > k_p$ thus allowing all the chains to start growing simultaneously.[60, 61]

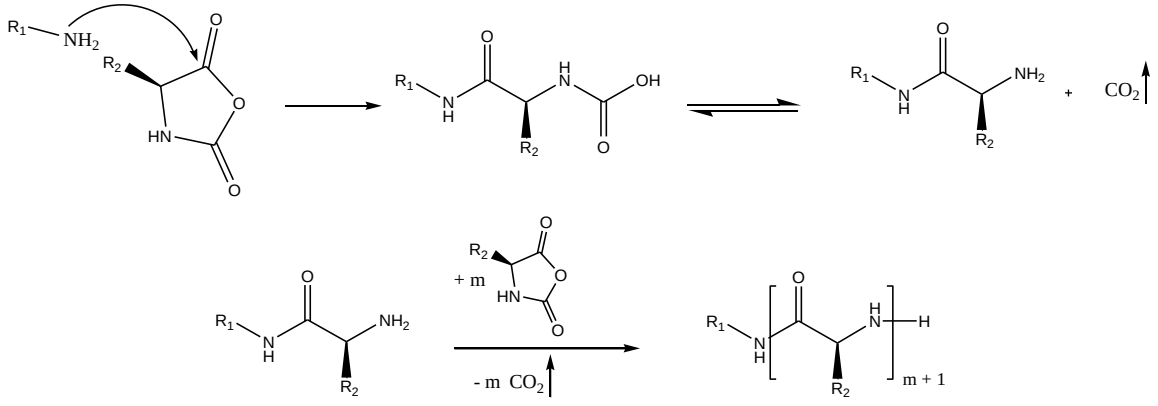

Scheme 1. 5 The normal amine mechanism (NAM).

In the case where the initiator acts like a base instead of a nucleophile and abstracts a proton from the NCA, it is referred to as the activated monomer mechanism (AMM). Here an NCA anion forms due to the abstraction of a proton from the nitrogen atom of the monomer, which then attacks the carbonyl group in the 5-position (Scheme 1.6). Subsequently, this method is limited to NCAs with an unsubstituted nitrogen atom in the ring.

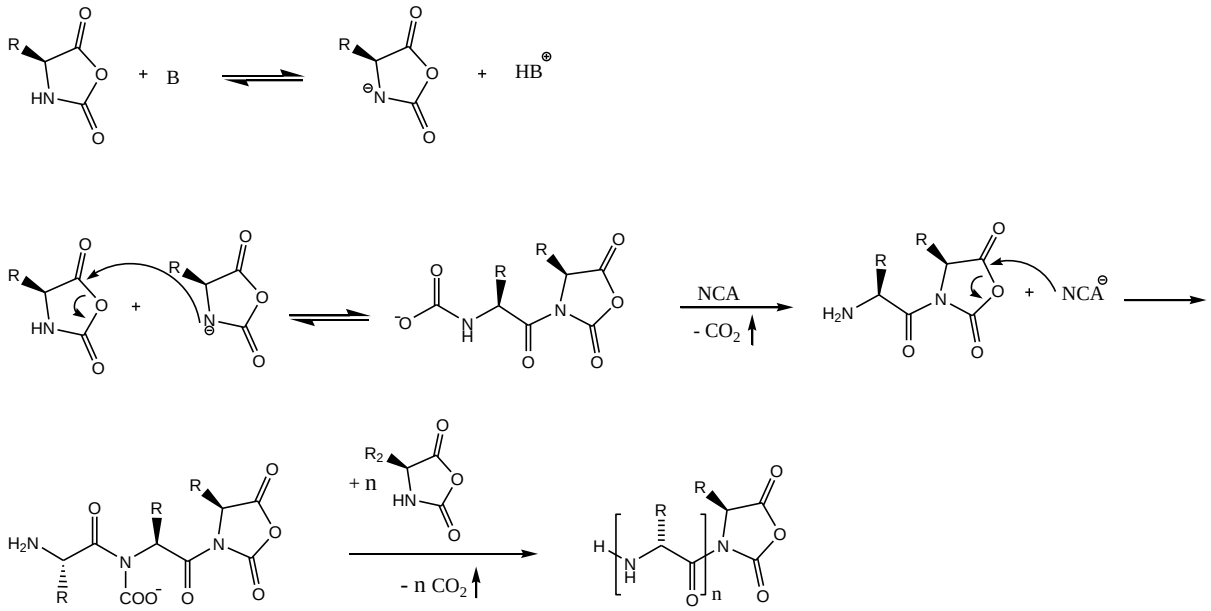

Scheme 1. 6 The activated monomer mechanism (AMM).

The effect of the two different mechanisms are clear when one compares achievable molecular weights as well as the control obtained. This is said to be due to the higher propagation rate of the anion which leads to higher molecular weight for AMM, but higher dispersities are expected due to $k_i < k_{p.}$[78]

Lu *et al.* have shown the control one can obtain when exploiting this fact as they synthesized poly(benzyl-L-glutamate (PBLG) with high molecular weight but a low *Đ* using the secondary amine, *N*-trimethylsilyl amine. Thus allowing the functionalization at the *C*-terminus, while still obtaining the control one expects of primary amines. The polymerization propagates *via* a trimethylsilyl carbamate (TMS-CBM) group which is unable to extract the proton of the nitrogen thus restricting the polymerization to the normal amine mechanism. Control of *Đ* = 1.1 is reported for PBLG (28 500 g/mol) using the selected initiators.[79]

Although optimization of the reaction is possible *via* the choice of initiator, it is also possible to follow a more facile route by optimizing the NAM conditions and thereby trying to reduce possible side reactions as well as accelerating reaction rates. This includes lowering the

temperature[80, 81] varying the solvent[82] or possibly working at higher vacuum,[68, 83] whereby the two greatest influences are arguably temperature and vacuum.

Lowering the temperature essentially increases the stability of the carbamic acid intermediate, which after decarboxylation, forms the primary amine and subsequently propagates the polymerization.[61] Kricheldorf *et al.*[82] have shown that some solvents can induce polymerization of α-amino acids resulting in cyclic polypeptides while working at high vacuum results in the removal of CO_2. This results in acceleration of the reaction as well as in minimization of possible side reactions that CO_2 can have with the solvent.[61, 68]

As mentioned before, the term 'living system' is used in the sense of the control achieved ($Đ$ < 1.2) as well as the ability to reinitiate polymer chains in the presence of more monomer. Using this term loosely, Kricheldorf described the ROP of NCAs as 'living polypeptides' when using primary amines as the initiator.[60] This was due to the fast initiation rate for small, unhindered amines, leading to excellent control as well as the ease of tailoring the degree of polymerization *via* the correct choice of the monomer/initiator molar ratio ($[NCA]_0/[I]_0$).

This has allowed for a wider scope of possible implementation of polypeptides as the incorporation of other living polymerization techniques in combination with NCA ROP allow for the efficient tailoring of composition and topology.[84-86]

1.3 Hybrid bioconjugates

Due to the biological importance of polypeptides and the previous discussion on the living nature of the NCA ROP, it is evident that an array of applications is possible. This is especially true for their use in the fields of biotechnology, biomedicine and pharmaceutical technologies where the combination of natural- and synthetically prepared polymers allow for the synthesis of biohybrid materials, some of which have enjoyed clinical success.[11-13, 87]

Several approaches exist for the preparation of hybrid conjugates, where typically a LRP technique is employed to synthesize the synthetic polymer and combined with the ROP of NCAs. The LRP techniques typically employed are ATRP, NMP and RAFT.[85, 88-91]

Knoop *et al.* reported the combination of NMP and NCA ROP whereby they synthesized PBLG-*b*-PS using a dual initiator. The polypeptide was chain extended using a primary amine on the dual initiator and subsequently used as a macroinitiator. Macroinitiation of styrene via NMP yielded the narrowly dispersed and well-defined hybrid copolymer (see Scheme 1.7).[85]

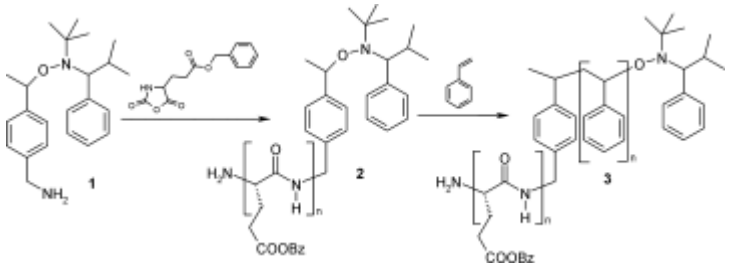

Scheme 1. 7 Synthetic pathway to P(BLG-*b*-styrene) from a dual initiator.[85]

The synthesis of polymer hybrids *via* ATRP and NCA ROP is well documented and recently Liu *et al.* have shown ability of preparing these conjugates with complex architectures such as molecular bottlebrushes. They synthesized Nϵ-bromoisobutyryl functionalized Nα-CBZ-L-lysine and converted this to a polymerizable NCA. This was subsequently polymerized using a transition metal and the subsequent bromo-functionalized poly-L-lysine backbone was used to further grow styrene and ethylene glycol methacrylate side-chains (Scheme 1.8).[92]

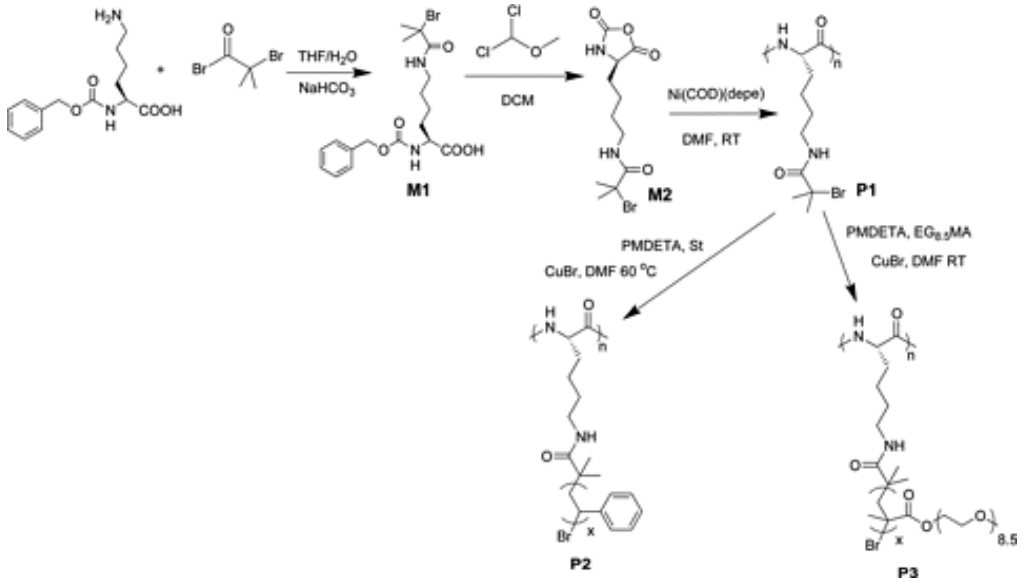

Scheme 1. 8 Synthetic route to poly(Br-L-lysine) (PBrLL) (P1), PLL-g-PS (P2), and PLL-g-PEGMA (P3) polypeptide bottlebrushes.[92]

The use of RAFT in combination with NCA ROP has some inherent difficulties as the amino group used to initiate the NCAs will also cleave the thiocarbonyl thio moiety of the CTA *via* aminolysis. Furthermore, the resulting free thiol has the ablility to further act as a initator, albeit in an uncontrolled manner.[91] Few modular routes are available as it needs effective tailoring of the CTA as well as a strategy which prevents the simultaneous presence of amino and CTA groups. Zhang *et al.* accomplished this with a new class of RAFT agents. A Boc protected amine is incorporated in to the RAFT CTA *via* a multi-step synthesis procedure

(Scheme 1.9).[93] The applicability of using a polypeptide macroCTA is compared to using a synthetic PNIPAM macroinitiator to chain extend BLG NCA. Well-defined PBLG-*b*-PNIPAM conjugates were prepared when utilizing the macroinitiator route where the thermo responsive properties of the hybrid where further investigated.

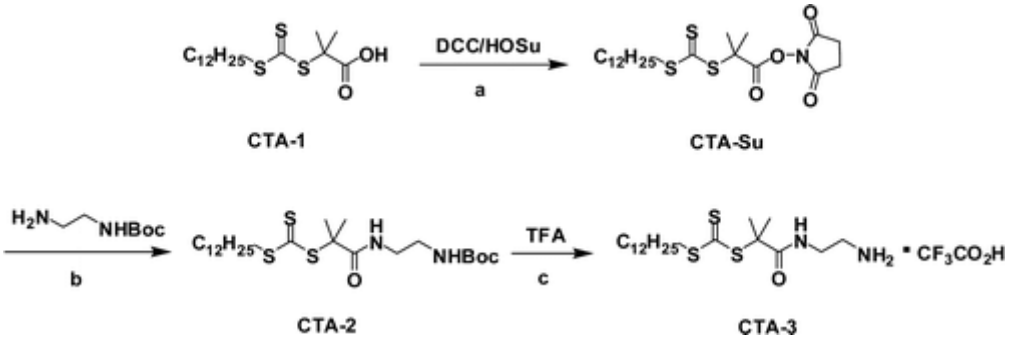

Scheme 1. 9 Synthesis if the Boc protected RAFT CTAs. [a] Reagents and conditions: (a) DCC, HOSu, DCM, −15 °C, 12 h (95%); (b) *N*-Boc-ethylenediamine, TEA, −10 °C ,12 h (90%); (c) TFA, 0 °C,1 h (70%).[93]

The structures formed *via* the self-assembly of these hybrid conjugates are able to utilize the polyelectrolyte type character of the polypeptide which allows for reversible transitions. Thus, at a certain pH, the chains can be ionized and present as water-soluble coils or neutral with a secondary structure that will always favour certain secondary conformations leading to decreased solubility. This, in combination with amphiphilic block copolypeptides or amphiphilic polymer-protein conjugates, make for interesting self-assembled structures such as vesicles,[94-96] aggregates,[94] micelles[97, 98] and organogels.[86]

1.4 Latex particles via heterophase polymerization techniques

1.4.1 Emulsion Polymerization

Emulsion polymerization is arguably one of the most utilized tools in the preparation of polymer latexes where applications range from industrial uses such as surface coatings, paints or bulk polymers to (bio)medical fields like nanomedicine for the design of nanosized diagnostic agents. There is a real incentive to use water as the dispersion system as it is ideal for large-scale productions being an inexpensive, environmentally friendly solvent which allows for excellent heat dissipation during the polymerization.[99, 100]

A simple system will typically start as an oil-in-water dispersion of monomer droplets in aqueous solution and once initiated, lead to a dispersion of polymer particles with mean diameters ranging from 50 – 500 nm. Sparingly water-soluble monomers such as styrenics,

acrylates and methacrylates are incorporated and partially stabilized by the addition of a stabilizer (above the critical micelle concentration). Colloidal stabilizers may be surfactants ranging from ionic, non-ionic or mixed systems to surfactant-free emulsions where high molecular weight polymer are incorporated in the particle and extend outward in a stabilizing capacitance, ensuring colloidal stability. Initiators are generally water-soluble, i.e. persulfates, ensuring that initiation starts in the aqueous phase.[101, 102]

Upon heating, the initiator decomposes and propagates with monomer in the aqueous phase. This is interval I (0 – 10% conversion) of an emulsion polymerization where the addition of several monomer units makes the oligoradicals sufficiently hydrophobic and they subsequently diffuse into micelles or polymer particles to intiate in the oil phase. Free radicals generated will preferentially enter the smaller unswollen micelles or polymer particles compared to the larger monomer reservoirs due to the favourable surface/volume ratios.

As the polymerization proceeds into interval II (10 – 40% conversion), any stabilizer/surfactant from the aqueous phase or that part of micelles which have not been nucleated will disappear as they are absorbed by the growing polymer particles. As propagation of the polymer chain ensues, the micelles grow (swell) *via* the diffusion of monomer from the aqueous phase and monomer reservoir. In interval III (conversion > 40%) the polymerization has proceeded to a stage where all the monomer reservoirs are depleted and any remaining monomer is solely present in the polymer particles.[103] The terminology for these intervals was defined by Smith and Ewart and the kinetics have been well documented (see Figure 1.3).[101, 104-107]

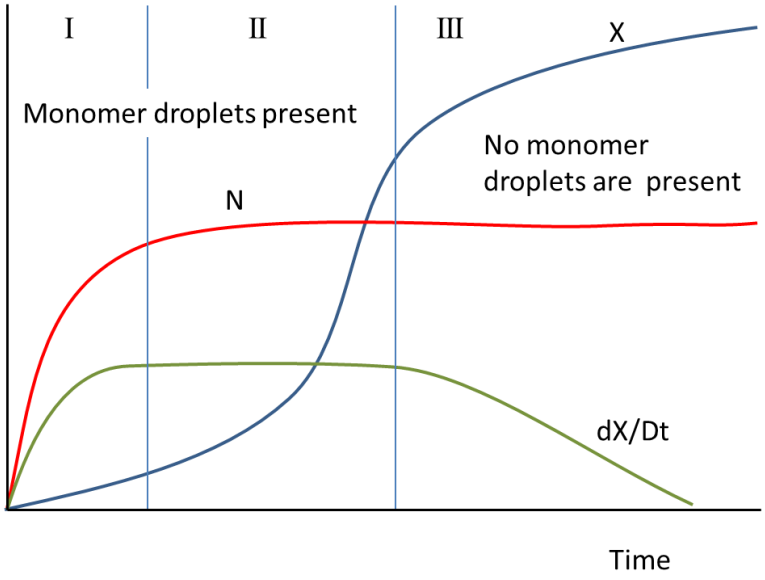

Figure 1. 3 Classical qualitative desorption of phases (intervals) I, II and III as a function of the evolution of monomer conversion (X), rate of polymerization (dX/dt) and number of particles (N).[107]

1.4.1 Mini-emulsion Polymerization

In some cases, the mechanism of an emulsion polymerization is not adequate for the synthesis of more compex materials. It is then possible to modify the technique via the introduction of an external shear force which subsequently reduces the size of the monomer droplets resulting in the latter becoming the loci of the polymerization themselves. This is known as a mini-emulsion polymerization, whereby the reaction mixture is readily formulated so that any aqueous mass transfer between droplets is considered negligible. Furthermore, this is an efficient method for templating particles as the final particle sizes are similar to the initial monomer droplet sizes (if only particle nucleation occurred).[22, 28, 108] This concept was first introduced by Higuchi and Misra[109] and subsequently utilized in the formation of polymeric nanoparticles by Ugelstadt *et al.*[110]

A typical mini-emulsion would involve a continuous phase, a dispersed phase, emulsifier and a co-stabilizer. The continuous phase is normally an aqueous solution which influences the reaction through pH and ionic strength. The dispersed phase contains the monomer and very often the co-stabilizer. The latter having excellent solubility in the dispersed phase while being badly soluble in the continuous phase, act as an osmotic pressure agent inside the droplet. The emulsifier is a surface active compound dissolved in the continuous phase. The emulsifier helps prevent coalescence during droplet formation as well as aggregation during

the polymerization itself. It has an direct influence on the final particels size, colloidal stability and surface characteristics of the final latex.[108] Initiation can proceed in either the dispersed or continuous phase as long as the polymerization proceeds inside the monomer droplets.

The greatest attribute of this technique is that particle nucleation is the main nucleating mechanism, meaning no monomer transfer takes place. Subsequently, an array of synthetic tools is available to polymerize the monomer in the droplets. These range from anionic polymerizations resulting in polybutylcyanoacrylate (PBCA) nanoparticles,[111] cationic polymerizations for the synthesis of poly-*p*-methoxystyreneparticles,[112] ring-opening metathesis polymerization (ROMP) in preparing polynorbornene nanoparticles[113, 114] and step-growth acylic diene metathesis (ADMET) polymerization leading to oligo(phenylene vinylenes) particles.[115]

1.6 References

1. DeRosa, M. C.; Monreal, C.; Schnitzer, M.; Walsh, R.; Sultan, Y. *Nat Nano* **2010,** 5, (2), 91-91.

2. Huang, Q.; Yu, H.; Ru, Q. *Journal of Food Science* **2009,** 75, (1), R50-R57.

3. Raj, S.; Jose, S.; Sumod, U. S.; Sabitha, M. *Journal of Pharmacy & Bioallied Sciences* **2012,** 4, (3), 186-193.

4. Bakhru, S. H.; Furtado, S.; Morello, A. P.; Mathiowitz, E. *Advanced Drug Delivery Reviews* **2013,** 65, (6), 811-821.

5. Ezhilarasi, P. N.; Karthik, P.; Chhanwal, N.; Anandharamakrishnan, C. *Food and Bioprocess Technology* **2012,** 6, (3), 628-647.

6. Sultana, S.; Khan, M. R.; Kumar, M.; Kumar, S.; Ali, M. *Journal of Drug Targeting* **2013,** 21, (2), 107-125.

7. Shokeen, M.; Pressly, E. D.; Hagooly, A.; Zheleznyak, A.; Ramos, N.; Fiamengo, A. L.; Welch, M. J.; Hawker, C. J.; Anderson, C. J. *ACS Nano* **2011,** 5, (2), 738-747.

8. Elsabahy, M.; Wooley, K. L. *Chemical Society Reviews* **2012,** 41, (7), 2545-2561.

9. Kamaly, N.; Xiao, Z.; Valencia, P. M.; Radovic-Moreno, A. F.; Farokhzad, O. C. *Chemical Society Reviews* **2012,** 41, (7), 2971-3010.

10. Duncan, R. *Current Opinion in Biotechnology* **2011,** 22, (4), 492-501.

11. Duncan, R.; Vicent, M. J. *Advanced Drug Delivery Reviews* **2013,** 65, (1), 60-70.

12. Duncan, R. *Journal of Controlled Release* **2014,** 190, (0), 371-380.

13. Matsumura, Y.; Kataoka, K. *Cancer Science* **2009,** 100, (4), 572-579.

14. Mai, Y.; Eisenberg, A. *Chemical Society Reviews* **2012,** 41, (18), 5969-5985.

15. Friedrich, H.; McKenzie, B.; Bomans, P. H. H.; Deng, Z.; Nudelman, F.; Holder, S. J.; de With, G.; Somerdijk, N. *Microscopy and Microanalysis* **2010,** 16, (SupplementS2), 832-833.

16. Rösler, A.; Vandermeulen, G. W. M.; Klok, H.-A. *Advanced Drug Delivery Reviews* **2012,** 64, Supplement, (0), 270-279.

17. Danhier, F.; Ansorena, E.; Silva, J. M.; Coco, R.; Le Breton, A.; Preat, V. *Journal of Controlled Release* **2012,** 161, (2), 505-522.

18. Owens Iii, D. E.; Peppas, N. A. *International Journal of Pharmaceutics* **2006,** 307, (1), 93-102.

19. Ma, Y.; Sadoqi, M.; Shao, J. *International Journal of Pharmaceutics* **2012,** 436, (1 - 2), 25-31.

20. Kamaly, N.; Fredman, G.; Subramanian, M.; Gadde, S.; Pesic, A.; Cheung, L.; Fayad, Z. A.; Langer, R.; Tabas, I.; Cameron Farokhzad, O. *Proceedings of the National Academy of Sciences* **2013,** 110, (16), 6506-6511.

21. Wu, J.; Kamaly, N.; Shi, J.; Zhao, L.; Xiao, Z.; Hollett, G.; John, R.; Ray, S.; Xu, X.; Zhang, X.; Kantoff, P. W.; Farokhzad, O. C. *Angewandte Chemie International Edition* **2014,** 53, (34), 8975-8979.

22. Landfester, K.; Mailander, V. *Expert Opinion on Drug Delivery* **2013,** 10, (5), 593-609.

23. Sakuma, S.; Kataoka, M.; Higashino, H.; Yano, T.; Masaoka, Y.; Yamashita, S.; Hiwatari, K.-i.; Tachikawa, H.; Kimura, R.; Nakamura, K.; Kumagai, H.; Gore, J. C.; Pham, W. *European Journal of Pharmaceutical Sciences* **2011,** 42, (4), 340-347.

24. Miki, K.; Kimura, A.; Oride, K.; Kuramochi, Y.; Matsuoka, H.; Harada, H.; Hiraoka, M.; Ohe, K. *Angewandte Chemie* **2011,** 123, (29), 6697-6700.

25. Holzapfel, V.; Musyanovych, A.; Landfester, K.; Lorenz, M. R.; Mailänder, V. *Macromolecular Chemistry and Physics* **2005,** 206, (24), 2440-2449.

26. Rao, J. P.; Geckeler, K. E. *Progress in Polymer Science* **2011,** 36, (7), 887-913.

27. Mahapatro, A.; Singh, D. *Journal of Nanobiotechnology* **2011,** 9, (1), 55.

28. Landfester, K.; Musyanovych, A.; Mailänder, V. *Journal of Polymer Science Part A: Polymer Chemistry* **2010,** 48, (3), 493-515.

29. Albanese, A.; Tang, P. S.; Chan, W. C. W. *Annual Review of Biomedical Engineering* **2012,** 14, (1), 1-16.

30. Caruso, F.; Stayton, P.; Ward, M. D. *Chemistry of Materials* **2012,** 24, (5), 727-727.

31. Dhar, S.; Gu, F. X.; Langer, R.; Farokhzad, O. C.; Lippard, S. J. *Proceedings of the National Academy of Sciences* **2008,** 105, (45), 17356-17361.

32. Singh, K., Choudhary, M. , Chianella, I. and Singh, P. *Advances in Nanoparticles* **2013**, (2), 182-190.

33. Ruoslahti, E. *Advanced Materials* **2012,** 24, (28), 3747-3756.

34. Medley, C. D.; Bamrungsap, S.; Tan, W.; Smith, J. E. *Analytical Chemistry* **2011,** 83, (3), 727-734.

35. Yu, B.; Tai, H. C.; Xue, W.; Lee, L. J.; Lee, R. J. *Molecular Membrane Biology* **2010,** 27, (7), 286-298.

36. Moad, G.; Rizzardo, E.; Thang, S. H. *Acc. Chem. Res.* **2008,** 41, (9), 1133-1142.

37. Moad, G.; Matyjaszewski, K.; Moller, M., Radical Polymerization. In *Polymer Science: A Comprehensive Reference*, Elsevier: Amsterdam, 2012; Vol. 3, pp 59-118.

38. Julien, N.; Giuseppe, M.; David, M. H. *Macromol. Rapid Commun.* **2007,** 28, (10), 1083-1111.

39. Braunecker, W. A.; Matyjaszewski, K. *Prog. Polym. Sci.* **2007,** 32, (1), 93-146.

40. Nicolas, J.; Guillaneuf, Y.; Lefay, C.; Bertin, D.; Gigmes, D.; Charleux, B. *Progress in Polymer Science* **2013,** 38, (1), 63-235.

41. Rizzardo, E.; Solomon, D. H. *Australian Journal of Chemistry* **2012,** 65, (8), 945-969.

42. Matyjaszewski, K.; Xia, J. *Chemical Reviews* **2001,** 101, (9), 2921-2990.

43. Matyjaszewski, K. *Macromolecules* **2012,** 45, (10), 4015-4039.

44. Barner-Kowollik, C.; Buback, M.; Charleux, B.; Coote, M. L.; Drache, M.; Fukuda, T.; Goto, A.; Klumperman, B.; Lowe, A. B.; McLeary, J. B.; Moad, G.; Monteiro, M. J.; Sanderson, R. D.; Tonge, M. P.; Vana, P. *J. Polym. Sci., Part A: Polym. Chem.* **2006,** 44, (20), 5809-5831.

45. Moad, G.; Rizzardo, E.; Thang, S. H. *Australian Journal of Chemistry* **2012,** 65, (8), 985-1076.

46. Keddie, D. J. *Chemical Society Reviews* **2014,** 43, (2), 496-505.

47. Le, T. P. M., G.; Rizzardo, E.; Thang, S. H. *PCT Int Appl WO 98/01478* **1998**.

48. Rhodia Chimie: Corpart, P. C., D.; Biadatti, T.; Zard, S.Z.; Michelet, D.; . *PCT Int. Appl. WO. 9858974* **1998**.

49. Perrier, S.; Takolpuckdee, P. *J. Polym. Sci., Part A: Polym. Chem.* **2005,** 43, (22), 5347-5393.

50. Moad, G.; Rizzardo, E.; Thang, S. H. *Chemistry – An Asian Journal* **2013,** 8, (8), 1634-1644.

51. Gody, G.; Maschmeyer, T.; Zetterlund, P. B.; Perrier, S. b. *Macromolecules* **2014,** 47, (2), 639-649.

52. Keddie, D. J.; Moad, G.; Rizzardo, E.; Thang, S. H. *Macromolecules* **2012,** 45, (13), 5321-5342.

53. Moad, G.; Rizzardo, E.; Thang, S. H. *Polymer* **2008,** 49, (5), 1079-1131.

54. Benaglia, M.; Chiefari, J.; Chong, Y. K.; Moad, G.; Rizzardo, E.; Thang, S. H. *J. Am. Chem. Soc.* **2009,** 131, (20), 6914-6915.

55. Destarac, M.; Brochon, C.; Catala, J.-M.; Wilczewska, A.; Zard, S. Z. *Macromol. Chem. Phys.* **2002,** 203, (16), 2281-2289.

56. McLeary, J. B.; McKenzie, J. M.; Tonge, M. P.; Sanderson, R. D.; Klumperman, B. *Chem. Commun. (Cambridge, U. K.)* **2004**, (17), 1950-1951.

57. Vana, P.; Davis, T. P.; Barner-Kowollik, C. *Macromol. Theory Simul.* **2002,** 11, (8), 823-835.

58. Marsden, H. R.; Handgraaf, J.-W.; Nudelman, F.; Sommerdijk, N. A. J. M.; Kros, A. *J. Am. Chem. Soc.* 132, (7), 2370-2377.

59. Merrifield, B. *Science* **1986,** 232, (4748), 341-347.

60. Kricheldorf, H. R. *Angew. Chem., Int. Ed.* **2006,** 45, (35), 5752-5784.

61. Hadjichristidis, N.; Iatrou, H.; Pitsikalis, M.; Sakellariou, G. *Chem. Rev. (Washington, DC, U. S.)* **2009,** 109, (11), 5528-5578.

62. Huang, J.; Heise, A. *Chemical Society Reviews* **2013,** 42, (17), 7373-7390.

63. Deming, T. J. *J. Polym. Sci., Part A: Polym. Chem.* **2000,** 38, (17), 3011-3018.

64. Gibson, M. I.; Cameron, N. R. *J. Polym. Sci., Part A: Polym. Chem.* **2009,** 47, (11), 2882-2891.

65. Papadopoulos, P.; Floudas, G.; Klok, H. A.; Schnell, I.; Pakula, T. *Biomacromolecules* **2003,** 5, (1), 81-91.

66. Deming, T. J. *Nature* **1997,** 390, (6658), 386.

67. Habraken, G. J. M.; Heise, A.; Thornton, P. D. *Macromolecular Rapid Communications* **2012,** 33, (4), 272-286.

68. Habraken, G. J. M.; Wilsens, K. H. R. M.; Koning, C. E.; Heise, A. *Polymer Chemistry* **2011,** 2, (6), 1322-1330.

69. Wang, J.; Lu, H.; Kamat, R.; Pingali, S. V.; Urban, V. S.; Cheng, J.; Lin, Y. *Journal of the American Chemical Society* **2011,** 133, (33), 12906-12909.

70. Appelhans, D.; Komber, H.; Kirchner, R.; Seidel, J.; Huang, C.-F.; Voigt, D.; Kuckling, D.; Chang, F.-C.; Voit, B. *Macromolecular Rapid Communications* **2005,** 26, (8), 586-591.

71. Sulistio, A.; Widjaya, A.; Blencowe, A.; Zhang, X.; Qiao, G. *Chemical Communications* **2011,** 47, (4), 1151-1153.

72. Byrne, M.; Thornton, P. D.; Cryan, S.-A.; Heise, A. *Polymer Chemistry* **2012,** 3, (10), 2825-2831.

73. Sulistio, A.; Blencowe, A.; Widjaya, A.; Zhang, X.; Qiao, G. *Polymer Chemistry* **2012,** 3, (1), 224-234.

74. Borase, T.; Iacono, M.; Ali, S. I.; Thornton, P. D.; Heise, A. *Polymer Chemistry* **2012,** 3, (5), 1267-1275.

75. Kar, M.; Vijayakumar, P. S.; Prasad, B. L. V.; Gupta, S. S. *Langmuir* **2010,** 26, (8), 5772-5781.

76. Balamurugan, S. S.; Soto-Cantu, E.; Cueto, R.; Russo, P. S. *Macromolecules* **2010,** 43, (1), 62-70.

77. Deming, T. J. *Wiley Interdisciplinary Reviews: Nanomedicine and Nanobiotechnology* **2014,** 6, (3), 283-297.

78. Peggion, E.; Cosani, A.; Mattucci, A. M.; Scoffone, E. *Biopolymers* **1964,** 2, (1), 69-78.

79. Lu, H.; Cheng, J. *J. Am. Chem. Soc.* **2008,** 130, (38), 12562-12563.

80. Vayaboury, W.; Giani, O.; Cottet, H.; Deratani, A.; Schué, F. *Macromol. Rapid Commun.* **2004,** 25, (13), 1221-1224.

81. Vayaboury, W.; Giani, O.; Cottet, H.; Bonaric, S.; Schué, F. *Macromol. Chem. Phys.* **2008,** 209, (15), 1628-1637.

82. Kricheldorf, H. R.; von Lossow, C.; Schwarz, G. *Macromolecules* **2005,** 38, (13), 5513-5518.

83. Pickel, D. L.; Politakos, N.; Avgeropoulos, A.; Messman, J. M. *Macromolecules* **2009,** 42, (20), 7781-7788.

84. Audouin, F.; Knoop, R. J. I.; Huang, J.; Heise, A. *J. Polym. Sci., Part A: Polym. Chem.* **2010,** 48, (20), 4602-4610.

85. Knoop, R. J. I.; Habraken, G. J. M.; Gogibus, N.; Steig, S.; Menzel, H.; Koning, C. E.; Heise, A. *Journal of Polymer Science Part A: Polymer Chemistry* **2008,** 46, (9), 3068-3077.

86. Gibson, M. I.; Cameron, N. R. *Angew. Chem., Int. Ed.* **2008,** 47, (28), 5160-5162.

87. Heredia, K. L.; Maynard, H. D. *Org. Biomol. Chem.* **2007,** 5, (1), 45-53.

88. Brzezinska, K. R.; Deming, T. J. *Macromolecular Bioscience* **2004,** 4, (6), 566-569.

89. Deng, L.; Shi, K.; Zhang, Y.; Wang, H.; Zeng, J.; Guo, X.; Du, Z.; Zhang, B. *Journal of Colloid and Interface Science* **2008,** 323, (1), 169-175.

90. Habraken, G. J. M.; Koning, C. E.; Heise, A. *Journal of Polymer Science Part A: Polymer Chemistry* **2009,** 47, (24), 6883-6893.

91. Zhang, X.; Oddon, M.; Giani, O.; Monge, S.; Robin, J.-J. *Macromolecules* **2010,** 43, (6), 2654-2656.

92. Liu, Y.; Chen, P.; Li, Z. *Macromolecular Rapid Communications* **2012,** 33, (4), 287-295.

93. Zhang, X.; Li, J.; Li, W.; Zhang, A. *Biomacromolecules* **2007,** 8, (11), 3557-3567.

94. Holowka, E. P.; Pochan, D. J.; Deming, T. J. *J. Am. Chem. Soc.* **2005,** 127, (35), 12423-12428.

95. Iatrou, H.; Frielinghaus, H.; Hanski, S.; Ferderigos, N.; Ruokolainen, J.; Ikkala, O.; Richter, D.; Mays, J.; Hadjichristidis, N. *Biomacromolecules* **2007,** 8, (7), 2173-2181.

96. Sun, J.; Chen, X.; Deng, C.; Yu, H.; Xie, Z.; Jing, X. *Langmuir* **2007,** 23, (16), 8308-8315.

97. Osada, K.; Christie, R. J.; Kataoka, K. *Journal of The Royal Society Interface* **2009,** 6, (Suppl 3), S325-S339.

98. Heffernan, M.; Murthy, N. *Annals of Biomedical Engineering* **2009,** 37, (10), 1993-2002.

99. Landfester, K. *Macromolecular Chemistry and Physics* **2003,** 204, (3), 542-542.

100. Urban, D.; Takamura, K., *Polymer dispersions and their industrial applications*. Wiley-VCH: 2002.

101. Thickett, S. C.; Gilbert, R. G. *Polymer* **2007,** 48, (24), 6965-6991.

102. Cunningham, M. F. *Progress in Polymer Science* **2008,** 33, (4), 365-398.

103. Zetterlund, P. B.; Kagawa, Y.; Okubo, M. *Chemical Reviews* **2008,** 108, (9), 3747-3794.

104. Smith, W. V.; Ewart, R. H. *The Journal of Chemical Physics* **1948,** 16, (6), 592-599.

105. Harkins, W. D. *Journal of the American Chemical Society* **1947,** 69, (6), 1428-1444.

106. Gardon, J. L. *Journal of Polymer Science Part A-1: Polymer Chemistry* **1968,** 6, (3), 623-641.

107. Okubo, M.; Nomura, M.; Tobita, H.; Suzuki, K., Emulsion Polymerization: Kinetic and Mechanistic Aspects. In *Polymer Particles*, Springer Berlin Heidelberg: 2005; Vol. 175, pp 1-128.

108. Durand, A.; Marie, E. *Advances in Colloid and Interface Science* **2009,** 150, (2), 90-105.

109. Higuchi, W. I.; Misra, J. *Journal of Pharmaceutical Sciences* **1962,** 51, (5), 459-466.

110. Ugelstad, J.; El-Aasser, M. S.; Vanderhoff, J. W. *Journal of Polymer Science: Polymer Letters Edition* **1973,** 11, (8), 503-513.

111. Weiss, C. K.; Ziener, U.; Landfester, K. *Macromolecules* **2007,** 40, (4), 928-938.

112. Cauvin, S.; Ganachaud, F.; Moreau, M.; Hemery, P. *Chemical Communications* **2005**, (21), 2713-2715.

113. Quemener, D.; Heroguez, V.; Gnanou, Y. *Macromolecules* **2005,** 38, (19), 7977-7982.

114. Quémener, D.; Héroguez, V.; Gnanou, Y. *Journal of Polymer Science Part A: Polymer Chemistry* **2006,** 44, (9), 2784-2793.

115. Pecher, J.; Mecking, S. *Macromolecules* **2007,** 40, (22), 7733-7735.

Chapter 2

Synthesis of polypeptide block copolymer hybrids by the combination of N-carboxyanhydride (NCA) polymerization with RAFT.

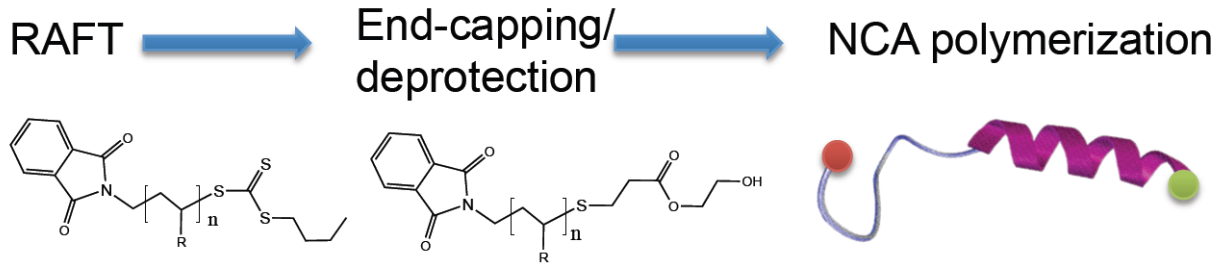

This work was published in the journal Macromolecular Rapid communications:

Jacobs, J.; Gathergood, N.; Heise, A., Synthesis of Polypeptide Block Copolymer Hybrids by the Combination of N-Carboxyanhydride Polymerization and RAFT. *Macromolecular Rapid Communications* **2013,** 34, (16), 1325-1329.

2.1 Abstract

The synthesis of hybrid bioconjugates *via* the ring-opening polymerization (ROP) of *N*-carboxyanhydrides (NCAs) using a synthetic macroinitiator is described. Poly(*n*-butyl acrylate), polystyrene and poly(*N*-isopropyl acrylamide) was synthesized ($Đ$ < 1.1) using reversible addition-fragmentation chain transfer (RAFT) as the synthetic tool. A phthalimidomethyl tritiocarbonate RAFT CTA was used to prepare well-defined, end-functional polymers, which after deprotection, resulted in amine terminal macroinitiators. The subsequent initiating systems could successfully be chain extended with ε-benzyloxycarbonyl-L-lysine (ZLL) or γ-benzyl-L-glutamate (BLG) as the NCAs to produce a library of polymer-polypeptide conjugates. In doing so, we describe a novel procedure for directly synthesizing bioconjugates *via* a non-modular route without the need for excessive purification and isolation steps.

2.2. Introduction

Protein-polymer conjugates have enjoyed increased awareness as promising materials in biomedicine, (nano)biotechnology and pharmaceutical technologies.[1-4] In view of their potential, researchers are also investigating fully synthetic biohybrid materials in which the natural protein segment is replaced by a synthetic polypeptide. While these are structurally simplistic mimics, the ability of synthetic polypeptides to adopt secondary structures allow for an inherent method of directing the formation of self-assembly in copolymers on the nanoscale.[5-9] Recent advances in controlled N-carboxyanhydrides (NCA) polymerization have significantly enhanced the capability to obtain synthetic polypeptides with well-defined molecular weight, polymer architecture and end-group fidelity.[10-13] Moreover, efficient orthogonal functionalization techniques have further expanded the scope for the design of functional polypeptides for example, stimuli-responsive materials.[14-24]

Additional macromolecular diversity and consequently property modulation can be achieved by the modular combination of the synthetic polypeptide segments with other functional polymer blocks. First reports employed atom transfer radical polymerization (ATRP) in a macroinitiation approach from synthetic polypeptides rationalized by the broad range of polymerizable monomers available in this methodology.[25-29] However, interference of the amide bonds with the catalytic system along with the added purification steps needed to remove the ATRP catalyst, supports the investigation of a possible alternative to ATRP.[26, 30, 31] The combination of NCA and nitroxide mediated polymerization (NMP) has shown promise, but the versatility of possible monomers using NMP is a drawback as well as the high temperatures required for NMP.[32, 33] Ring-opening metathesis polymerization (ROMP) was also successfully applied in combination with NCA polymerization.[34, 35] While both techniques show very good compatibility, the limited choice of ROMP monomers could be a restricting factor. In contrast, reversible addition-fragmentation chain transfer (RAFT)-mediated polymerization is one of the most versatile and robust methods for synthesizing well-defined, high molecular weight polymers from a wide range of monomers.[36-40] However, due to the inherent possibility of side reactions, there is minimal work reported combining RAFT and the ring-opening polymerization of NCAs. One challenge is the inherent instability of RAFT agents in the presence of primary amines either required as initiators for the NCA polymerization or present as polypeptide chain ends. Nevertheless, the combination of RAFT and NCA ROP has enjoyed some success, for example Zhang *et. al.* have shown

that it is possible to initiate NCAs with a thiol end-functional initiator.[41] γ-Benzyl-L-glutamate (BLG) was successfully initiated with an aminolysed RAFT CTA resulting, however, in a multimodal distribution of products. Furthermore, to the authors' knowledge, only one direct method of obtaining a synthetic amine-functional macroinitiator and chain extending with NCAs has been reported.[42] Synthesizing bioconjugates *via* a non-modular route thus calls for a carefully chosen synthetic pathway to ensure the efficiency of the macroinitiator.

We report the synthesis of hybrid polypeptide polymers by facilitating NCA polymerization from a synthetic RAFT macroinitiator. A protected amine functionality was incorporated in the RAFT CTA for subsequent chain extension of the polypeptide. A library of polypeptide-polymer conjugates could be built up by varying the synthetic polymers used as the macroinitiator and after the subsequent deprotection, BLG or ε-benzyloxycarbonyl-L-lysine (ZLL) was incorporated as the NCAs.

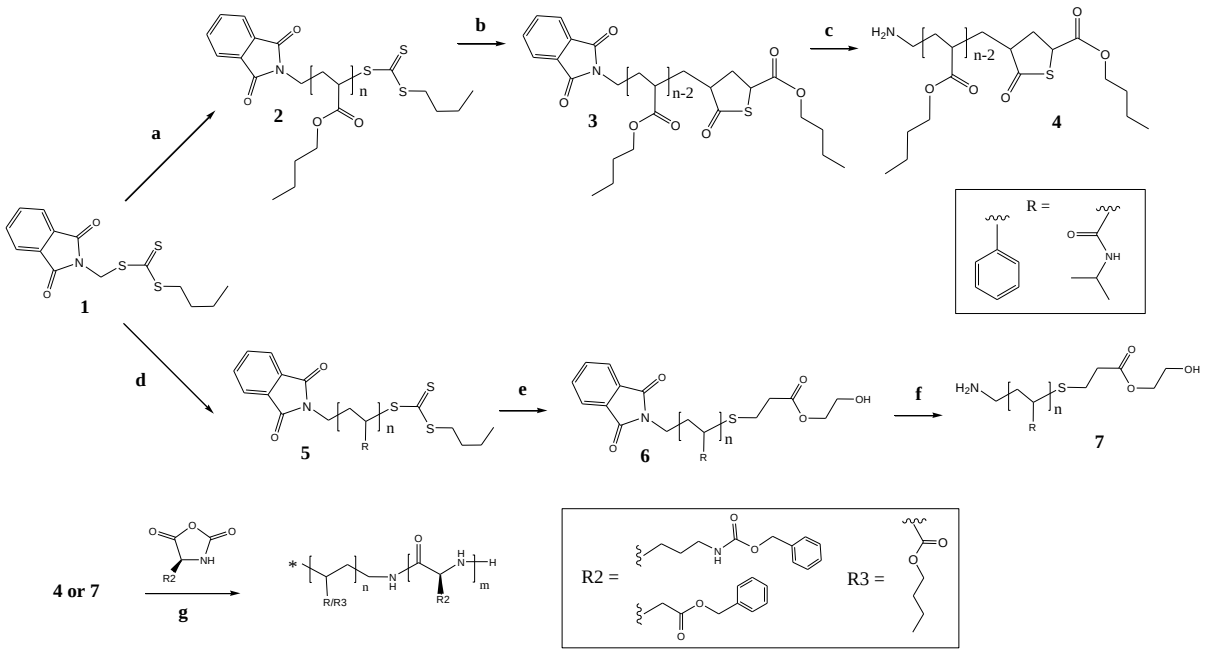

Scheme 2. 1: Synthesis of block copolymers combining RAFT and NCA polymerization. (a) n-butyl acrylate, AIBN, 2 h, 60 °C; (b) 2-aminoethanol (10 eq.), 12 h, r.t.; (c) DMF, NH_2NH_2 (30 eq.), 2 h, 60 °C; (d) styrene or N-isopropyl acrylamide, AIBN, 16 h, 60 °C; (e) DMF, 2-aminoethanol (5 eq.), hydroxylethyl acrylate (5 eq.), 24 h, r.t.; (f) DMF, NH_2NH_2 (30 eq.), 4 h, 75 °C; (g) DMF or $CHCl_3$, BLG or ZLL NCA.

2.3 Experimental Procedures

2.3.1 Materials

All chemicals were purchased from Sigma-Aldrich and used as received unless otherwise noted. γ-Benzyl-L-glutamate and ε-benzyloxycarbonyl-L-Lysine were supplied by Bachem. Anhydrous DMF, chloroform, ethyl acetate, methanol were used directly from the bottle under an inert and dry atmosphere.γ-Benzyl-L-glutamate (BLG) and ε-benzyloxycarbonyl-L-Lysine (ZLL) NCA was synthesised following a literature procedure.[43] Butyl phthalimidomethyl tritiocarbonate, RAFT CTA, was synthesized according to a literature procedure by Moad *et. al.*[44]

2.3.2 Synthesis of PBA, PS and PNIPAM homopolymer using RAFT CTA (1).

The homopolymer was prepared according to a literature procedure by Moad *et. al.*[44]

The following is representative procedure. *n*-BA (10 g, 78 mmol), RAFT CTA 1 (230 mg, 0.71 mmol) and AIBN (23 mg, 0.14 mmol) were placed in a Schlenk flask and degassed via 4 freeze-pump-thaw cycles. The flask was immersed in a preheated oil bath (60˚C) and left under magnetic stirring for a 2 hour period. The reaction was quenched by cooling the reaction flask and exposing the polymer solution to air. The product, PBA, was then isolated by dialyzing against methanol using Spectra/Por dialysis membranes (MWCO, 1000 Da) for 24 h at room temperature. The excess methanol was removed under high vacuum and the resulting polymer dried under vacuum. The product was analyzed by ^{1}H NMR spectroscopy ($CDCl_3$) and SEC. Conversion as determined *via* ^{1}H NMR spectroscopy: 54%. Isolated yield: 4.3 g.

2.3.3 Synthesis of amine end-functional PBA, PS and PNIPAM.

2.3.3.1 Synthesis of Amine end-functionalized PBA. Trithiocarbonate end-functional PBA (4 g, 53 mmol) was dissolved in DMF (10 mL) and added to a 50 mL round-bottomed flask equipped with a magnetic stirring bar. 15 Molar equivalents of 2-aminoethanol was added and then left to stir for 6 hours at room temperature. The solution was purified by dialysis against methanol using Spectra/Por dialysis membranes (MWCO, 1000 Da) for 24 h at room temperature. The thiolactone end-functional polymer was

recovered by removing the solvent under high vacuum. The product was identified via ^{1}H NMR spectroscopy ($CDCl_3$) and MALDI-ToF MS. Product 3.6 g, 90% yield.

The subsequent thiolactone end-functional polymer (3 g, 40 mmol) was dissolved in 8 mL DMF and added to a 50 mL Schlenck tube equipped with a magnetic stirring bar. The reaction mixture was placed in a preheated oil bath of 60 °C and 30 molar equivalents of hydrazine (0.6 mL) was added. The reaction mixture was left under stir for 2 hours. The solution was purified by dialysis against methanol using Spectra/Por dialysis membranes (MWCO, 1000 Da) for 24 h at room temperature. The product was recovered by removing the solvent under high vacuum and further drying in a vacuum oven for 40 hours at 40 °C. The product was identified via ^{1}H NMR spectroscopy ($CDCl_3$) and MALDI-ToF MS. Product 2.6 g, 87% yield.

General procedure for the synthesis of amine end-functional polystyrene and poly(N-isopropyl acrylamide) via a One-Pot Aminolysis/Thiol-Ene Reaction.

2.3.3.2 Synthesis of Amine end-functionalized PNIPAM. PNIPAM-TTC (1.0 g, 0.18 mmol), triethylphosphite (0.30 g, 1.8 mmol) and 2-aminoethanol (0.43 mL, 9 mmol) were dissolved in 8 mL DMF. The solution was degassed with nitrogen and left to stir for 3 h at room temperature. After this time had elapsed, a solution of hydroxylethyl acrylate (0.81 g, 9 mmol) and triethylamine (0.091 mL, 0.91 mol) was added via a syringe to the reaction mixture. The reaction mixture was left to stir for 24 h at 25 °C. The solution was purified by dialysis against DDI water using Spectra/Por dialysis membranes (MWCO, 1000 Da) for 24 h at room temperature. After lyophilization, the product obtained as a white powder was analyzed by ^{1}H NMR spectroscopy ($CDCl_3$) and SEC. Yield: 0.82 g.

The subsequent phthalimide and hydroxyl end-functional polymer (0.6 g, 0.11 mmol) was dissolved in 5 mL DMF and added to a 50 mL Schlenk tube equipped with a magnetic stirring bar. The reaction mixture was placed in a preheated oil bath of 75 °C and 30 molar equivalents of hydrazine (0.17 mL) was added. The reaction mixture was left under stir for 4 hours. The solution was purified by dialysis against DDI water using Spectra/Por dialysis membranes (MWCO, 1000 Da) for 24 h at room temperature. The resulting solution was lyophilized and the product collected as a white powder. The product was analyzed by ^{1}H NMR spectroscopy ($CDCl_3$) and SEC. Yield: 0.48 g.

2.3.3.3 Synthesis of Amine end-functionalized PS. A similar procedure was followed to prepare the amine end-functional PS.

2.3.4 General Procedure for Synthesis of the Hybrid Block Copolymers via NCA ROP.

2.3.4.1 Typical synthesis procedure of PBA-b-PZLL at room temperature: The NCA monomer of ε-benzyloxycarbonyl-L-Lysine (0.74 g, 2.4 mmol) was dissolved in 30 ml anhydrous chloroform in a Schlenk tube and degassed *via* three successive freeze-pump-thaw cycles and then backfilled with nitrogen. A solution of PBA-NH_2 (200 mg, 0.027 mmol) in 2 mL anhydrous chloroform was injected through a rubber septum with a syringe. The reaction was left to stir at room temperature overnight until the ZLL NCA had been completely consumed as monitored by ATR FTIR spectroscopy. The reaction mixture was concentrated under vacuum and precipitated into an excess of diethylether, filtered and dried under vacuum. The product was identified via ^{1}H NMR spectroscopy (DMSO) and SEC. Yield: 75%

2.3.4.2 **Typical synthesis procedure of PBA-b-PZLL at 0 °C*:*** The NCA monomer of ε-benzyloxycarbonyl-L-Lysine (0.74 g, 2.4 mmol) was dissolved in 6 ml anhydrous DMF in a Schlenk tube. The solution was degassed *via* three successive freeze-pump-thaw cycles and kept under vacuum. The reaction flask was immersed in a 0 °C water bath and a solution of PBA-NH_2 (200 mg, 0.027 mmol) in 1 mL anhydrous DMF was injected through a rubber septum with a syringe. The reaction was left to stir for several days until the ZLL NCA had been completely consumed as monitored by ATR FTIR spectrosocopy. The reaction mixture was precipitated into an excess of diethylether, filtered and dried under vacuum. The product was identified via ^{1}H NMR spectroscopy (DMSO) and SEC. Yield: 70%

Similar procedures were followed to prepare PBA-*b*-PBLG, PS-*b*-PZLL and PNIPAM-*b*-PZLL.

2.3.5 Methods

Nuclear magnetic resonance (NMR) spectra were recorded on a Bruker Avance 400 (400 MHz) in DMSO-d6 and $CDCl_3$ as solvents. All chemical shifts are reported in parts per million (ppm) with tetramethylsilane (TMS) as an internal reference.

Attenuated Total Reflection (ATR) FTIR measurements were performed on a Perkin-Elmer Spectrum 100 instrument. Spectra were obtained from 4 scans with a resolution of 2 cm^{-1} in the spectral region of 650 – 4000 cm^{-1}. A background measurement was taken before the sample was loaded onto the ATR for measurement. Samples could be characterized in the liquid state without prior sample preparation.

Size Exclusion Chromatography (SEC) was performed on an Agilent 1200 system in conjunction with two PSS GRAM analytical (8 x 300 and 8 x 100, 10 μ) columns, a Wyatt Dawn Heleos 8 multi angle light scattering (MALS) detector and Wyatt Optilab rEX differential refractive index (DRI) detector with a 658 nm light source. The eluent was DMF containing 0.1 M LiBr at a flow rate of 1 mL/min. The column temperature was set to 40 °C with the MALS detector at 35 °C and the DRI detector at 40 °C. Molar masses and dispersities were calculated from the MALS signal by the Astra software (Wyatt) using the refractive index increment (dn/dc) as determined or found in literature.[45, 46] The specific refractive index increments for the colopymers were calculated relative to the ratio of the homopolymer. The dn/dc values used for PZLL and PBLG were 0.120 and 0.118 respectively, while the synthetic and copolymer values are summarized in Table 2.1. All samples for SEC analysis were filtered through a 0.45 mm PTFE filter (13 mm, PP housing, Whatman) prior to injection.

MALDI-ToF-MS analysis was carried out on a Voyager-DE STR form Applied Biosystems. The matrix used was trans-2-[3-(4-tert-butylphenyl)-2-methyl-2-propenylidene]malononitrile (DCTB) with potassium trifluoroacetic acid (KTFA) added as cationic ionization agent.

Table 2. 1 dn/dc values for the library of hybrid bioconjugates successfully prepared using synthetic macroinitiators synthesized via RAFT mediated polymerization.

Entry	Copolymer[a]	dn/dc[b]
A	PBA_{60}-NH_2	0.041
1*	PBA_{60}-*b*-$PZLL_{98}$	0.103
2*	PBA_{60}-*b*-$PZLL_{127}$	0.106
3**	PBA_{60}-*b*-$PZLL_{68}$	0.096
B	PBA_{60}-NH_2	0.041
1**	PBA_{60}-*b*-$PBLG_{49}$	0.115
C	PS_{80}-NH_2	0.159
1**	PS_{80}-*b*-PZLL	0.135[e]
D	$PNIPAM_{62}$-NH_2	0.094
1**	$PNIPAM_{62}$-*b*-PZLL	0.105[e]

[a]The DP was determined *via* ^{1}H-NMR. [b]dn/dc values where calculated based on the molar fraction of the individual homopolymer. [e]Initial [NCA]/[MacroI] ratios were used for the dn/dc calculation. * Bioconjugate synthesized *via* the chain extension of the subsequent NCA in $CHCl_3$ at RT. **Bioconjugate synthesized *via* the chain extension of the subsequent NCA in DMF at 0 °C.

2.4 Results and Discussion

Due to the incompatibility of amino groups used for NCA initiation and CTA for RAFT polymerization we adopted a strategy by which the RAFT polymerization was carried out first followed by NCA macroinitiation. A phthalimide functional trithiocarbonate (TTC)[44] (**1**) was used as the RAFT CTA to prepare the synthetic polymer (Scheme 2.1). The robustness of RAFT in this process is evident from the range of monomers successfully polymerized to prepare poly(n-butyl acrylate) (PBA), polystyrene (PS) and poly(N-isopropyl acrylamide) (PNIPAM). Well-defined, narrowly distributed ($Đ$ = 1.1) homopolymers were synthesized with a protected amine at the α-chain-end and a TTC moiety at the ω-chain-end.

To further employ the polymers as macroinitiator in NCA polymerization, it was necessary to selectively and quantitatively cleave the TTC moiety before deprotecting the phthalimide as the amine would readily react *via* an aminolysis reaction. Purification is arguably the most important factor when synthesizing the macroinitiator as residual by-products will readily initiate the NCA ROP and any method should thus be straightforward and simple. The cleaving is achieved by reacting the TTC moiety with a nucleophile such as a primary or secondary amine.[47, 48] During these post-polymerization reactions, it was found that aminoethanol was most suitable for the selective cleavage of the TTC moiety. This was partly due to the compound's aminolysis efficiency, but more importantly the ability to completely remove the excess aminoethanol and the subsequent by-products by dialysis. Xu *et. al.* have shown that acrylates and specifically poly(methyl methacrylate) readily form a terminal thiolactone functionality after aminolysis of a dithiobenzoate end-functionality due to backbiting of the subsequent free thiol.[49] This was also observed for the PBA with ^{1}H-NMR and MALDI-ToF MS indicating complete thiolactone formation (Figure 2.1). This has the advantages as it circumvents possible side-reactions when deprotecting the amine as NCA propagation will not be able to proceed *via* the thiol as a possible nucleophilic initiator.[41]

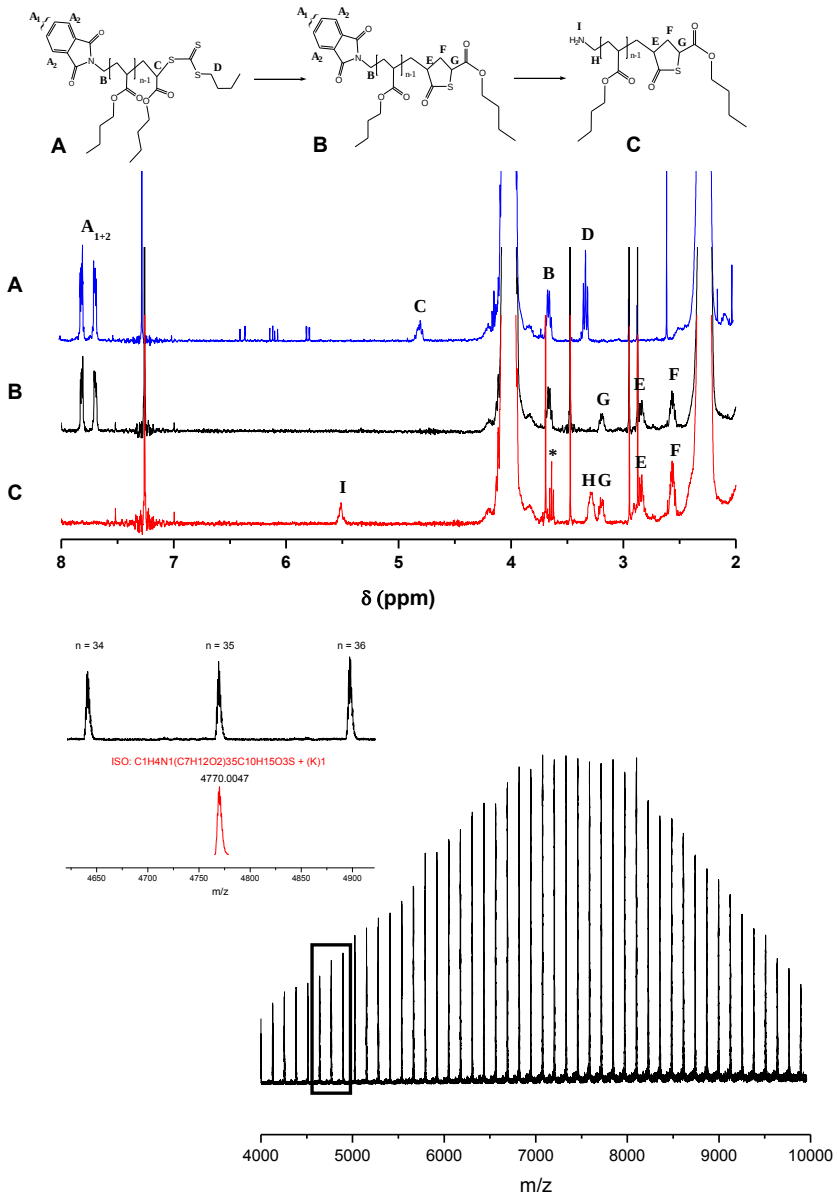

Figure 2. 1: ^{1}H-NMR spectra of poly(n-butyl acrylate) before (A) and after the selective cleavage of the TTC moiety (B) via an aminolysis reaction and subsequent phthalimide deprotection (C). MALDI-ToF mass spectra of the amine end-functional poly(n-butyl acrylate) (C) with insert of experimental (top) and theoretical (bottom) results for DP = 35.

The phthalimide was deprotected using 30 molar equivalents of hydrazine at an elevated temperature (dependent on the susceptibility of the homopolymer to side-reactions) resulting in the amine end-functional macroinitiator.[44] The removal of the phthalimide can be quantified by the disappearance of the characteristic phthalimido aromatic signals between δ 7.5 and 8.0 ppm (Figure 2.1, A_{1+2}) as well as the appearance of the amine signal (Figure 2.1, I) (confirmed *via* a D_2O shake). The efficiency of the PBA macroinitiator was investigated by chain extension using different NCA in anhydrous DMF or chloroform, respectively. In

general, we found that the propagation rate is enhanced in chloroform, but due to solubilization problems this method is limited to only certain NCAs for example ZLL and BLG while working with low concentrations. Alternatively the macroinitiator was chain extended in anhydrous DMF at 0 °C under vacuum.[50]

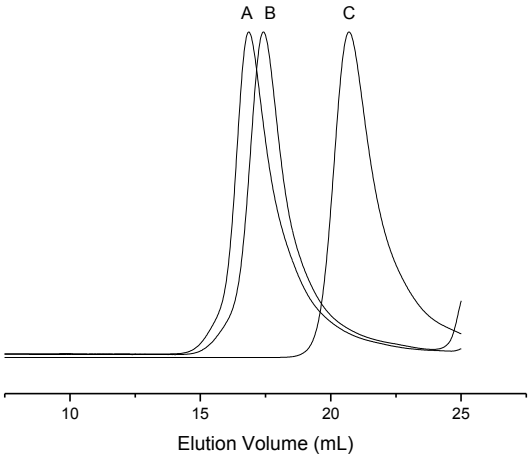

Figure 2. 2: SEC traces of PBA_{60}-*b*-$PZLL_{127}$ (A), PBA_{60}-*b*-$PZLL_{98}$ (B) and PBA-NH_2 (C).

For the PBA (7500 g/mol) (**4**, Scheme 2.1) chain extension with ZLL NCA, polypeptide chains of 20 000 - 40 000 g/mol were targeted. The reaction in chloroform is rapid and reaches completion in less than 10 hours when targeting up to 120 repeat units. Furthermore, when characterized by SEC, no residual homopolymer is evident after chain extension and a monomodal distribution of the higher molecular weight bioconjugates is present (Figure 2.2). The reaction was repeated at low temperature in DMF due to the enhanced end-group control, which would be important for further NCA chain extension.[50] Only 60 repeat units were targeted due to the long reaction times associated with 0 °C NCA polymerization (Figure 2.3).

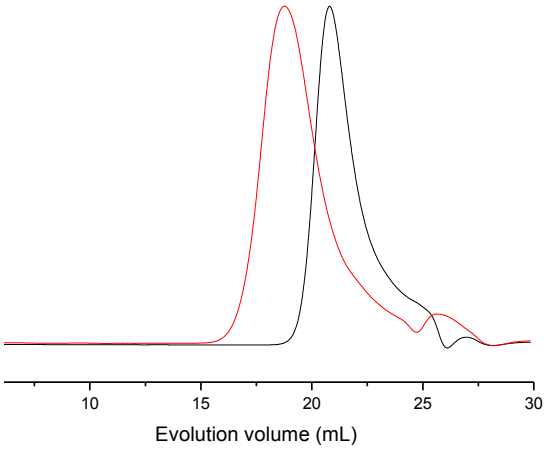

Figure 2. 3 SEC trace PBA_{60}-*b*-$PZLL_{68}$ (red) and PBA-NH_2 (black) after chain extension in DMF at 0 °C.

By referencing the methyl signal of the PBA (0.80 – 0.92 ppm, Figure 2.4) to the two-proton peak of the ZLL repeat unit (4.7 – 5.2 ppm) the molecular weights of the block copolymer could be determined *via* ^{1}H-NMR spectroscopy. A good agreement was found between the theoretical and experimental values (Table 2.2).

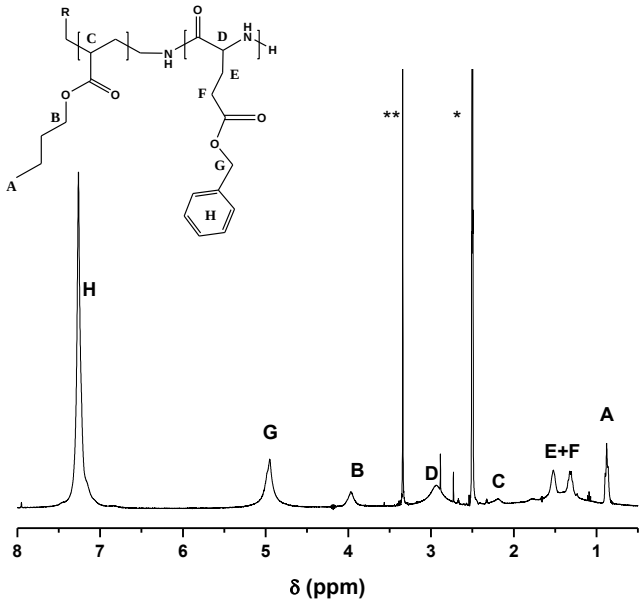

Figure 2. 4 ^{1}H-NMR spectra of PBA-*b*-PZLL after chain extension with ZLL NCA (*, DMSO-d6; **, water).

The versatility of the PBA macroinitiator was further indicated by chain extending with BLG NCA (**4**, Scheme 2.1), resulting in a monomodal distribution of PBA_{60}-*b*-$PBLG_{49}$ conjugates (Figure 2.5). Once again, a monomodal distribution was obtained where the molecular weight compared well with the expected value.

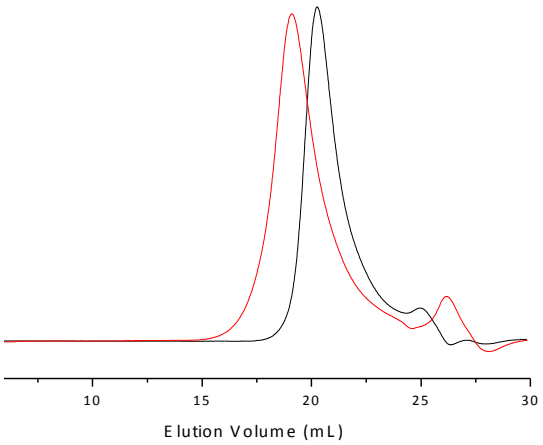

Figure 2. 5 SEC trace of PBA_{60}-*b*-$PBLG_{49}$ (red) and PBA-NH_2 (black) after chain extension in DMF at 0 °C.

The strategy was applied to PS and PNIPAM in an effort to extend the bioconjugate library while using the same RAFT CTA. However, the synthetic pathway had to be modified slightly in order to cap the free thiol obtained during aminolysis to inhibit possible initiation of the NCAs and to prevent reaction of TTC with the amine.[41] This was overcome *via* a simultaneous aminolysis/thiol-ene reaction with hydroxyl ethylacrylate, effectively allowing us to engineer the ω-chain-end by introducing a functionality of our choice by the selection of the acrylate (**5**, Scheme 2.1).

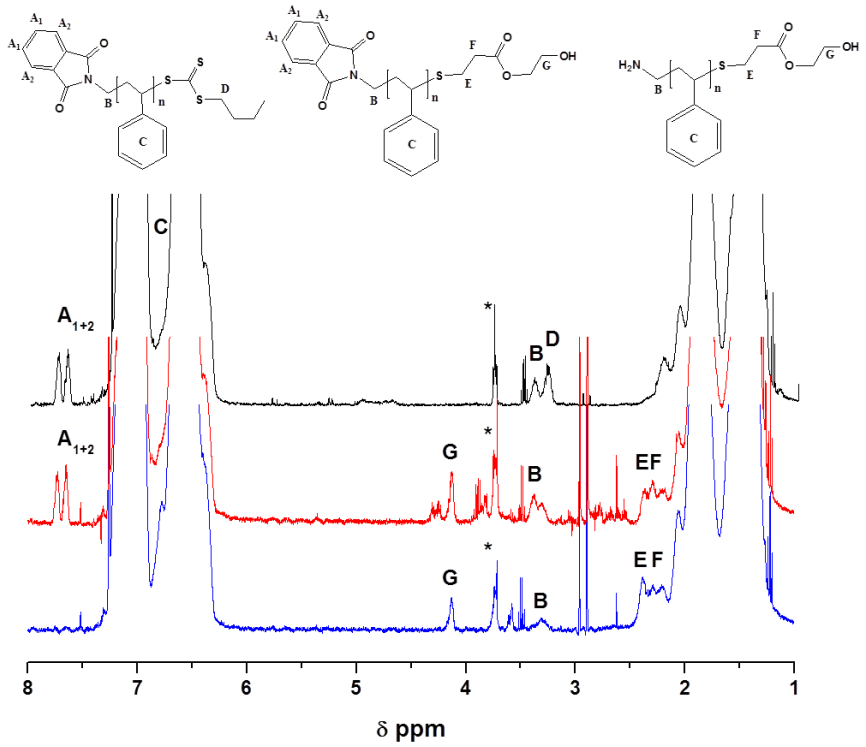

Figure 2. 6 ^{1}H-NMR spectra of PS-TTC before (black) and after (red) a simultaneous aminolysis/thiol-ene reaction, yielding hydroxyl end-functional PS. The bottom (blue) ^{1}H-NMR spectra indicates the signal disappearance of the amine protecting phthalimide moiety after hydrazinolysis (* indicates solvent peaks).

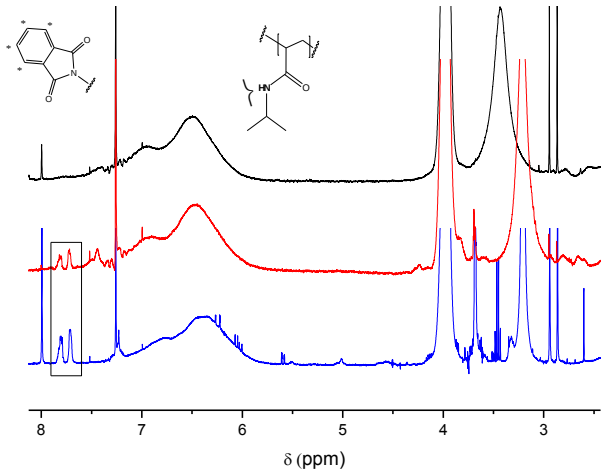

Figure 2. 7 ^{1}H-NMR spectra of PNIPAM before (blue) and after (red) a simultaneous aminolysis/thiol-ene reaction, yielding hydroxyl end-functional PS. The top (black) ^{1}H-NMR spectra indicates the signal disappearance of the amine protecting phthalimide moiety after hydrazinolysis.

After the simultaneous aminolysis and thiol-ene reaction of both PS and PNIPAM, ^{1}H-NMR spectra show the absence of the TTC proton signals (Figure 2.6 and Figure 2.7) while the subsequent SEC trace indicates no higher molecular weight shift due to disulfide coupling (Figure 2.8 and Figure 2.9). This is indicative of successful conjugation of the ene and the thiol end-functional polymer.

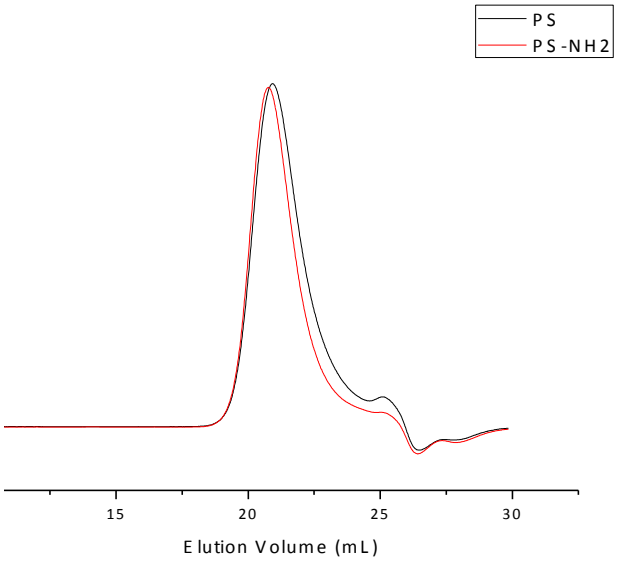

Figure 2. 8 SEC trace of PS before (black) the one-pot aminolysis/thiol-ene reaction as well as after amine deprotection (red) yielding the α-amine and ω-hydroxyl end-functional polymer.

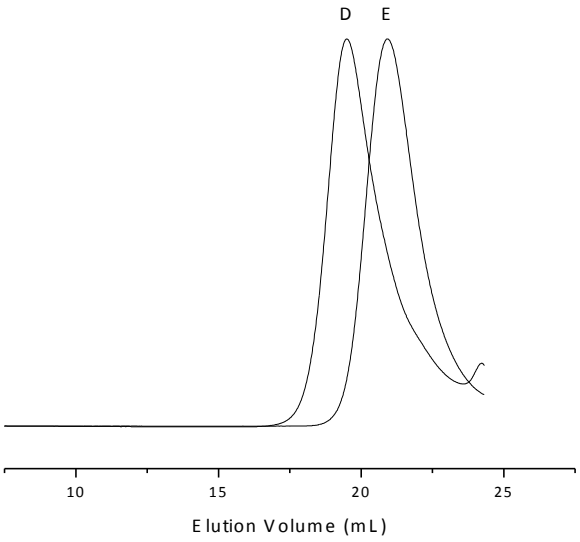

Figure 2. 9 SEC traces of PS_{80}-*b*-$PZLL_{60}$ (D) and PS-NH_2 (E).

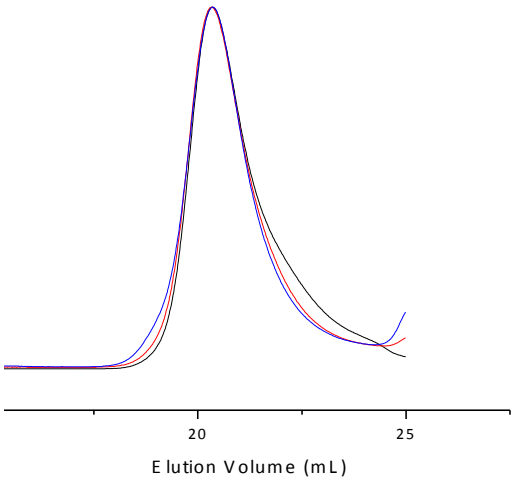

Figure 2. 10 SEC trace of PNIPAM before (black) and after (red) the one-pot aminolysis/thiol-ene reaction, as well as the subsequent amine deprotection (blue) yielding the α-amine and ω-hydroxyl end-functional polymer.

Subsequently, PS and PNIPAM macroinitiators of 8300 and 7000 g/mol respectively, were synthesized and chain extended with ZLL as the NCA in DMF. Both the PS and PNIPAM macroinitiators indicate effective copolymerization of the polypeptide chain as illustrated in both Figure 2.9 and Figure 2.11. The PNIPAM system did however display a lower molecular weight shoulder, indicating the presence of some starting material and effectively increasing the [NCA]/[MacroI] ratio.

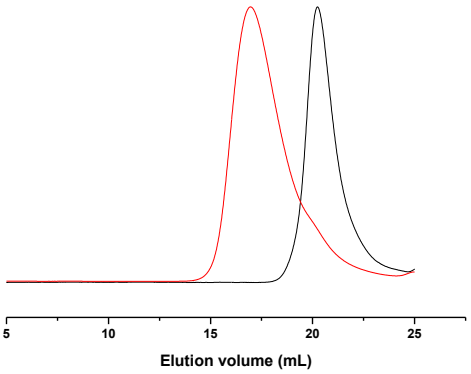

Figure 2. 11 SEC trace of $PNIPAM_{62}$-*b*-PZLL (red) and PNIPAM-NH_2 (black).

Table 2. 2 Library of hybrid block copolymer successfully prepared using RAFT macroinitiators and NCA polymerization.

Copolymer[a]	$[NCA]_0/[MI]_0$	Reaction time (h)	$M_n^{theo\ (b)}$ g/mol	$M_w^{(c)}$ g/mol	$M_n^{NMR\ (a)}$ g/mol	*Đ*
PBA_{60}-NH_2	-	2	-	8000	7500	1.1
PBA_{60}-*b*-$PZLL_{98}$	90	8*	31 100	48200	33200	1.1
PBA_{60}-*b*-$PZLL_{127}$	120	<10*	39 000	61100	40800	1.1
PBA_{60}-*b*-$PZLL_{68}$	60	72**	23 200	31400	25300	1.1
PBA_{60}-NH_2	-	2	-	8000	7500	1.1
PBA_{60}-*b*-$PBLG_{49}$	45	72**	17 400	18100	20400	1.1
PS_{80}-NH_2	-	24	-	8700	8300	1.1
PS_{80}-*b*-PZLL	60	72**	24 000	29800	N/A	1.1
$PNIPAM_{62}$-NH_2	-	16	-	7300	7000	1.1
$PNIPAM_{62}$-*b*-PZLL	90	120**	30 600	58 100	N/A	1.2

(a) Molecular weights and DP were determined by ^{1}H-NMR using signals of the initiator and the polymer. (b) Theoretical M_n calculated using the original target $[NCA]_0/[MI]_0$ ratios. (c) M_w determined by SEC in DMF using Multi Angle Light Scattering with dn/dc values calculated based on the molar fraction of the individual homopolymer. (e) Initial [NCA]/[MacroI] ratios were used for the dn/dc calculation. * NCA chain extension in $CHCl_3$ at RT. ** NCA chain extension in DMF at 0 °C under high vacuum.

2.5 Conclusions

We have demonstrated the versatility of the synthesis of polypeptide-polymer hybrids combining RAFT and NCA polymerization. Key to this successful approach is an end-group engineering strategy that prevents the simultaneous presence of amino and CTA groups. We devised two such strategies, which are simple and highly efficient, i.e. the aminoethanol CTA removal with in-situ thiolactone formation for PBA and simultaneous aminolysis/thiol-ene reaction with hydroxyl ethylacrylate for PS and PNIPAM. The combination of these two polymerization techniques has shown to be effective in synthesizing a wide range of hybrid conjugates only limited by the compatibility of the RAFT CTA and monomer while the presented end-capping strategies allow the introduction of a range of functional end-groups.

2.6 References

1. Bulmus, V. *Polymer Chemistry* **2011,** 2, (7), 1463-1472.

2. Duncan, R. *Nat Rev Drug Discov* **2003,** 2, (5), 347.

3. Heredia, K. L.; Maynard, H. D. *Organic & Biomolecular Chemistry* **2007,** 5, (1), 45-53.

4. Klok, H.-A. *Macromolecules* **2009,** 42, (21), 7990-8000.

5. Choi, Y. Y.; Joo, M. K.; Sohn, Y. S.; Jeong, B. *Soft Matter* **2008,** 4, (12), 2383-2387.

6. Heffernan, M.; Murthy, N. *Annals of Biomedical Engineering* **2009,** 37, (10), 1993-2002.

7. Holowka, E. P.; Pochan, D. J.; Deming, T. J. *Journal of the American Chemical Society* **2005,** 127, (35), 12423-12428.

8. Iatrou, H.; Frielinghaus, H.; Hanski, S.; Ferderigos, N.; Ruokolainen, J.; Ikkala, O.; Richter, D.; Mays, J.; Hadjichristidis, N. *Biomacromolecules* **2007,** 8, (7), 2173-2181.

9. Osada, K.; Christie, R. J.; Kataoka, K. *Journal of The Royal Society Interface* **2009,** 6, (Suppl 3), S325-S339.

10. Cheng, J.; Deming, T., Synthesis of Polypeptides by Ring-Opening Polymerization of alpha-Amino Acid N-Carboxyanhydrides. In *Peptide-Based Materials*, Springer Berlin Heidelberg: 2012; Vol. 310, pp 1-26.

11. Deming, T. J., Polypeptide and Polypeptide Hybrid Copolymer Synthesis via NCA Polymerization. In *Peptide Hybrid Polymers*, Springer Berlin Heidelberg: 2006; Vol. 202, pp 1-18.

12. Habraken, G. J. M.; Heise, A.; Thornton, P. D. *Macromolecular Rapid Communications* **2012,** 33, (4), 272-286.

13. Kricheldorf, H. R. *Angewandte Chemie International Edition* **2006,** 45, (35), 5752-5784.

14. Borase, T.; Ninjbadgar, T.; Kapetanakis, A.; Roche, S.; O'Connor, R.; Kerskens, C.; Heise, A.; Brougham, D. F. *Angewandte Chemie International Edition* **2013,** 52, (11), 3164-3167.

15. Engler, A. C.; Bonner, D. K.; Buss, H. G.; Cheung, E. Y.; Hammond, P. T. *Soft Matter* **2011,** 7, (12), 5627-5637.

16. Engler, A. C.; Lee, H.-i.; Hammond, P. T. *Angewandte Chemie International Edition* **2009,** 48, (49), 9334-9338.

17. Huang, J.; Bonduelle, C.; Thevenot, J.; Lecommandoux, S.; Heise, A. *Journal of the American Chemical Society* **2012,** 134, (1), 119-122.

18. Huang, J.; Habraken, G.; Audouin, F.; Heise, A. *Macromolecules* **2010,** 43, (14), 6050-6057.

19. Huang, J.; Heise, A. *Chemical Society Reviews* **2013,** 42, (17), 7373-7390.

20. Kramer, J. R.; Deming, T. J. *Journal of the American Chemical Society* **2012,** 134, (9), 4112-4115.

21. Krannig, K.-S.; Schlaad, H. *Journal of the American Chemical Society* **2012,** 134, (45), 18542-18545.

22. Sun, J.; Schlaad, H. *Macromolecules* **2010,** 43, (10), 4445-4448.

23. Tang, H.; Zhang, D. *Biomacromolecules* **2010,** 11, (6), 1585-1592.

24. Xiao, C.; Zhao, C.; He, P.; Tang, Z.; Chen, X.; Jing, X. *Macromolecular Rapid Communications* **2010,** 31, (11), 991-997.

25. Brzezinska, K. R.; Deming, T. J. *Macromolecular Bioscience* **2004,** 4, (6), 566-569.

26. Habraken, G. J. M.; Koning, C. E.; Heise, A. *Journal of Polymer Science Part A: Polymer Chemistry* **2009,** 47, (24), 6883-6893.

27. Liu, Y.; Chen, P.; Li, Z. *Macromolecular Rapid Communications* **2011,** 33, (4), 287-295.

28. Steig, S.; Cornelius, F.; Witte, P.; Staal, B. B. P.; Koning, C. E.; Heise, A.; Menzel, H. *Chemical Communications* **2005**, (43), 5420-5422.

29. Zhang, X.; Li, J.; Li, W.; Zhang, A. *Biomacromolecules* **2007,** 8, (11), 3557-3567.

30. Li, Y.; Tang, Y.; Narain, R.; Lewis, A. L.; Armes, S. P. *Langmuir* **2005,** 21, (22), 9946-9954.

31. Limer, A.; Haddleton, D. M. *Macromolecules* **2006,** 39, (4), 1353-1358.

32. Knoop, R. J. I.; de Geus, M.; Habraken, G. J. M.; Koning, C. E.; Menzel, H.; Heise, A. *Macromolecules* **2010,** 43, (9), 4126-4132.

33. Knoop, R. J. I.; Habraken, G. J. M.; Gogibus, N.; Steig, S.; Menzel, H.; Koning, C. E.; Heise, A. *Journal of Polymer Science Part A: Polymer Chemistry* **2008,** 46, (9), 3068-3077.

34. Bai, Y.; Lu, H.; Ponnusamy, E.; Cheng, J. *Chemical Communications* **2011,** 47, (38), 10830-10832.

35. Lu, H.; Wang, J.; Lin, Y.; Cheng, J. *Journal of the American Chemical Society* **2009,** 131, (38), 13582-13583.

36. Barner, L.; Davis, T. P.; Stenzel, M. H.; Barner-Kowollik, C. *Macromolecular Rapid Communications* **2007,** 28, (5), 539-559.

37. Benaglia, M.; Chiefari, J.; Chong, Y. K.; Moad, G.; Rizzardo, E.; Thang, S. H. *Journal of the American Chemical Society* **2009,** 131, (20), 6914-6915.

38. Moad, G.; Chong, Y. K.; Postma, A.; Rizzardo, E.; Thang, S. H. *Polymer* **2005,** 46, (19), 8458-8468.

39. Moad, G.; Rizzardo, E.; Thang, S. H. *Australian Journal of Chemistry* **2012,** 65, (8), 985-1076.

40. Perrier, S.; Takolpuckdee, P. *Journal of Polymer Science Part A: Polymer Chemistry* **2005,** 43, (22), 5347-5393.

41. Zhang, X.; Oddon, M.; Giani, O.; Monge, S.; Robin, J.-J. *Macromolecules* **2010,** 43, (6), 2654-2656.

42. Deng, L.; Shi, K.; Zhang, Y.; Wang, H.; Zeng, J.; Guo, X.; Du, Z.; Zhang, B. *Journal of Colloid and Interface Science* **2008,** 323, (1), 169-175.

43. Habraken, G. J. M.; Koning, C. E.; Heuts, J. P. A.; Heise, A. *Chem. Commun. (Cambridge, U. K.)* **2009**, (24), 3612-3614.

44. Postma, A.; Davis, T. P.; Li, G.; Moad, G.; O'Shea, M. S. *Macromolecules* **2006,** 39, (16), 5307-5318.

45. Yip, J.; Duhamel, J.; Qiu, X. P.; Winnik, F. o. M. *Canadian Journal of Chemistry* **2011,** 89, (2), 163-172.

46. Deming, T. J. *Nature* **1997,** 390, (6658), 386-389.

47. Boyer, C.; Granville, A.; Davis, T. P.; Bulmus, V. *Journal of Polymer Science Part A: Polymer Chemistry* **2009,** 47, (15), 3773-3794.

48. Willcock, H.; O'Reilly, R. K. *Polymer Chemistry* **2010,** 1, (2), 149-157.

49. Xu, J.; He, J.; Fan, D.; Wang, X.; Yang, Y. *Macromolecules* **2006,** 39, (25), 8616-8624.

50. Habraken, G. J. M.; Wilsens, K. H. R. M.; Koning, C. E.; Heise, A. *Polymer Chemistry* **2011,** 2, (6), 1322-1330.

Chapter 3

Fluorescent latex nanoparticles with selective binding and imaging properties using amphiphilic glycosylated polypeptide surfactants.

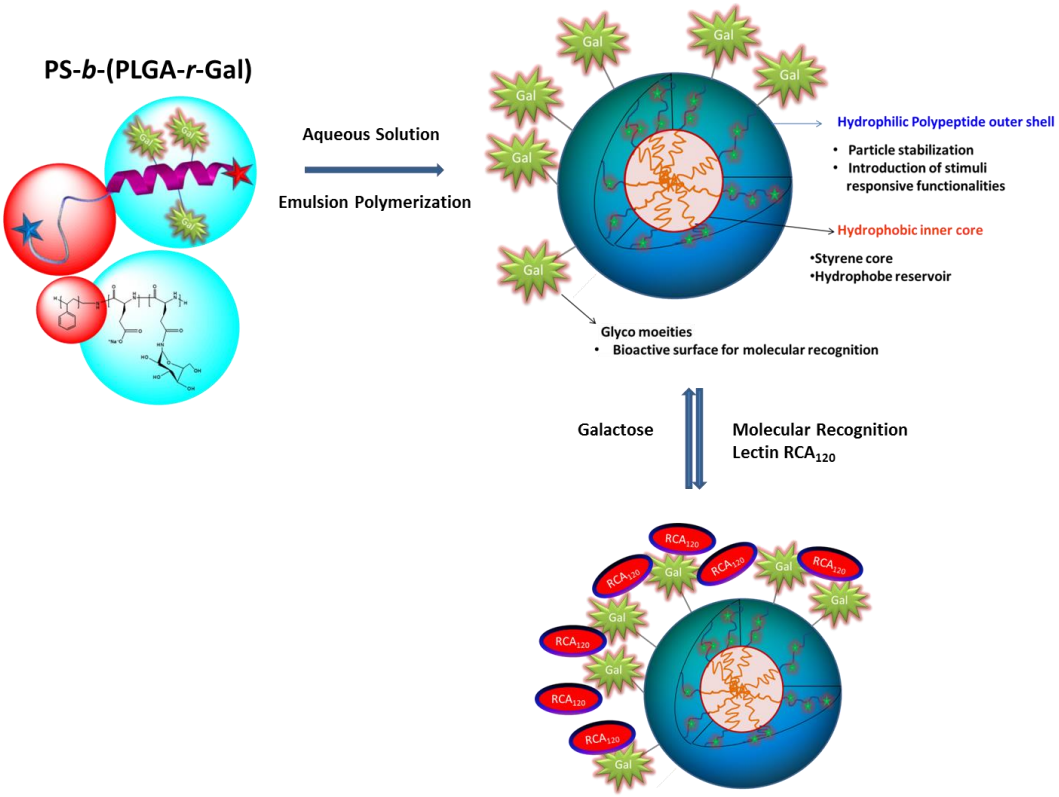

This work was published in the journal Macromolecules:

Jacobs, J.; Byrne, A.; Gathergood, N.; Keyes, T. E.; Heuts, J. P. A.; Heise, A., Facile Synthesis of Fluorescent Latex Nanoparticles with Selective Binding Properties Using Amphiphilic Glycosylated Polypeptide Surfactants. *Macromolecules* **2014,** 47, (21), 7303-7310.

3.1 Abstract

Block copolymers comprising a poly(styrene) and a poly(L-lysine) or poly(L-glutamic acid) block, respectively, were obtained by sequential Reversible Addition–Fragmentation chain Transfer (RAFT) and N-carboxyanhydride (NCA) polymerization. Subsequent partial glycosylation of the poly(L-glutamic acid) block with D-galactosamine (GA) and the poly(L-lysine) block with lactobionic acid (LA) yielded block copolymers with a degree of glycosylation of 50 % and 35 %, respectively, in the poly(amino acid) block. These amphiphilic block copolymers were successfully employed as macromolecular surfactants in the emulsion polymerization of styrene to produce uniform 100-150 nm size nanoparticles with a poly(styrene) core and galactose containing poly(L-amino acid) periphery. Introduction of fluorescence was achieved by incorporation of Nile Red during latex formation and reaction of remaining lysine functionalities on the nanoparticle periphery with fluorescein isothiocyanate (FITC). The availability of the galactose units at the nanoparticles surface for selective binding was demonstrated by lectin binding experiments and binding to Chinese hamster ovary (CHO) cells. Confocal images of live CHO cells following incubation with fluorescent glycosylated nanoparticles confirmed that the nanoparticles bound strongly to the cell surface and could only be removed by addition of free lactobionic acid highlighting selective binding of the nanoparticles on the cell surface. This approach provides a straightforward route to highly fluorescent nanoparticles with selective binding properties for imaging applications avoiding particle post-modification.

3.2 Introduction

The interest in advanced nanoparticles has significantly increased recently with the technological demands from emerging applications in biomedical devices. In particular in the area of diagnostics, functional nanoparticles with high contrast imaging capabilities combined with highly specific targeting properties towards clinically relevant targets are sought.[1-4] . Inorganic nanoparticles are well documented for these tasks where some examples include iron oxide nanoparticles (IONPs) as a contrast-enhancing agent of magnetic resonance imaging (MRI). The large surface area of IONPs are ideal for carrying drugs and genes, however, surface modification is necessary for binding enhancement as well as for effective stabilization to prevent aggregation.[5-7] Fluorescent silica nanoparticles (FSNPs) are another example of inorganic optical probes whereby silica NPs are loaded with a fluorescent dye as probes for sensitive imaging of, for example, cancer cells.[8-10]

Polymer based NPs offer a highly promising alternative to inorganic nanoparticles for diagnostic applications.[4, 11] Most reported examples of polymer NPs rely on the self-assembly of amphiphilic block copolymers into various three dimensional nanostructures such as micelles, vesicles, rods and worms.[12-14] One drawback of these structures is their dynamic nature, which could cause stability issues under application conditions. Moreover, protocols of self-assembly and functionalisation often require multiple steps, which could compromise scalability of the materials. Solid polymer NPs are a promising alternative as they combine characteristics of solid inorganic NPs with the synthetic variability of polymers. Poly(lactic-co-glycolic acid)s (PLGA) have already been utilized for NPs owing to their excellent biocompatibility and biodegradability.[15] As the core material, PLGA has been combined with poly(ethylene glycol) (PEG) for several systems where NPs are typically prepared *via* nanoprecipitation or emulsification.[16, 17] Furthermore, non-degradable fluorescent polystyrene (PS) and poly(methyl methacrylate) NPs have also been investigated successfully offering higher long-term stability for *in vitro* and *in vivo* cell imaging.[18, 19] In a specific example Landfester reported the synthesis of functional fluorescent polystyrene NPs by miniemulsion polymerization incorporating functional acrylates for colloidal stability and as potential handles for post-modification. Cell uptake was visualized by fluorescent spectroscopy.[19]

A critical aspect is in the design to produce NPs tailored to its final application. Size, shape and surface properties are parameters that need to be tuned as these are critical for *in vitro* and *in vivo* performance.[20, 21] Furthermore, diagnostic agents need to be specific in the

detection of compromised cells and for this reason active targeting concepts are desirable. This involves the conjugation of targeting ligands to the exposed surface of NPs, which interact with receptors expressed on the targeted cells. Targeting ligands, which have been successfully utilized thus far include antibodies, peptides, aptamers and carbohydrates (glycans).[22-26]

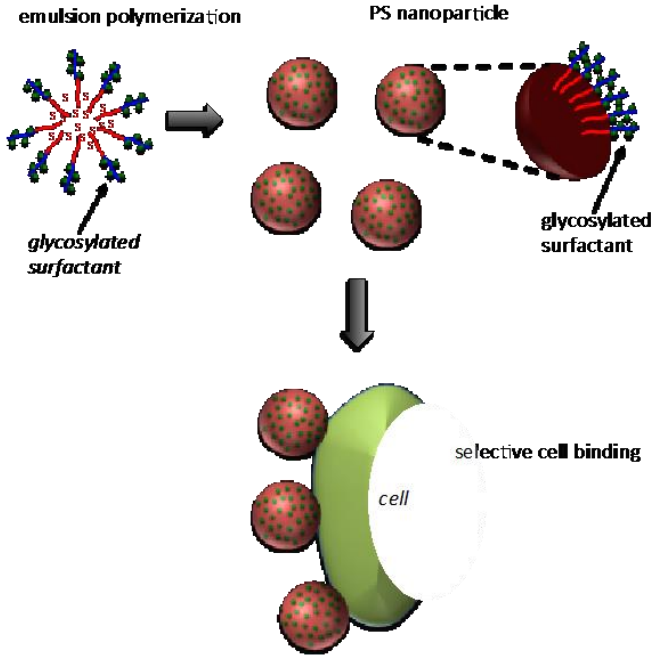

Figure 3. 1 Schematic route for the synthesis of glycosylated poly(styrene) nanoparticles with selective binding properties.

The latter has come to the forefront of the scientific community in the past number of years with the discovery that glycans regulate numerous biological processes such as cell communication, selective binding of other biological species among others, which makes glycochemistry an attractive tool in the design of materials for selective targeting.[27-29] In particular complex (surface) glycoproteins are involved in biological binding events and this has inspired research into the development of simplistic synthetic glycoprotein mimics[30-37] Of particular attraction are glycopolypeptides derived from the polymerization of amino acid N-carboxyanhydrides (NCA) due to their ready availability and structural similarity to natural proteins.[38-48] The successful formulation of these glycopolypeptides into bioactive nanomaterials has been demonstrated albeit mostly by self-assembly.[49-51]

In this work we devise a novel one-step strategy to prepare glycosylated fluorescent polystyrene nanoparticles in an emulsion using glycosylated polypeptide-PS conjugates as

macromolecular surfactants. Its attractiveness lies in the fact that the glycans play a large part in stabilizing the polymer latex while at the same time are presented at the final nanoparticle surface available for selective binding (Figure 3.1). This approach overcomes challenges associated with the bioconjugation of polymer particles by post-modification or surface grafting. The obtained PS NPs have a glycosylated periphery, which provides molecular recognition capabilities demonstrated by the specific binding to lectin and Chinese hamster ovary (CHO) cells.

3.3 Experimental Procedures

3.3.1 Materials.

All chemicals were purchased from Sigma-Aldrich and used as received unless otherwise noted. γ-Benzyl-L-glutamate and ε-benzyloxycarbonyl-L-Lysine were supplied by Bachem. Anhydrous dimethyl formamide (DMF), chloroform, ethyl acetate and methanol were used directly from the bottle under an inert and dry atmosphere. γ-Benzyl-L-glutamate (BLG) and ε-benzyloxycarbonyl-L-Lysine (ZLL) NCA was synthesized following a literature procedure.[52] Butyl phthalimidomethyl trithiocarbonate (RAFT CTA 1) and the PS homopolymer (PS TTC) were synthesized according to a literature procedure by Moad *et. al.*[53]

3.3.2 Polystyrene-trithiocarbonate (PS-TTC) cleavage using Bu_3SnH.

PS-TTC (1) (2.5 g, 0.46 mmol) was dissolved in THF (15 mL) and added to a 50 mL round-bottomed flask equipped with a magnetic stirring bar. The mixture was degassed with nitrogen for 30 minutes before the addition of Bu_3SnH (1.03 mL, 3.8 mmol) and AIBN (0.19 g, 1.2 mmol). The reaction was left to stir for 3 hours at 60 ºC. The solution was purified by precipitation into a 400 mL 80/20 mixture of methanol/n-heptane under vigorous stirring. This was repeated and washed twice with the same mixture to remove any excess Bu_3SnH. The product was identified via ^1H NMR spectroscopy ($CDCl_3$). Isolated yield: 2.1 g.

3.3.3 Phthalimide deprotection to produce PS-NH2 (2).

Phthalimide end-functional polymer (1.7 g, 0.31 mmol) was dissolved in 10 mL DMF and added to a 50 mL Schlenk tube equipped with a magnetic stirring bar. The reaction mixture was placed in a preheated oil bath of 70 °C and hydrazine monohydrate (0.28 mL, 20 molar equivalents Hydrazine) added. The reaction mixture was stirred for 3 hours. The solution was purified by precipitation into 300 mL methanol and subsequently washed twice with

methanol. The product was dried under high vacuum at 40 ºC and isolated as a white powder. The product was identified by ^{1}H NMR spectroscopy ($CDCl_3$) (see Fig 3.2). M_w: 4800 g/mol, Đ = 1.05, dn/dc = 0.159 mL/g. Isolated yield: 1.5 g.

3.3.4. General procedure for the synthesis of hybrid block copolymers via NCA ROP.

Chain extension of the PS-NH_2 macroinitiator was done according to a method described in previous work.[54] PS_{45}-*b*-$PBLG_{66}$: M_w: 18200 g/mol, Đ = 1.06, dn/dc = 0.192 mL/g (^{1}H-NMR spectrum Figure 3.5, SEC Figure 3.4). PS_{45}-*b*-$PZLL_{73}$: M_w: 22300 g/mol, Đ = 1.07, dn/dc = 0.129 mL/g (^{1}H-NMR spectrum Figure 3.5, SEC Figure 3.3).

3.3.5 Polypeptide deprotection.

A general procedure was used for the deprotection of both the PBLG and PZLL pendant groups: PS_{45}-*b*-$PBLG_{66}$ (1.35 g, 7.4 x 10^{-5} mmol) was dissolved in trifluoroacetic acid (12 mL) and a minimal amount of THF to improve solubility. A solution of HBr (33 wt. % in acetic acid) (3 mL, 15 mmol, 3-fold excess with respect to γ-benzyl-L-glutamate repeat units)) was added slowly to the reaction at 0 ºC. After 4 h, the solution was added to 200 mL diethyl ether and the precipitate washed several times with diethyl ether. The subsequent product was redissolved in a 0.5M NaOH solution (aqua) to obtain the polymer in the sodium salt form. The sodium salt polymer was dialyzed against double deionized (DDI) water using Spectra/Por dialysis membranes (MWCO, 3.5 kDa) for 72 h at room temperature. The product was lyophilized and isolated as a white powder. Yield: 0.80 g, 6.1 x 10^{-5} mmol, 82 % yield.

3.3.6 Glycosylation

3.3.6.1 PS_{45}-*b*-$(PLGA_{31}$-*r*-$GA_{35})_{66}$ (5).

Glycosylation of the carboxylic acid moieties was achieved according to a modified literature procedure.[44] PS_{45}-*b*-$PLGA_{66}$ (0.75 g, 5.7 x 10^{-5} mol) and galactosamine hydrochloride (0.43 g, 2.0 mmol, 0.5 eq w.r.t. the glutamate repeating units) was dissolved in deionized water (12 mL) and stirred for 15 min. 4-(4,6-Dimethoxy-1,3,5-triazin-2-yl)-4-methylmorpholinium chloride (DMT-MM) (0.55 g, 2.0 mmol, 1 eq to Galactosamine HCl) was dissolved in 5 mL of deionized water and added to the reaction mixture. After stirring for 24 h at room temperature the reaction mixture was dialyzed against DDI water using Spectra/Por dialysis membranes (MWCO, 3.5 kDa) for 72 h at room temperature. The polymer was subsequently

lyophilized and isolated as a white powder. ^{1}H NMR spectrum see Figure 3.6. Isolated yield: 1.1 g.

3.3.6.2 PS_{45}-*b*-$(PLL_{47}$-*r*-$LA_{28})_{75}$ (6).

A general procedure for 1-Ethyl-3-[3-dimethylaminopropyl]carbodiimide hydrochloride (EDC)/*N*-hydroxysuccinimide (NHS) coupling was employed to attach lactobionic acid to the lysine residues of the amphiphile. Lactobionic acid (0.64 g, 1.8 mmol, 0.35 eq w.r.t the lysine repeat units), EDC (0.45 g, 2.3 mmol, 1.3 equiv.) and NHS (0.43 g, 3.7 mmol, 2 equiv.) were dissolved in 2 mL 10 mM MES buffer (pH 4.7) and stirred for 20 minutes, then PS_{45}-*b*-PLL_{73} (1 g, 7.2 x 10^{-5} mol in 8 mL of DDI water) added. The reaction mixture was stirred overnight. The resulting product was purified *via* dialysis against DDI water using Spectra/Por dialysis membranes (MWCO, 3.5 kDa) for 72 h at room temperature. The product was subsequently lyophilized and isolated as a white powder. ^{1}H NMR spectroscopy see Figure 3.7. Isolated yield: 1.4 g.

3.3.7 Preparation of polystyrene nanoparticles *via* emulsion polymerization.

Batch emulsion polymerizations of styrene were all carried in a three-neck reactor equipped with a reflux condenser, nitrogen inlet and mechanical stirrer. A typical reaction proceeded as follows: PS_{45}-*b*-$(PLGA_{31}$-*r*-$GA_{35})$ (0.25 g) was added to the reactor under an inert atmosphere and dissolved in 34 mL of distilled water under stirring at 70 ºC. 4 mL of a sodium carbonate buffer solution (80 mg) was deoxygenated and injected into the reactor. The styrene monomer (4.80 g) was deoxygenated separately for 20 min by bubbling nitrogen through it and injected into the reactor. A deoxygenated initiator solution (50 mg of potassium persulfate in 2 mL of water) was injected to start the polymerization. The nitrogen flow was maintained throughout the reaction. Samples were withdrawn at regular times to determine the conversion. A small amount of hydroquinone was added to these aliquots to quench the radical polymerization where the monomer conversion was then determined *via* gravimetry.

3.3.8 Nile Red encapsulated NPs.

Nile Red (NR) was encapsulated in the polystyrene nanoparticles by dissolving NR (0.1 wt% with regard to monomer) in the styrene monomer and subsequently forming the particles via an emulsion polymerization (as previously described).

3.3.9 PS_{45}-*b*-(PLL_{45}-*r*-LA_{26}-*r*-$FITC_2$).

Fluorescein isothiocyanate (FITC) was attached to the lysine residues at 1.5 molar equivalents per chain. FITC was dissolved in DMSO and added to PS_{45}-*b*-$(PLL_{47}$-*r*-$LA_{28})_{75}$ solubilized in PBS pH 7.2. The resulting polymer was purified *via* dialysis against DDI water using Spectra/Por dialysis membranes (MWCO, 3.5 kDa) for 72 h and isolated as an orange powder.

3.3.10 Lectin binding.

The selective lectin-carbohydrate binding between the galactose moieties and RCA_{120} was done on a qualitative basis. After particle synthesis, the polystyrene latex was diluted with PBS buffer (pH 7.2) and a solution of the RCA_{120} lectin (1mg/mL) was added until the system collapsed. The reversibility of the system was indicated *via* the addition of dissolved lactobionic acid in PBS buffer.

3.3.11 Cell binding.

Chinese hamster ovary (CHO) cells were seeded at 2 x 10^5 in 2 mL media on a 35 mm glass bottom culture dish for 24 h at 37ºC at 5% CO_2. The media was removed and cells were washed with PBS (supplemented with 1.1mM $MgCl_2$ and 0.9 mM $CaCl_2$). The particles were added to the cells in phenol red-free media (1:4 dilution) and were incubated for 2 h at 37 ºC at 5% CO_2 in the dark. Cells were washed with 1mM lactobionic acid in PBS for 15 minutes at 37 ºC to assess displacement of any bound particles.

3.3.12 Methods.

Nuclear magnetic resonance (NMR) spectra were recorded on a Bruker Avance 400 (400 MHz) in DMSO-d6 and CDCl3 as solvents. All chemical shifts are reported in parts per million (ppm) with tetramethylsilane (TMS) as an internal reference. Size Exclusion Chromatography (SEC) was performed on an Agilent 1200 system in conjunction with two PSS GRAM analytical (8 x 300 and 8 x 100, 10 μ) columns, a Wyatt Dawn Heleos 8 multi angle light scattering (MALS) detector and Wyatt Optilab rEX differential refractive index (DRI) detector with a 658 nm light source. The eluent was DMF containing 0.1 M LiBr at a flow rate of 1 mL/min. The column temperature was set to 40 °C with the MALS detector at 35 °C and the DRI detector at 40 °C. Molar masses and dispersities were calculated from the MALS signal by the Astra software (Wyatt) using the refractive index increment (dn/dc) as determined experimentally. The specific refractive index increments for the copolymers were

calculated relative to the ratio of the homopolymer. The dn/dc values used for PS, PZLL and PBLG were 0.159, 0.120 and 0.118 mL/g respectively. All samples for SEC analysis were filtered through a 0.45 mm PTFE filter (13 mm, PP housing, Whatman) prior to injection. Dynamic light scattering (DLS) experiments were performed at 25 °C on a Malvern NanoZS (Malvern Instruments, Malvern UK) which uses a detection angle of 173°, and a 3 mW He-Ne laser operating at a wavelength of 633 nm. The hydrodynamic diameter and polydispersity index (PDI) values were obtained using cumulated analysis. Field emission scanning electron microscopy (FESEM) images were obtained on a Hitachi S5500 SEM. Cells were imaged using a Zeiss LSM510 Meta confocal microscope using a 63x oil immersion objective lens and heated stage set to 37 ºC. The particles were excited using 514 nm laser, and the emission collected using a long pass 560 nm filter set.

3.4 Results and Discussion

3.4.1 Synthesis of glycosylated amphiphilic block copolymers.

The synthesis of polypeptide-PS block copolymers was achieved following a strategy previously reported from our group by the macroinitiation of NCA ring-opening polymerization from amine-functional PS 2 obtained by reversible addition–fragmentation chain transfer (RAFT) polymerization (Scheme 3.1).[54]

Briefly, a phthalimide protected amine is incorporated in a trithiocarbonate RAFT chain transfer agent (CTA, 1) which allows for effective control over the polymerization of styrenics. Tributyltin hydride in the presence of AIBN was used successfully to quantitatively remove the trithiocarbonate group.[54-56] Quantitative deprotection of the phthalimide protecting group followed on treatment with excess hydrazine monohydrate (Scheme 3.1, Figure 3.2) resulting in the PS-NH_2 macroinitiator 2 (4700 g/mol, Đ = 1.1).

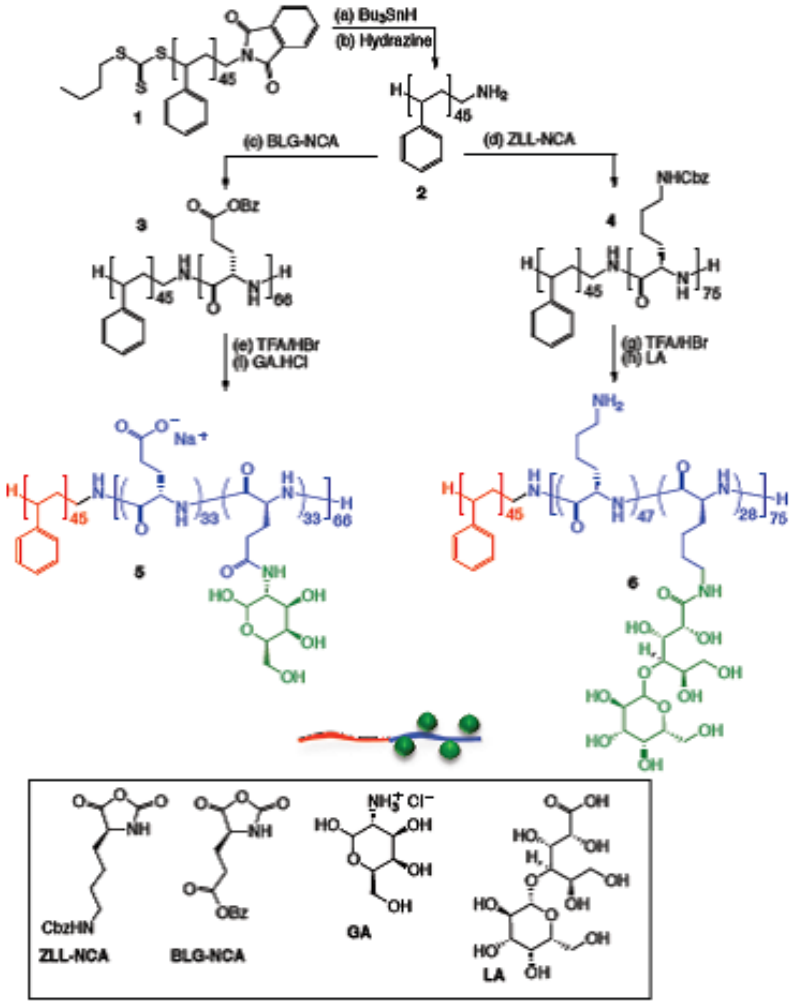

Scheme 3. 1 Synthesis of glycosylated block copolymers[a]

[a]Reagents and conditions: (a) Bu_3SnH (8 eq), AIBN (3 eq) THF, 60 °C; (b) NH_2NH_2 (20 eq), DMF, 70 °C; (c) BLG-NCA (70 $[M]_0/[MI]_0$), DMF, HV, 0 °C; (d) ZLL-NCA (70 $[M]_0/[MI]_0$), DMF, HV, 0 °C; (e) HBr (33 wt. % in AcOH), TFA; 0.5 M NaOH (aq); (f) DMT-MM, DDI; (g) HBr (33 wt. % in AcOH), TFA; (h) LA, EDC/NHS, pH 4.7, 10 mM MES buffer; DDI. MI = macroinitiator, HV = high vacuum, DDI = distilled deionized water.

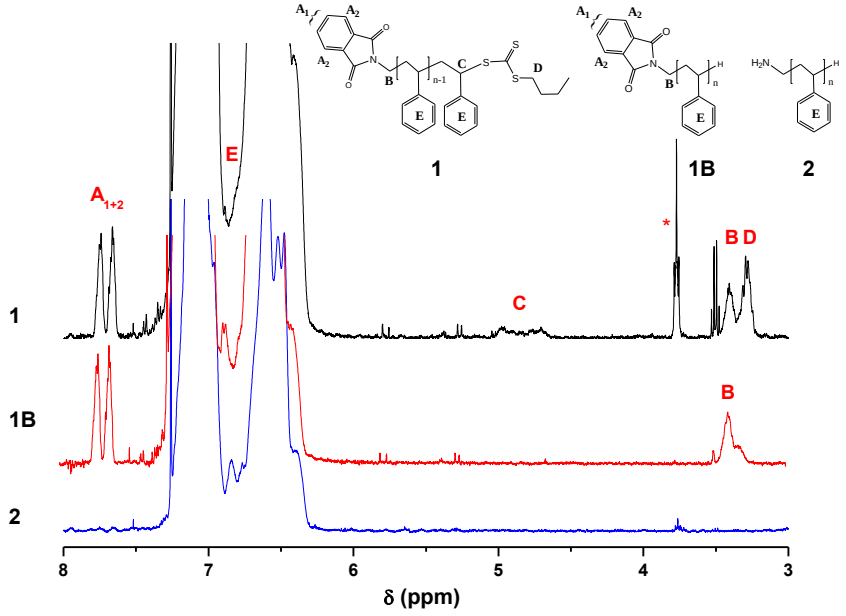

Figure 3. 2 ^{1}H-NMR spectra indicating selective deprotection of the α- and ω-end-functional PS homopolymer (1). Cleavage of the trithiocarbonyl moeity (1B) with tributyltin hydride and subsequent hydrazinolysis of the pthtalimide protecting group leads to the amine end-functional PS homopolymer (2).

The subsequent NCA polymerizations were run at 0 °C under high vacuum to combine high polymerization control with efficient removal of the reaction by-product CO_2 to accelerate the polymerization rate.[57, 58] The PS-NH_2 macroinitiator was chain extended with ε-benzyloxycarbonyl-L-lysine (ZLL) (Figure 3.3) and γ-benzyl-L-glutamate (BLG) NCAs where chain lengths of 70 repeat units were targeted (Scheme 3.1). Figure 3.4 shows the size exclusion chromatography (SEC) traces of the PS_{45}-*b*-$PBLG_{66}$ (**3**) and the PS macroinitiator (**2**). A shift in the elution time upon macroinitiation confirms the formation of the block copolymer with no residual homopolymer present highlighting efficient initiation.

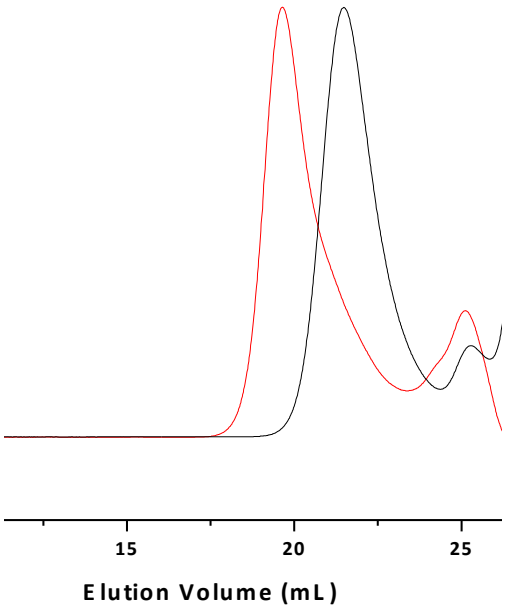

Figure 3. 3 SEC traces of PS_{45}-NH_2 (2, black) and PS_{45}-*b*-$PZLL_{73}$ (4, red).

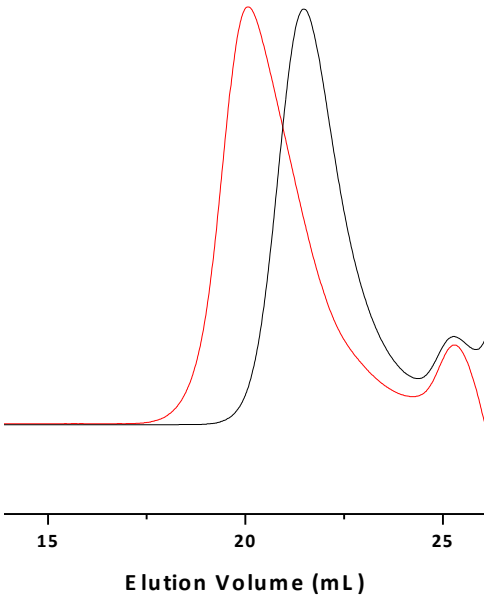

Figure 3. 4 SEC traces of PS_{45}-NH_2 macroinitiator (2, black) and PS_{45}-*b*-$PBLG_{66}$ (3, red).

Table 3. 1 Characteristics of poly(styrene) macro-initiator (MI) and block copolymers.

Polymer[(a)]	**$[NCA]_0/[MI]_0$**	**M_w**[(b)] **(g/mol)**	**Đ**
PS_{45}-NH_2 (MI) (2)	**-**	**4800**	**1.1**
PS_{45}-*b*-$PZLL_{75}$ (4)	**70**	**22 300**	**1.1**
PS_{45}-*b*-$PBLG_{66}$ (3)	**70**	**18 200**	**1.1**

(a) Degree of polymerization was determined via ^{1}H-NMR spectroscopy by calculating the ratio of styrene to polypeptide repeat units using the methylene protons of the polypeptide protecting group (5.0 ppm) to that of the combined signals of the aromatic protons of styrene and the polypeptide protecting group (6.2 – 7.5 ppm) (Figure S3). (b) Values obtained from multi angle light scattering (MALS) detection.

Both block copolymers were further characterized using ^{1}H-NMR, where comparison of the polypeptide protecting group signals with that of the characteristic aromatic polystyrene signals allowed determining the respective degrees of polymerization as summarized in Table 3.1 (see Figure 3.5). For both block copolymers there is a good agreement between the monomer to macroinitiator feed ratio (70) and the calculated degree of polymerization (75 and 66, respectively).

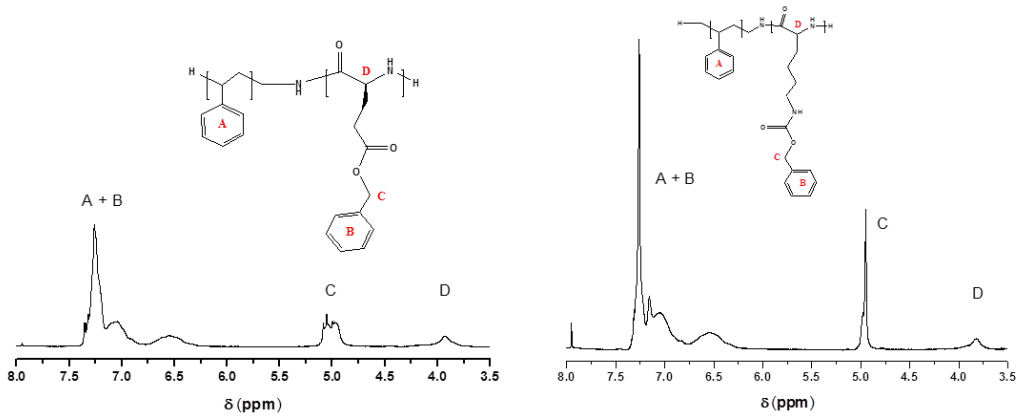

Figure 3. 5 ^{1}H-NMR spectra (TFA-d, 400 MHz) of PS_{45}-*b*-$PZLL_{75}$ (4) and PS_{45}-*b*-$PBLG_{66}$ (3)

After quantitative deprotection of the polypeptide block, galactose was covalently attached to the amino acid units via two different strategies targeting 35 % and 50 % glycosolation (Scheme 3.1) depending on the size of the sugar. A procedure described by Menzel et. al. was employed to attach D-galactosamine (GA) to the carboxylic acid moieties of the PS_{45}-*b*-$PLGA_{66}$ to prepare PS_{45}-*b*-$(PLGA_{31}$-r-$GA_{35})_{66}$ (5) (Figure 3.6).[44] 4-(4,6-Dimethoxy-1,3,5-triazin-2-yl)-4-methylmorpholinium chloride (DMT-MM) is a mild and efficient amide-coupling agent, which was used to facilitate the reaction. DMT-MM allows for a high degree of substitution while it has been shown to be a very versatile component in preparing polyglutamic acid derivatives with orthogonal reactive sites.[59]

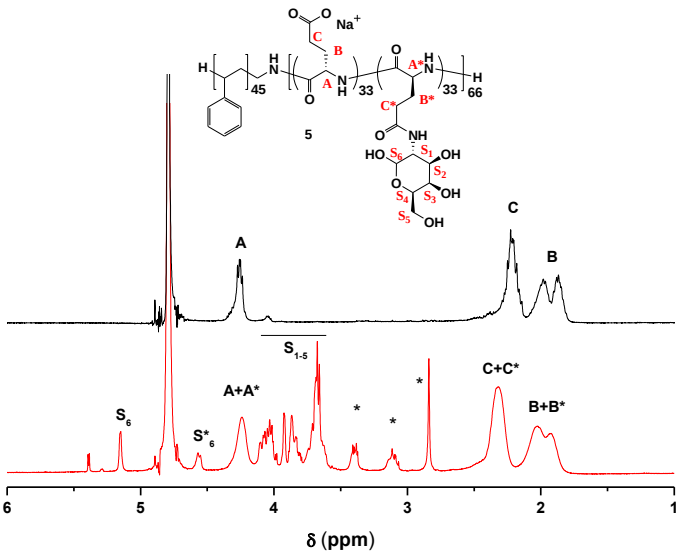

Figure 3. 6 ^{1}H-NMR spectra (D_2O, 400 MHz) of PS_{45}-*b*-$PLGA_{66}$ (3, top) and PS_{45}-*b*-$(PLGA_{31}$-*r*-$GA_{35})_{66}$ (5, bottom). The * signals are due to the residual DMT-MM.

For PS_{45}-*b*-PLL_{75}, EDC/NHS coupling chemistry was used to attach lactobionic acid (LA, 4-O-β-galactopyranosyl-D-gluconic acid, 7) to the lysine residues typically targeting 35% glycosylation of the PLL block. LA is a readily available disaccharide with a galactose moiety and a cost effective alternative to the functional sugars typically incorporated in other glycosylation strategies.

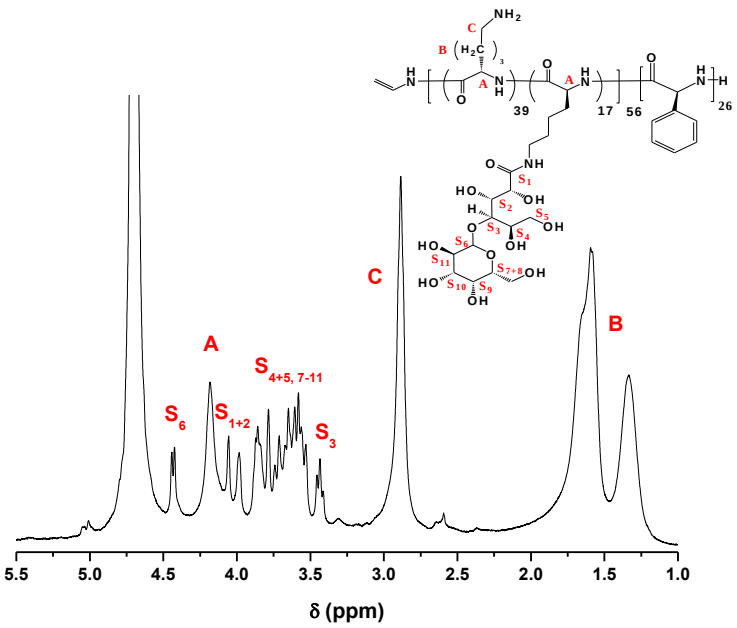

Figure 3. 7 ^{1}H-NMR spectra (in D_2O) of PS_{45}-*b*-PLL_{75} (top) and PS_{45}-*b*-(PLL_{46}-*r*-LA_{28}) (6) (bottom).

Figure 3.7 shows the ^{1}H-NMR spectra of the PS_{45}-*b*-(PLL_{47}-*r*-LA_{28})$_{75}$ copolymer (**6**) and the corresponding precursor block copolymer. The success of the glycosylation is evident from the presence of characteristic LA signals between 3.5 and 4.6 ppm.

3.4.2 Emulsion polymerization to obtain polystyrene nanoparticles

Glycosylation of the polypeptide block permitted to impart certain traits necessary for the effective stabilization of the targeted polymer NPs. It was envisaged that by attaching highly water-soluble carbohydrate moieties the electrolytic nature of the polypeptide would decrease. At the same time, the effective range of macromolecular stabilization during the synthesis of the hydrophobic latex particles was expected to increase. To the best of our knowledge glycosylated polypeptide hybrid block copolymers have not yet been investigated in emulsion polymerization.

The emulsion polymerization of styrene stabilized by either PS_{45}-*b*-($PLGA_{31}$-*r*-GA_{35})$_{66}$ (**5**) or PS_{45}-*b*-(PLL_{47}-*r*-LA_{28})$_{75}$ (**6**) was carried out in order to evaluate the ability of the hybrid conjugates to form stable polystyrene nanoparticles with a brush-like periphery. All reactions were performed using potassium persulfate as a water-soluble initiator at 70 °C and a concentration of 1 wt% with respect to monomer (1 pphm). Monomer contents of 12 and 15 wt%, and block copolymer contents of 2 and 5 pphm were used for both block copolymers. In

all but one experiment high styrene conversion and stable particle dispersion were obtained. Only in the case of using a low concentration of PS_{45}-*b*-$(PLL_{47}$-*r*-$LA_{28})_{75}$ (i.e., 2 pphm) a stable latex could not obtain, which implies that PS_{45}-*b*-$(PLGA_{31}$-*r*-$GA_{35})_{66}$ has better stabilizing properties than PS_{45}-*b*-$(PLL_{47}$-*r*-$LA_{28})_{75}$. Conversion-time curves for the PS_{45}-*b*-$(PLGA_{31}$-*r*-$GA_{35})_{66}$-stabilized emulsion polymerizations are shown in Figure 3.8. All three curves show the absence of a nucleation period typical for a conventional *ab initio* emulsion polymerization. This behavior, which we observed before, suggests that the block copolymer micelles present at the start of the reaction act as a seed and are converted into particles.[60-63]

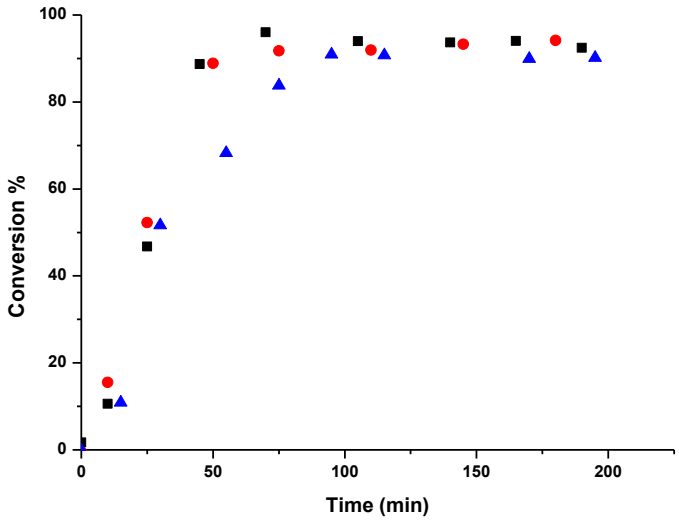

Figure 3. 8 Evolution of monomer conversion with time for the emulsion polymerization of styrene using KPS as initiator (1 wt%), a monomer content of 12 wt% and surfactant content of 5 wt% (■), a monomer content of 15 wt% and surfactant content of 5 wt% (●),a monomer content of 15 wt% and surfactant content of 2 wt% (▲) with PS_{45}-*b*-$(PLGA_{31}$-*r*-$Gal_{35})$ as stabilizer.

Furthermore it is clear from this Figure that higher block copolymer concentrations lead to faster rates. This observation is consistent with the smaller particle diameters as determined using dynamic light scattering (Table 3.2) (Figure 3.9) for the higher block copolymer concentrations; smaller diameters imply larger particle numbers, which in turn lead to higher polymerization rates. The increase in monomer content while maintaining a constant surfactant/monomer ratio does not significantly affect either particle size (Table 3.2) or the polymerization rate (Figure 3.8), implying that in both cases very similar particles are produced, i.e., particles of the same size and same glycopolymer periphery. These results, in

combination with the narrow particle size distributions (PDI < 0.02, see Table 3.2), clearly demonstrate the high amount of control over particle synthesis with these block copolymer surfactants.

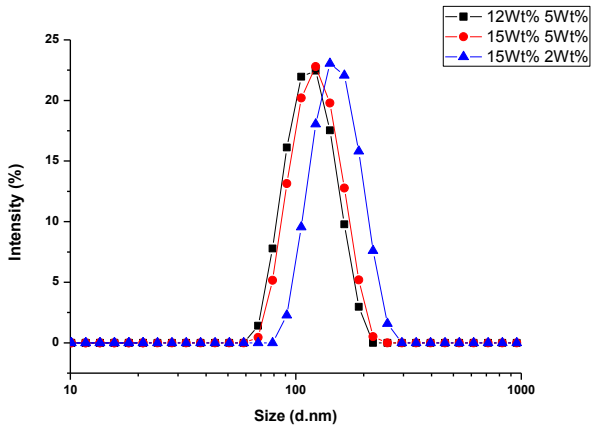

Figure 3. 9 Intensity particle size distribution (DLS) for the latex particles prepared with a monomer content of 12 wt% and surfactant content of 5 wt% (■), a monomer content of 15 wt% and surfactant content of 5 wt% (●),a monomer content of 15 wt% and surfactant content of 2 wt% (▲) with PS45-b-(PLGA31-r-GA35)66 as stabilizer.

In the case of PS_{45}-*b*-$(PLL_{47}$-*r*-$LA_{28})_{75}$ **6** as the macromolecular surfactant, it was found that the stabilization was not as effective as for PS_{45}-*b*-$(PLGA_{31}$-*r*-$GA_{35})_{66}$ **5**; only at block copolymer contents of 5 pphm stable dispersions were obtained. Interestingly, at block copolymer contents of 5 pphm both block copolymers seem to be able to stabilize very similar particle surface areas as can be concluded from the similar particle diameters listed in Table 3.2 (Also see Figure 3.10 and Figure 3.11).

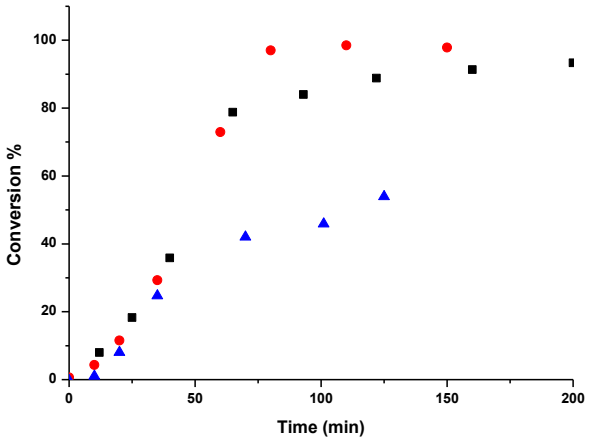

Figure 3. 10 Evolution of monomer conversion with time for the emulsion polymerization of styrene using KPS as initiator (1 wt%), a monomer content of 12 wt% and surfactant content of 5 wt% (●), a monomer content of 15 wt% and surfactant content of 5 wt% (■),a monomer content of 15 wt% and surfactant content of 2 wt% (▲) with PS_{45}-*b*-(PLL_{47}-*r*-LA_{28})$_{75}$ as stabilizer.

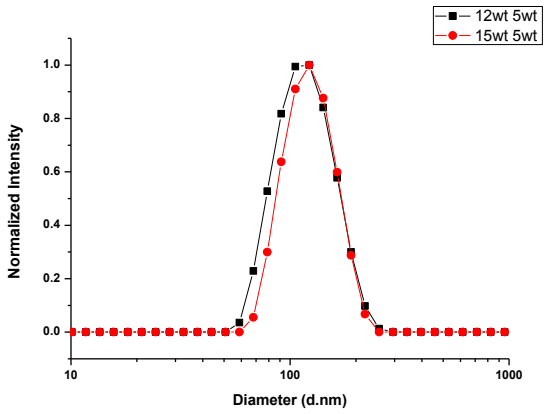

Figure 3. 11 . Intensity particle size distribution (DLS) for the latex particles prepared with a monomer content of 15wt% and surfactant content of 5 wt% (●), a monomer content of 12 wt% and surfactant content of 5 wt% (■) with PS_{45}-*b*-(PLL_{47}-*r*-LA_{28})$_{75}$ as stabilizer.

All particles were further investigated with FE-SEM highlighting the uniformity of the particles, all ranging between in 80 – 90 nm in diameter (Figure 3.9).

Table 3. 2 Results from the emulsion polymerization of styrene using glycosylated block copolymers as surfactants

block copolymer	**Solids content (Wt%)[a]**	**[block copolymer] (pphm)[b]**	**D_z (nm)[c]**	**PDI[d]**
PS_{45}-*b*-($PLGA_{31}$-*g*-Gal_{35})	12	5	114	0.02
PS_{45}-*b*-($PLGA_{31}$-*g*-Gal_{35})	15	5	120	0.02
PS_{45}-*b*-($PLGA_{31}$-*g*-Gal_{35})	15	2	147	0.02
PS_{45}-*b*-(PLL_{47}-*g*-LA_{28})	12	5	111	0.06
PS_{45}-*b*-(PLL_{47}-*g*-LA_{28})	15	5	119	0.04
PS_{45}-*b*-(PLL_{47}-*g*-LA_{28})	15	2	n/a	n/a

[a] solid content = mass polymer/mass dispersion. [b] 1 pphm = 1 g block copolymer/100 g monomer. [c] Z-average particle diameter from Dynamic Light Scatering (DLS). [d] Polydispersity Index of particle size distribution from cumulative DLS analysis.

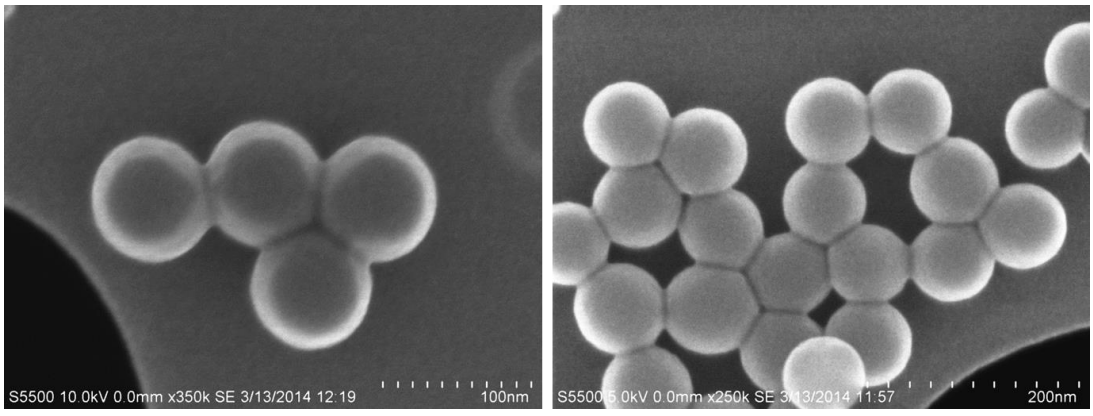

Figure 3. 12 FE-SEM images of polystyrene latex stabilized by PS_{45}-*b*-($PLGA_{31}$-*r*-GA_{35})$_{66}$ (5) with a monomer content of 12 wt% and surfactant content of 5 wt% (Table 3.2).

3.4.3 Biological screening

Various methods are available to prepare functional polystyrene microspheres, where the most common method would arguably be to engineer functional layers on existing microspheres by post-modification.[64, 65] Divinylbenzene (DVB) as well as ethylene glycol

dimethacrylate (EGDMA) are typically incorporated to crosslink the PS particle resulting in free vinyl groups at the surface. Surface modification using thiol–ene chemistry can then be utilized to introduce glyco-functionalities as was demonstrated on microspheres by Alvarez-Paino *et. al*.[66]

The use of functional macromolecular surfactants during an emulsion polymerization of hydrophobic monomer allow for a straightforward strategy to functional polymer NPs. Furthermore, the introduction of fluorescent tags to track the polystyrene particles as they target specific biological entities can readily be achieved. This is demonstrated using two different strategies. In the first instance a highly hydrophobic dye, Nile Red was incorporated during the emulsion polymerization of styrene at 0.1 wt% with regards to the monomer. Figure 3.13A depicts the PS particles stabilized by PS_{45}-*b*-$(PLGA_{31}$-*r*-$GA_{35})_{66}$ in water under UV light. Here the incorporation of NR is evident as well as the effective stabilization due to the glycosylated hydrophilic shell. After the addition of a galactose binding lectin, RCA_{120}, the hydrophilic nature of the carbohydrates are nullified and effectively forces the whole system to collapse upon itself (Figure 3.13B). The effects are however reversible as the addition of excess lactobionic acid and thus competing galactose moieties allow the system to revert to the original stabilized state. The same was observed for the system incorporating PS_{45}-*b*-$(PLL_{47}$-*r*-$LA_{28})_{75}$ (Figure 3.14).

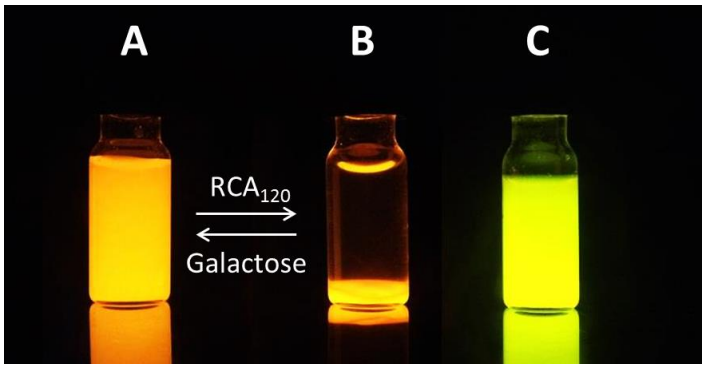

Figure 3. 13 Image of Nile Red encapsulated PS_{45}-*b*-$(PLGA_{31}$-*r*-$GA_{35})$ stabilized PS NPs in water before (A) and after (B) the addition of the lectin RCA_{120}. PS_{45}-*b*-$(PLL_{45}$-*r*-LA_{26}-*r*-$FITC_2)$ is represented by C.

In a second system, the excess lysine residues of PS_{45}-*b*-$(PLL_{47}$-*r*-$LA_{28})_{75}$ was utilized to prepare fluorescein labeled PS particles. The reactivity of fluorescein isothiocyanate (FITC) towards primary amines are well known and thus the synthesis of PS_{45}-*b*-$(PLL_{45}$-*r*-LA_{28}-*r*-$FITC_2)_{75}$ is a facile approach to fluorescent PS particles. Subsequently, PS_{45}-*b*-$(PLL_{45}$-*r*-LA_{28}-*r*-$FITC_2)_{75}$ was used to stabilize the emulsion polymerization of styrene to produce fluorescent glycosylated PS particles (Figure 3.13C).

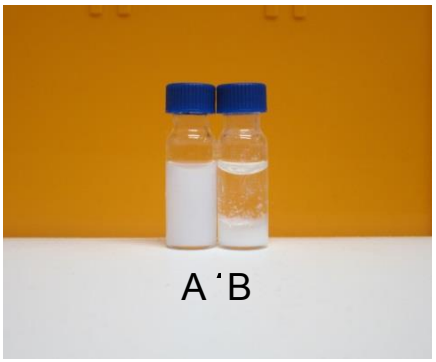

Figure 3. 14 Comparison of PS latex stabilized by PS_{45}-*b*-$(PLL_{47}$-*r*-$LA_{28})_{75}$ before (A) and after (B) the addition of lectin RCA_{120}.

These results demonstrate the feasibility of the proposed approach allowing two methods of labeling, i.e. in the NP core and the periphery by simple chemistry. While this was not further pursuit here, this would allow the introduction of two different labels for imaging. Such an approach is potentially of significant value in fluorescence sensing applications where two probes are used to permit referencing of the transduction signal by an analytically inert probe. Such an approach has been described for dye encapsulation, for example in silicate or polystyrene spheres but the advantage of this approach is that the probes are physically separated between core and shell of the nanoparticle, which can reduce potential probe cross talk.[67]

While lectin binding experiments provide a conceptual proof for selective binding, *in vitro* cellular binding of the nanoparticles was investigated in CHO cells.[67]Carbohydrate receptors such as lectins are prevalent on cell surfaces, and CHO-K1 was used in the present study because this cell line has been demonstrated previously to express relatively large amounts of Galectin 1, which resides at the plasma membrane and can bind to extracellular glycoconjugate ligands.[68, 69] Figure 3.15 shows confocal images of live CHO cells following 2 h incubation with 1:4 PS_{45}-*b*-$(PLGA_{31}$-*r*-$GA_{35})_{66}$ (**5)** nanoparticles in cell media (A and B). It was found that the particles bound strongly to the cell surface, and remained bound after

washing several times with PBS (supplemented with 0.9 mM $CaCl_2$ and 1.1 mM $MgCl_2$). Using confocal imaging, scanning in the Z-direction, it was confirmed that the particles did not permeate the cells.

To confirm surface binding was specific, lactobionic acid containing a galactose moiety was used in order to remove any specifically bound particles on the cell surface. This was achieved by incubating CHO cells with 1 mM lactobionic acid in PBS for 15 minutes at 37 °C. The media was removed from the cells and they were washed with PBS buffer (supplemented with 0.9 mM $CaCl_2$ and 1.1 mM $MgCl_2$). Figure 3.15C shows that particles were displaced by the wash step with lactobionic acid.

To assess if the binding process to the cell surface could be blocked, CHO cells were incubated with 300 µM lactobionic acid in cell media for 1 h at 37 ºC and particles were added to give the final concentration (a 1 in 4 dilution) for a further 2 h. Figure 3.15D confirmed that the particles could not bind to the cell surface in the presence of lactobionic acid. It is important to note that in the control described above where the cells were washed extensively with PBS buffer in the absence of lactobionic acid, the particles remained bound to the cell surface, ie. they were not removed by washing. These results indicate that the galactose modified particles bound in a receptor specific way to the cell surface.

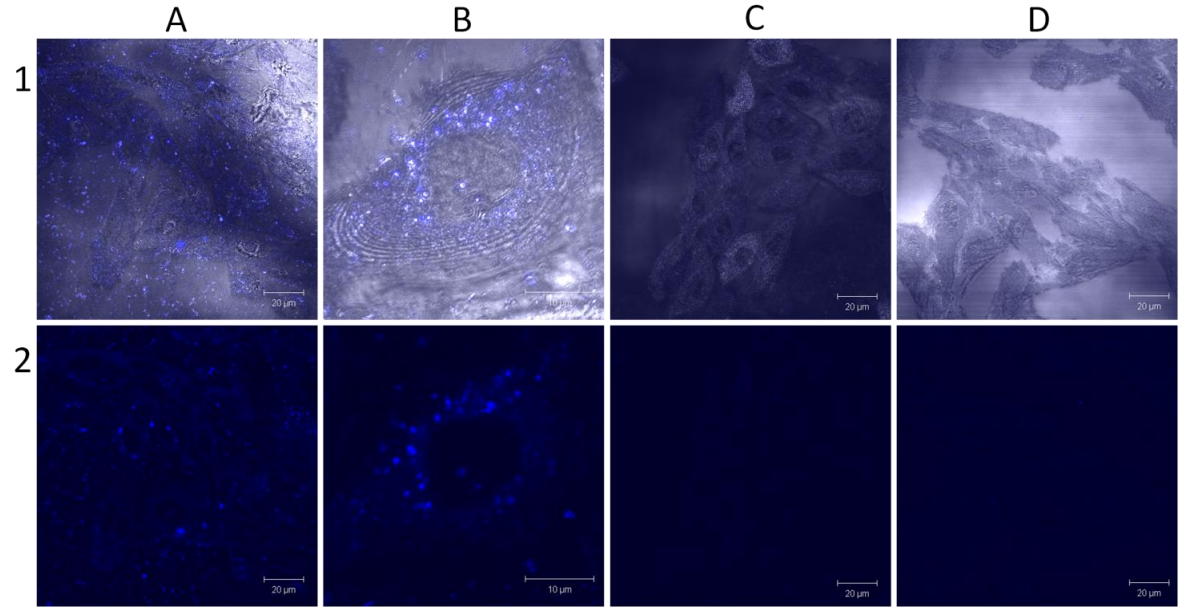

Figure 3. 15 Confocal fluorescence imaging showing binding of nanoparticles (1:4 dilution) to live CHO cells following a 2 h incubation at 37 ºC (Fig 2A) where Fig 2B expands a single cell image to show the distribution of particles at the cell surface (z = 3.5). Figures 1A and 1B show the reflectance images of the cells superimposed on the fluorescence images. Fig 2C shows the fluorescence images of the CHO cells treated with the nanoparticles, after they had been washed with 1mM lactobionic acid in PBS for 15 minutes at 37 ºC, the absence of fluorescence confirmed binding was reversed. Fig 2D shows that following incubation with 300 µM lactobionic acid for 1 h, prior to the addition of nanoparticles (1:4 dilution) for 2 h, no particle binding occurred. Figures 1C and 1D show the reflectance images for these studies superimposed on the fluorescence images to confirm that the cells were present but unmodified by the particles.

3.5 Conclusion

Hybrid block copolymers consisting of poly(styrene) and a poly(amino acid) segments were synthesized via combination of RAFT and NCA polymerization. The polypeptide segments were glycosolated with galactose moieties using traditional coupling chemistry. The resulting amphiphilic block copolymers were found to be efficient stabilizers in the emulsion polymerization of styrene offering a facile method for the synthesis of fluorescent glycosylated polystyrene nanoparticles. The availability of the galactose units introduced through the glycopolymer surfactant at the nanoparticles surface for selective binding was successfully demonstrated by lectin binding experiments and binding to Chinese hamster ovary (CHO) cells. This approach provides a straightforward route to highly fluorescent

nanoparticles with selective binding properties for imaging applications avoiding particle post-modification.

3.6 References

1. Elsabahy, M.; Wooley, K. L. *Chemical Society Reviews* **2012,** 41, (7), 2545-2561.

2. Parveen, S.; Misra, R.; Sahoo, S. K. *Nanomedicine: Nanotechnology, Biology and Medicine* **2012,** 8, (2), 147-166.

3. Ryu, J. H.; Koo, H.; Sun, I.-C.; Yuk, S. H.; Choi, K.; Kim, K.; Kwon, I. C. *Advanced Drug Delivery Reviews* **2012,** 64, (13), 1447-1458.

4. Vollrath, A.; Schubert, S.; Schubert, U. S. *Journal of Materials Chemistry B* **2013,** 1, (15), 1994-2007.

5. Gupta, A. K.; Gupta, M. *Biomaterials* **2005,** 26, (18), 3995-4021.

6. Maeng, J. H.; Lee, D.-H.; Jung, K. H.; Bae, Y.-H.; Park, I.-S.; Jeong, S.; Jeon, Y.-S.; Shim, C.-K.; Kim, W.; Kim, J.; Lee, J.; Lee, Y.-M.; Kim, J.-H.; Kim, W.-H.; Hong, S.-S. *Biomaterials* **2010,** 31, (18), 4995-5006.

7. Borase, T.; Ninjbadgar, T.; Kapetanakis, A.; Roche, S.; O'Connor, R.; Kerskens, C.; Heise, A.; Brougham, D. F. *Angewandte Chemie International Edition* **2013,** 52, (11), 3164-3167.

8. Grobmyer, S. R.; Moudgil, B. M.; Santra, S., Fluorescent Silica Nanoparticles for Cancer Imaging. In *Cancer Nanotechnology*, Humana Press: 2010; Vol. 624, pp 151-162.

9. Santra, S.; Malhotra, A. *Wiley Interdisciplinary Reviews: Nanomedicine and Nanobiotechnology* **2011,** 3, (5), 501-510.

10. Ow, H.; Larson, D. R.; Srivastava, M.; Baird, B. A.; Webb, W. W.; Wiesner, U. *Nano Letters* **2004,** 5, (1), 113-117.

11. Kamaly, N.; Xiao, Z.; Valencia, P. M.; Radovic-Moreno, A. F.; Farokhzad, O. C. *Chemical Society Reviews* **2012,** 41, (7), 2971-3010.

12. Mai, Y.; Eisenberg, A. *Chemical Society Reviews* **2012,** 41, (18), 5969-5985.

13. Friedrich, H.; McKenzie, B.; Bomans, P. H. H.; Deng, Z.; Nudelman, F.; Holder, S. J.; de With, G.; Somerdijk, N. *Microscopy and Microanalysis* **2010,** 16, (SupplementS2), 832-833.

14. Rösler, A.; Vandermeulen, G. W. M.; Klok, H.-A. *Advanced Drug Delivery Reviews* **2012,** 64, Supplement, (0), 270-279.

15. Danhier, F.; Ansorena, E.; Silva, J. M.; Coco, R.; Le Breton, A.; Preat, V. *Journal of Controlled Release* **2012,** 161, (2), 505-522.

16. Owens Iii, D. E.; Peppas, N. A. *International Journal of Pharmaceutics* **2006,** 307, (1), 93-102.

17. Ma, Y.; Sadoqi, M.; Shao, J. *International Journal of Pharmaceutics* **2012,** 436, (1 - 2), 25-31.

18. Sakuma, S.; Kataoka, M.; Higashino, H.; Yano, T.; Masaoka, Y.; Yamashita, S.; Hiwatari, K.-i.; Tachikawa, H.; Kimura, R.; Nakamura, K.; Kumagai, H.; Gore, J. C.; Pham, W. *European Journal of Pharmaceutical Sciences* **2011,** 42, (4), 340-347.

19. Holzapfel, V.; Musyanovych, A.; Landfester, K.; Lorenz, M. R.; Mailänder, V. *Macromolecular Chemistry and Physics* **2005,** 206, (24), 2440-2449.

20. Albanese, A.; Tang, P. S.; Chan, W. C. W. *Annual Review of Biomedical Engineering* **2012,** 14, (1), 1-16.

21. Caruso, F.; Stayton, P.; Ward, M. D. *Chemistry of Materials* **2012,** 24, (5), 727-727.

22. Dhar, S.; Gu, F. X.; Langer, R.; Farokhzad, O. C.; Lippard, S. J. *Proceedings of the National Academy of Sciences* **2008,** 105, (45), 17356-17361.

23. Singh, K., Choudhary, M. , Chianella, I. and Singh, P. *Advances in Nanoparticles* **2013**, (2), 182-190.

24. Ruoslahti, E. *Advanced Materials* **2012,** 24, (28), 3747-3756.

25. Medley, C. D.; Bamrungsap, S.; Tan, W.; Smith, J. E. *Analytical Chemistry* **2011,** 83, (3), 727-734.

26. Yu, B.; Tai, H. C.; Xue, W.; Lee, L. J.; Lee, R. J. *Molecular Membrane Biology* **2010,** 27, (7), 286-298.

27. Cummings, R. D.; Pierce, J. M. *Chemistry & Biology* **2014,** 21, (1), 1-15.

28. Hudak, J. E.; Bertozzi, Carolyn R. *Chemistry & Biology* **2014,** 21, (1), 16-37.

29. Lowary, T. L. *Current Opinion in Chemical Biology* **2013,** 17, (6), 990-996.

30. Gamblin, D. P.; Scanlan, E. M.; Davis, B. G. *Chemical Reviews* **2008,** 109, (1), 131-163.

31. Ting, S. R. S.; Chen, G.; Stenzel, M. H. *Polymer Chemistry* **2010,** 1, (9), 1392-1412.

32. Spain, S. G.; Cameron, N. R. *Polymer Chemistry* **2011,** 2, (1), 60-68.

33. Spain, S. G.; Gibson, M. I.; Cameron, N. R. *Journal of Polymer Science Part A: Polymer Chemistry* **2007,** 45, (11), 2059-2072.

34. Kiessling, L. L.; Gestwicki, J. E.; Strong, L. E. *Angewandte Chemie International Edition* **2006,** 45, (15), 2348-2368.

35. Huang, J.; Zhang, Q.; Li, G.-Z.; Haddleton, D. M.; Wallis, R.; Mitchell, D.; Heise, A.; Becer, C. R. *Macromolecular Rapid Communications* **2013,** 34, (19), 1542-1546.

36. Zhang, Q.; Collins, J.; Anastasaki, A.; Wallis, R.; Mitchell, D. A.; Becer, C. R.; Haddleton, D. M. *Angewandte Chemie International Edition* **2013,** 52, (16), 4435-4439.

37. Becer, C. R. *Macromolecular Rapid Communications* **2012,** 33, (9), 742-752.

38. Kramer, J. R.; Deming, T. J. *Journal of the American Chemical Society* **2010,** 132, (42), 15068-15071.

39. Krannig, K.-S.; Doriti, A.; Schlaad, H. *Macromolecules* **2014,** 47, (7), 2536-2539.

40. Huang, J.; Heise, A. *Chemical Society Reviews* **2013,** 42, (17), 7373-7390.

41. Krannig, K.-S.; Huang, J.; Heise, A.; Schlaad, H. *Polymer Chemistry* **2013,** 4, (14), 3981-3986.

42. Krannig, K.-S.; Schlaad, H. *Journal of the American Chemical Society* **2012,** 134, (45), 18542-18545.

43. Tang, H.; Zhang, D. *Biomacromolecules* **2010,** 11, (6), 1585-1592.

44. Mildner, R.; Menzel, H. *Journal of Polymer Science Part A: Polymer Chemistry* **2013,** 51, (18), 3925-3931.

45. Xiao, C.; Zhao, C.; He, P.; Tang, Z.; Chen, X.; Jing, X. *Macromolecular Rapid Communications* **2010,** 31, (11), 991-997.

46. Kramer, J. R.; Deming, T. J. *Polymer Chemistry* **2014,** 5, (3), 671-682.

47. Bonduelle, C.; Lecommandoux, S. *Biomacromolecules* **2013,** 14, (9), 2973-2983.

48. Huang, J.; Habraken, G.; Audouin, F.; Heise, A. *Macromolecules* **2010,** 43, (14), 6050-6057.

49. Huang, J.; Bonduelle, C.; Thevenot, J.; Lecommandoux, S.; Heise, A. *Journal of the American Chemical Society* **2012,** 134, (1), 119-122.

50. Bonduelle, C.; Huang, J.; Mena-Barragan, T.; Ortiz Mellet, C.; Decroocq, C.; Etame, E.; Heise, A.; Compain, P.; Lecommandoux, S. *Chemical Communications* **2014,** 50, (25), 3350-3352.

51. Bonduelle, C.; Mazzaferro, S.; Huang, J.; Lambert, O.; Heise, A.; Lecommandoux, S. *Faraday Discussions* **2013,** 166, (0), 137-150.

52. Habraken, G. J. M.; Peeters, M.; Dietz, C. H. J. T.; Koning, C. E.; Heise, A. *Polymer Chemistry* **2010,** 1, (4), 514-524.

53. Postma, A.; Davis, T. P.; Evans, R. A.; Li, G.; Moad, G.; O'Shea, M. S. *Macromolecules* **2006,** 39, (16), 5293-5306.

54. Jacobs, J.; Gathergood, N.; Heise, A. *Macromolecular Rapid Communications* **2013,** 34, (16), 1325-1329.

55. Xu, J.; He, J.; Fan, D.; Wang, X.; Yang, Y. *Macromolecules* **2006,** 39, (25), 8616-8624.

56. Boyer, C.; Granville, A.; Davis, T. P.; Bulmus, V. *Journal of Polymer Science Part A: Polymer Chemistry* **2009,** 47, (15), 3773-3794.

57. Vayaboury, W.; Giani, O.; Cottet, H.; Deratani, A.; Schué, F. *Macromol. Rapid Commun.* **2004,** 25, (13), 1221-1224.

58. Habraken, G. J. M.; Wilsens, K. H. R. M.; Koning, C. E.; Heise, A. *Polymer Chemistry* **2011,** 2, (6), 1322-1330.

59. Barz, M.; Duro-Castano, A.; Vicent, M. J. *Polymer Chemistry* **2013,** 4, (10), 2989-2994.

60. Munoz-Bonilla, A.; van Herk, A. M.; Heuts, J. P. A. *Macromolecules* **2010,** 43, (6), 2721-2731.

61. Munoz-Bonilla, A.; van Herk, A. M.; Heuts, J. P. A. *Polymer Chemistry* **2010,** 1, (5), 624-627.

62. Munoz-Bonilla, A.; Ali, S. I.; del Campo, A.; Fernandez-Garcia, M.; van Herk, A. M.; Heuts, J. P. A. *Macromolecules* **2011,** 44, (11), 4282-4290.

63. Rager, T.; Meyer, W. H.; Wegner, G.; Mathauer, K.; Mächtle, W.; Schrof, W.; Urban, D. *Macromolecular Chemistry and Physics* **1999,** 200, (7), 1681-1691.

64. Kawaguchi, H. *Progress in Polymer Science* **2000,** 25, (8), 1171-1210.

65. Goldmann, A. S.; Barner, L.; Kaupp, M.; Vogt, A. P.; Barner-Kowollik, C. *Progress in Polymer Science* **2012,** 37, (7), 975-984.

66. Alvarez-Paino, M.; Munoz-Bonilla, A.; Marcelo, G.; Rodriguez-Hernandez, J.; Fernandez-Garcia, M. *Polymer Chemistry* **2012,** 3, (12), 3282-3288.

67. Wang, X.-d.; Gorris, H. H.; Stolwijk, J. A.; Meier, R. J.; Groegel, D. B. M.; Wegener, J.; Wolfbeis, O. S. *Chemical Science* **2011,** 2, (5), 901-906.

68. Cho, M.; Cummings, R. D. *Journal of Biological Chemistry* **1995,** 270, (10), 5198-5206.

69. Cho, M.; Cummings, R. D. *Journal of Biological Chemistry* **1995,** 270, (10), 5207-5212.

Chapter 4

Amphiphilic glycosylated block copolypeptides as macromolecular surfactants in the emulsion polymerization of styrene.

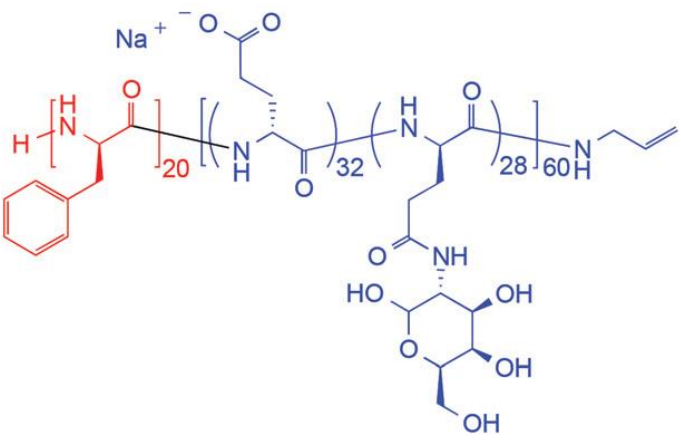

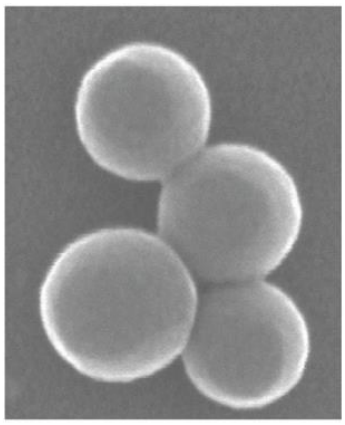

This work was published in the journal Polymer Chemistry:

Jacobs, J.; Gathergood, N.; Heuts, J. P. A.; Heise, A., Amphiphilic glycosylated block copolypeptides as macromolecular surfactants in the emulsion polymerization of styrene. *Polymer Chemistry* **2015,** 6, (25), 4634-4640.

4.1 Abstract

Diblock copolymers consisting of poly(L-phenyl alanine) and poly(benzyl-L-glutamate) or poly(CBZ-L-lysine), respectively, were synthesized via sequential NCA polymerization. After deprotection, subsequent partial glycosylation of the glutamic acid and lysine units with galactosamine hydrochloride or lactobionic acid yielded amphiphilic block copolypeptides. Moreover, a triblock copolymer poly(L-phenyl alanine-*b*-L-benzyl glutamate-b-propargylglycine) was obtained and glycosylated by 'click' chemistry. Glycosylated block copolypeptides showed improved water solubility and circular dichroism (CD) confirmed the pH dependence of the helix-coil transition. The block copolypeptides were found to be efficient stabilizers in the emulsion polymerization of styrene offering a facile method for the synthesis of polystyrene nanoparticles in the range of 100-140 nm depending on the block copolymer composition and emulsion concentration. This establishes an example of functional polymer additives fully based on renewable building blocks in nanomaterial synthesis.

4.2 Introduction

Over the last decade significant efforts have been made to introduce green approaches in polymer science. Prominent examples include polymers from renewable raw materials and bio-based feedstock.[1-3] Notably most of these renewable polymers are polycondensates and some of these materials have shown academic and industrial merit.[4-7] Another important class of monomers are acrylates and the corresponding polyacrylates are very versatile and adoptable to a range of applications due to their side chain functionality. A class of monomers similar in functionality yet fully bio-based is amino acids. Although it cannot be expected that poly(amino acids) can be a broad substitute for polyacrylics, they might be an alternative in some segments.

Significant advances in the controlled ring-opening polymerisation of amino acid N-carboxyanhydrides (NCA)[8, 9] has fuelled opportunities for the design of well-defined macromolecular structures such as block[9-11], graft[12], star (co)polymers[13-16], polymer brushes[17-19], etc., which shows parallels to the development in controlled radical polymerisation. While most authors propose such structures in the wider context of biomedical applications, we believe that there is scope in exploring poly(amino acid)s or synthetic polypeptides in non-medical applications. One such area is surface-active amphiphilic block copolymers as surfactants or emulsifiers. A few examples of amphiphilic block copolypeptides have been reported primarily with the aim to study their self-organisation into micelles and vesicles.[20-22] The use of polypeptides as macromolecular emulsifiers is largely unexplored despite the fact that proteins are the stabilizers in natural rubber latex.[23] Reported examples are generally limited to lower molecular weight analogues.[24-28] Only recently Deming has shown that it was possible to stabilize water-in-oil-in-water double emulsions using racemic amphiphilic copolypeptides prepared *via* NCA polymerisation.[29] Here we report glycosylated polypeptide block copolymers as efficient surfactants in emulsion polymerisation. This process was selected as it will provide not only information about the initial stability of an emulsion but also the ability of the amphiphilic block copolypeptides to provide emulsion stability throughout the demanding process of latex formation.

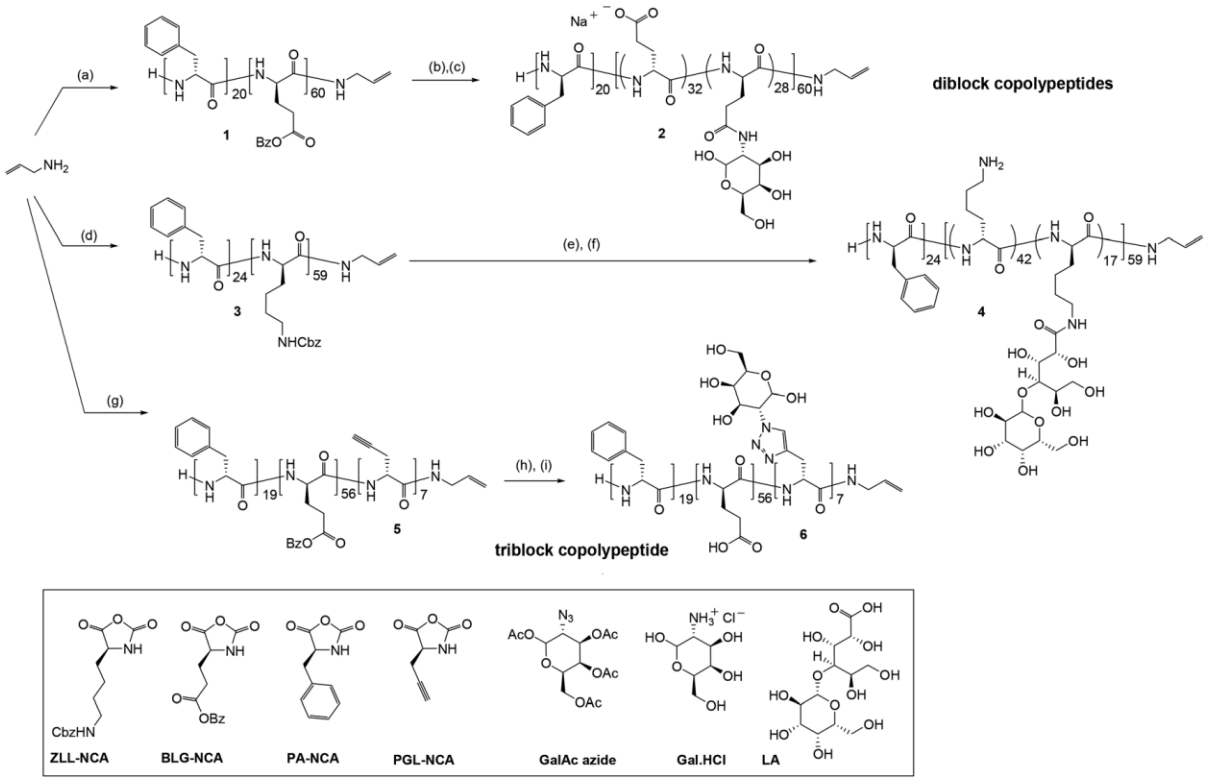

Scheme 4.1 Reagents and conditions: (a) BLG-NCA ([M]0/[I]0 = 60); PA NCA DMF ([M]0/[I]0 = 20), HV, 0 °C; (b) HBr (33 wt. % in AcOH), TFA; 0.5 M NaOH (aq); (c) GA.HCl, DMT-MM, DDI (d) ZLL-NCA ([M]0/[I]0 = 60); PA NCA DMF ([M]0/[I]0 = 20), HV, 0 °C (e) HBr (33 wt. % in AcOH), TFA; (f) LA, EDC/NHS, pH 4.7, 10 mM MES buffer; DDI (g) PGL NCA ([M]0/[I]0 = 7); BLG-NCA ([M]0/[I]0 = 60); PA NCA DMF ([M]0/[I]0 = 20), HV, 0 °C; (h) GalAc, Cu(PPh3)3Br, Et3N, DMF, 30 °C; (i) HBr (33 wt. % in AcOH), TFA. I = allylamine, HV = high vacuum, DDI = distilled deionized water.

4.3 EXPERIMENTAL

4.3.1 Materials

All chemicals were purchased from Sigma-Aldrich and used as received unless otherwise noted. γ-Benzyl-L-glutamate and ε-benzyloxycarbonyl-L-lysine were supplied by Bachem. Anhydrous DMF, chloroform, ethyl acetate, methanol were used directly from the bottle under an inert and dry atmosphere. γ-Benzyl-L-glutamate (BLG), ε-benzyloxycarbonyl-L-lysine (ZLL), Phenyl alanine (PA) and DL-propargylglycine (PGL) NCA was synthesised following literature procedures.[21, 30, 31] 1-β-Azido-2,3,4,6-tetraacetyl-D-galactose (GalAc) was synthesized following a literature procedure.[32]

4.3.2 Preparation of copolypeptides $PBLG_{60}$-*b*-PPA_{20} (1).

The NCA monomer of BLG (2.5 g, 9.5 mmol) was dissolved in 20 mL anhydrous DMF in a Schlenk tube. The solution was degassed *via* three successive freeze-pump-thaw cycles and kept under vacuum. The reaction flask was immersed in a 0 °C water bath and a solution of 12 μL allylamine in 1 mL anhydrous DMF ($[M]_0/[I]_0$ = 60) was injected through a rubber septum with a syringe. The reaction was left to stir until the BLG NCA had been completely consumed as monitored by ATR-FTIR spectroscopy. The polypeptide was further chain extended *via* the introduction of phenyl alanine NCA (0.60 g, 3.1 mmol, $[M]_0/[I]_0$ = 20) dissolved in 5 mL DMF. After full monomer conversion monitored via ATR FTIR spectroscopy the polymer was precipitated into an excess of diethyl ether, filtered and dried under vacuum. Isolated yield: 2.2 g.

Similar procedures were used to synthesize $PZLL_{59}$-*b*-PPA_{24} (**3**) and PGL_7-*b*-$PBLG_{56}$-*b*-PPA_{19} (**5**).

4.3.3 Block copolypeptide deprotection.

A general procedure was used for the deprotection of both the PBLG and PZLL pendant groups. $PBLG_{60}$-*b*-PPA_{20} (2.0 g, 0.13 mmol) was dissolved in trifluoroacetic acid (20 mL). 4 mL of HBr solution (33 wt.% in acetic acid; 3-fold excess with respect to γ-benzyl-L-glutamate repeat units) was added slowly to the reaction at 0 °C. After 2 h, the solution was added to 300 mL diethyl ether and the precipitate washed three times with 50 mL diethyl ether. The subsequent product was dissolved in a 0.5M NaOH solution (aqua) to obtain the polymer in the sodium salt form. The sodium salt polymer was dialyzed against double deionized (DDI) water using Spectra/Por dialysis membranes (MWCO, 3.5 kDa) for 72 h at room temperature. The product $PLGA_{60}$-*b*-PPA_{20} was lyophilized and isolated as a white powder. Isolated yield: 1.4 g.

$PZLL_{59}$-*b*-PPA_{24} was deprotected in a similar fashion to yield **PLL_{59}-*b*-PPA_{24}**.

4.3.4 Glycosylation reactions

4.3.4.1 (GA_{28}-*r*-$PLGA_{32}$)-*b*-PPA20 (2)

Glycosylation of the carboxylic acid moieties was achieved according to a modified literature procedure.[33] $PLGA_{60}$-*b*-PPA_{20} (1.3 g, 0.12 mmol) and galactosamine hydrochloride (GA.HCl) (0.79 g, 3.7 mmol, 0.5 eq w.r.t. the glutamate repeating units) was dissolved in

deionized water (10 mL) and stirred for 15 min. 4-(4,6-Dimethoxy-1,3,5-triazin-2-yl)-4-methylmorpholinium chloride (DMT-MM) (1.2 g, 4.4 mmol, 1.2 eq. to Galactosamine HCl) was dissolved in 5 mL of deionized water and added to the reaction mixture. After stirring for 24 h at room temperature 2 mL of a 1M NaOH aqueous solution was added to the reaction mixture and stirred for 3 hours. The mixture was then dialyzed against DDI water using Spectra/Por dialysis membranes (MWCO, 3.5 kDa) for 72 h at room temperature. The polymer was lyophilized and isolated as a white powder. Isolated yield: 1.7 g.

4.3.4.2 $(LA_{17}$-*r*-$PLL_{42})$-*b*-PPA_{24} (4)

A general procedure for 1-Ethyl-3-[3-dimethylaminopropyl]carbodiimide hydrochloride (EDC)/*N*-hydroxysulfosuccinimide (Sulfo-NHS) coupling was employed to attach lactobionic acid to the lysine residues of the amphiphilic copolypeptide. Lactobionic acid (LA) (0.7 g, 2 mmol, 0.3 eq w.r.t lysine repeat units), EDC (0.45 g, 2.3 mmol, 1.2 eq w.r.t. the LA) and sulfo-NHS (50 mg, 0.23 mmol, 0.1 eq w.r.t. EDC) were dissolved in 3 mL 10 mM MES buffer (pH 4.7) and stirred for 20 minutes. The latter was added to a solution of PLL_{59}-*b*-PPA_{24} (1.2 g, 0.11 mol) in 10 mL of DDI water. The reaction mixture was stirred overnight. The resulting product was purified *via* dialysis against DDI water using Spectra/Por dialysis membranes (MWCO, 3.5 kDa) for 72 h at room temperature. The product was subsequently lyophilized and isolated as a white powder. Isolated yield: 1.5 g.

4.3.4.3 GA_7-*b*-$PBLG_{56}$-*b*-PPA_{19} (6)

Glycosylation was achieved via a modified procedure previously utilized in our group.[21] PGL_7-*b*-$PBLG_{56}$-*b*-PPA_{19} (1.5 g, 0.66 mmol of alkyne units), 1-β-Azido-2,3,4,6-tetraacetyl-D-galactose 0.3 g, 0.8 mmol, 1.2 eq. to alkyne groups) and triethylamine (40 μL, 0.5 eq.) was dissolved in 20 mL of anhydrous DMF in a Schlenk tube. The mixture was stirred and degassed by bubbling nitrogen for 30 min. $(PPh_3)_3CuBr$ (60 mg, 0.1 eq.) was then added and nitrogen was bubbled through the resulting solution for another 30 min. The Schlenk tube was placed in an oil bath at 30 °C for 24 h under nitrogen atmosphere. 100 mg of Amberlite® IR120 hydrogen form ion exchange resin was added and the suspension gently stirred at ambient temperature overnight. After filtration and centrifugation, the polymer solution was precipitated in a 3:2 THF/diethyl ether mixture and washed with THF. Isolated yield: 1.6 g. Subsequent deprotection as described above results in the simultaneous deprotection of the benzyl ester and tetraacetate groups to yield **GA_7-*b*-$PLGA_{56}$-*b*-PPA_{19}.**

4.3.5 Preparation of polystyrene latex via emulsion polymerization.

Styrene was polymerized using a similar method described previously.[34] Batch emulsion polymerizations were all carried out in a three-neck reactor equipped with a reflux condenser, nitrogen inlet and mechanical stirrer. A typical reaction proceeded as follows: GA_{28}-*r*-$PLGA_{32}$-*b*-PPA_{20} (0.24 g) was added to the reactor under an inert atmosphere and dissolved in 38 mL of distilled water under stirring at 70 °C. The styrene monomer (4.8 g) was deoxygenated separately for 20 min by bubbling nitrogen through it and injected into the reactor. A deoxygenated initiator solution (50 mg of potassium persulfate in 2 mL of water) was injected to start the polymerization. The nitrogen flow was maintained throughout the reaction. Samples were withdrawn at regular times to determine the conversion. A small amount of hydroquinone was added to these aliquots to quench the radical polymerization where the monomer conversion was then determined gravimetrically.

4.3.6 Methods.

Nuclear magnetic resonance (NMR) spectra were recorded on a Bruker Avance 400 (400 MHz) in DMSO-d6 and $CDCl_3$ as solvents. All chemical shifts are reported in parts per million (ppm) with tetramethylsilane (TMS) as an internal reference. Attenuated Total Reflection (ATR) FTIR measurements were performed on a Perkin-Elmer Spectrum 100 instrument. Spectra were obtained from 4 scans with a resolution of 2 cm^{-1} in the spectral region of 650 – 4000 cm^{-1}. A background measurement was taken before the sample was loaded onto the ATR for measurement. Samples could be characterized in the liquid state without prior sample preparation. Size Exclusion Chromatography (SEC) was performed on an Agilent 1200 system in conjunction with two PSS GRAM analytical (8 x 300 and 8 x 100, 10 μ) columns, a Wyatt Dawn Heleos 8 multi angle light scattering (MALS) detector and Wyatt Optilab rEX differential refractive index (DRI) detector with a 658 nm light source. The eluent was DMF containing 0.1 M LiBr at a flow rate of 1 mL/min. The column temperature was set to 40 °C with the MALS detector at 35 °C and the DRI detector at 40 °C. Molar masses and dispersities were calculated from the MALS signal by the Astra software (Wyatt) using the refractive index increment (d*n*/d*c*) as calculated relative to the ratio of the homopolymer. The dn/dc values used for the polymers were experimentally determined or as found in literature.[9, 35] All samples for SEC analysis were filtered through a 0.45 mm PTFE filter (13 mm, PP housing, Whatman) prior to injection. Dynamic light scattering (DLS) experiments were performed at 25°C on a Malvern NanoZS (Malvern Instruments, Malvern

UK) which uses a detection angle of 173°, and a 3 mW He-Ne laser operating at a wavelength of 633 nm. Field emission scanning electron microscopy (FESEM) images were obtained on a Hitachi S5500 scanning electron microscope. CD spectra were recorded on a Jasco J-715 spectropolarimeter at ambient temperature. A quartz cell with 0.1 cm path length was used. Spectra were recorded between 250 and 190 nm. Each spectrum represents the average of five measurements. A baseline was taken from the pure solvent and subtracted from the spectra. The spectra were smoothed using a Savitzky–Golay smoothing filter. For the pH-dependent measurements, a stock solution of the copolypeptide (c.a. 0.3 mg/mL) in 0.01 M NaCl solution was titrated with aqueous HCl or aqueous NaOH. Mean residue ellipticities were calculated using the equation $[\Theta]_{MRW} = (\Theta_{MRW})/(10 \times c \times l)$ with experimental ellipticity Θ in mdeg, mean residue weight M_{MRW} in g/mol, mass concentration c in mg/mL and path length l in cm.[36] Helicities f_α were calculated from the mean residue ellipticities at λ = 222 nm using the following equation: $f_{222} = (-[\theta_{222}]_{MRW} + 3000)/39000$ (**1**).

4.4 Results and discussion

4.4.1 Synthesis of glycosylated block copolypeptides

With the increasing interest in functional polymer nanoparticles, various strategies are available for preparing polymer colloids via block copolymer-stabilized emulsion polymerisation.[37-39] Previously we demonstrated that hybrid amphiphilic block copolymers comprising a hydrophilic glycosylated polypeptide block and a hydrophobic polystyrene block could efficiently stabilise styrene latex formation.[34] Using a polystyrene block, high compatibility with the styrene latex was achieved. For the purpose of utilizing polypeptide block copolymers as macromolecular stabilisers in this process, it was necessary to carefully select the hydrophobic polypeptide block. In order to obtain uniform polystyrene latex nanoparticles it is critically important that the hydrophobic block remains embedded in the latex particle throughout the polymerisation process.[40] Phenyl-L-alanine (PA) was chosen as the amino acid for this block due to the structural resemblance of the phenyl substituent with styrene.

Initially, two different diblock copolymers were synthesised by sequential NCA polymerisation from poly(benzyl-L-glutamate) (PBLG) and poly(Z-L-lysine) (PZLL), respectively (Scheme 4.1), i.e. $PBLG_{60}$-*b*-PPA_{20} (**1**) and $PZLL_{59}$-*b*-PPA_{24} (**3**) in DMF at 0 °C under vacuum using allylamine as an initiator.[11] Due to the insolubility of PPA in DMF it

was necessary to first prepare the PBLG or PZLL block to prevent precipitation. The monomer conversion was followed by ATR-FTIR and the PA-NCA was added after complete disappearance of the initial NCAs anhydride peaks (1850 and 1790 cm^{-1}). An increase in molecular weight as well as narrow, monomodal distributions are evident from the SEC traces (Figure 4.1 and 4.2; Table 4.1) highlighting the successful synthesis of the block copolymers. Notably, the synthesis of these amphiphilic block copolypeptides is more straightforward than the previously reported synthesis of amphiphilic hybrid block copolymers[34].

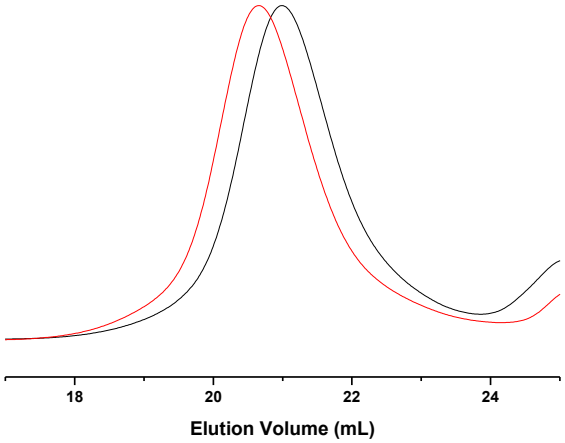

Figure 4. 1 SEC traces of $PBLG_{60}$ (red) and $PBLG_{60}$-*b*-PPA_{20} (**2**, black)

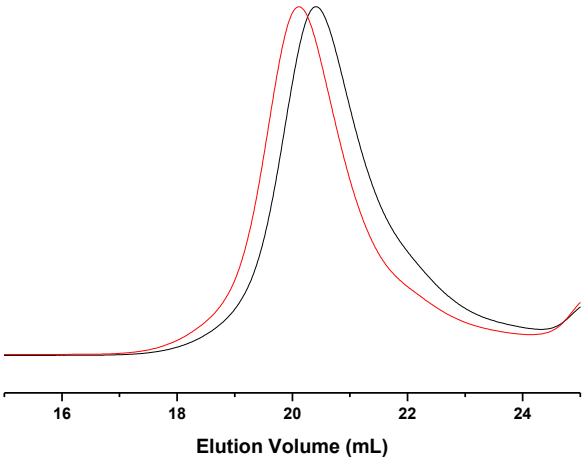

Figure 4. 2 SEC traces of $PZLL_{59}$ (black) and $PZLL_{59}$-*b*-PPA_{24} (**1,** red).

To enhance amphiphilicity, the deprotected poly(L-glutamic acid) (PGA) and poly(L-lysine) (PLL) blocks were glycosylated using previously reported strategies.[33, 34] The lysine residues of PLL_{59}-*b*-PPA_{24} were coupled with lactobionic acid (LA) using traditional EDC/NHS coupling chemistry (Scheme 4.1) targeting 30% glycosylation (LA_{17}-*r*-PLL_{42}-*b*-PPA_{24}, **4**). The carboxylic acid residues of $PLGA_{60}$-*b*-PPA_{20} were converted to the sodium salt form and galactosamine hydrochloride attached using an aqueous amide coupling approach in the presence of 4-(4,6-dimethoxy-1,3,5-triazin-2-yl)-4-methylmorpholinium chloride (DMT-MM) (Scheme 1) targeting 50% glycosylation (GA_{28}-*r*-$PLGA_{32}$-*b*-PPA_{20}, **2**). ^{1}H-NMR spectra confirm the successful deprotection as well as the glycosylation for both polymers (Figures 4.3 and 4.4).

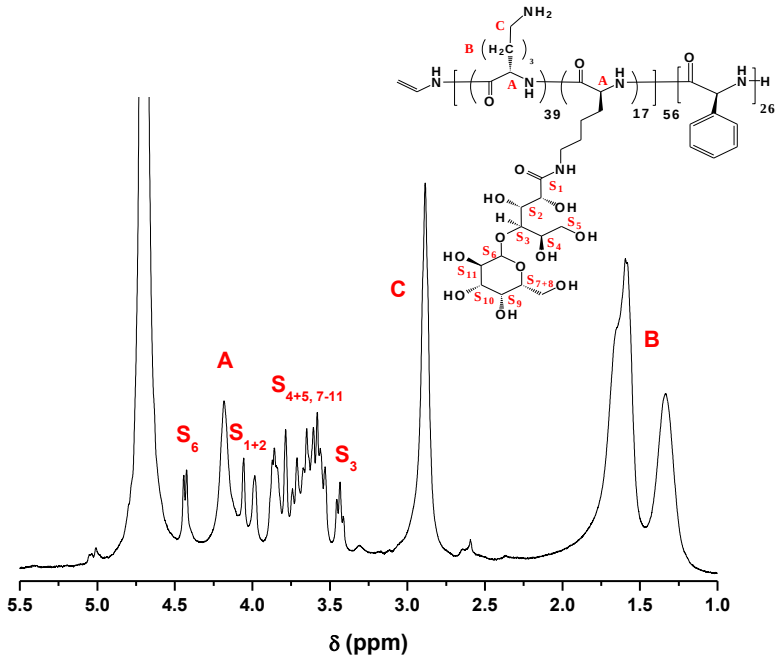

Figure 4. 3 ^{1}H-NMR spectra (D2O, 400 MHz) of LA_{17}-*r*-PLL_{42}-*b*-PPA_{24} (**4**).

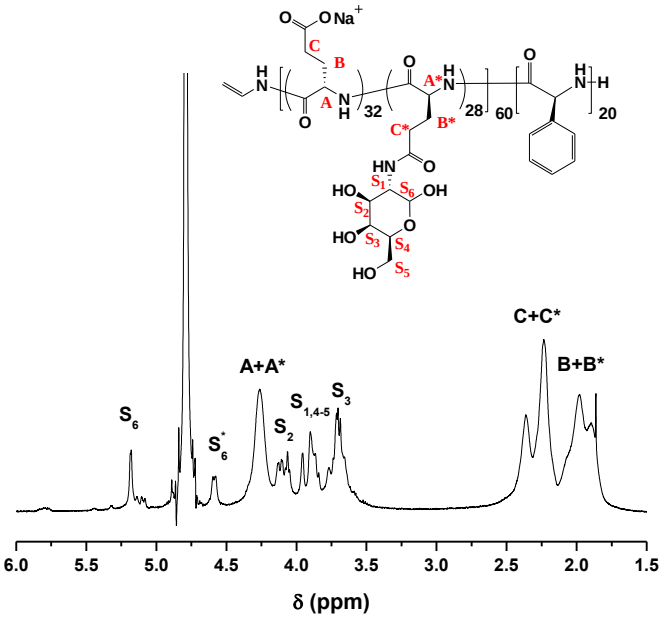

Figure 4. 4 ^{1}H-NMR spectra (D2O, 400 MHz) of GA_{28}-*r*-$PLGA_{32}$-*b*-PPA_{20} (**2**).

To further illustrate the versatility of the system a triblock copolymer PGL_{7}-*b*-$PBLG_{56}$-b-PPA_{19} (Scheme 1, **5**) was synthesised by sequential NCA polymerisation. Glycosylation was achieved by click chemistry of GA-azide with the alkyne groups of the propargylglycine block to yield GA_{7}-*b*-$PLGA_{56}$-*b*-PPA_{19} (**6**).[41] While the total composition of this triblock copolypeptide is similar to **2**, the amphiphilic block is arranged in a block rather than a random fashion. SEC and ^{1}H-NMR analysis confirm the well-defined block structure and efficient glycosylation (Figures 4.5 and 4.6).

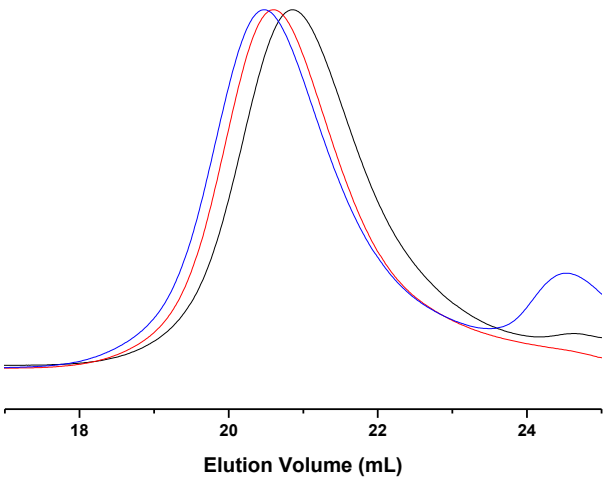

Figure 4. 5 SEC traces of PGL_7-*b*-$PBLG_{56}$ (black), $PArg_7$-*b*-$PBLG_{56}$-*b*-PPA_{19} (**5**, red) and $GalAc_7$-*b*-$PBLG_{60}$-*b*-PPA_{19} (blue).

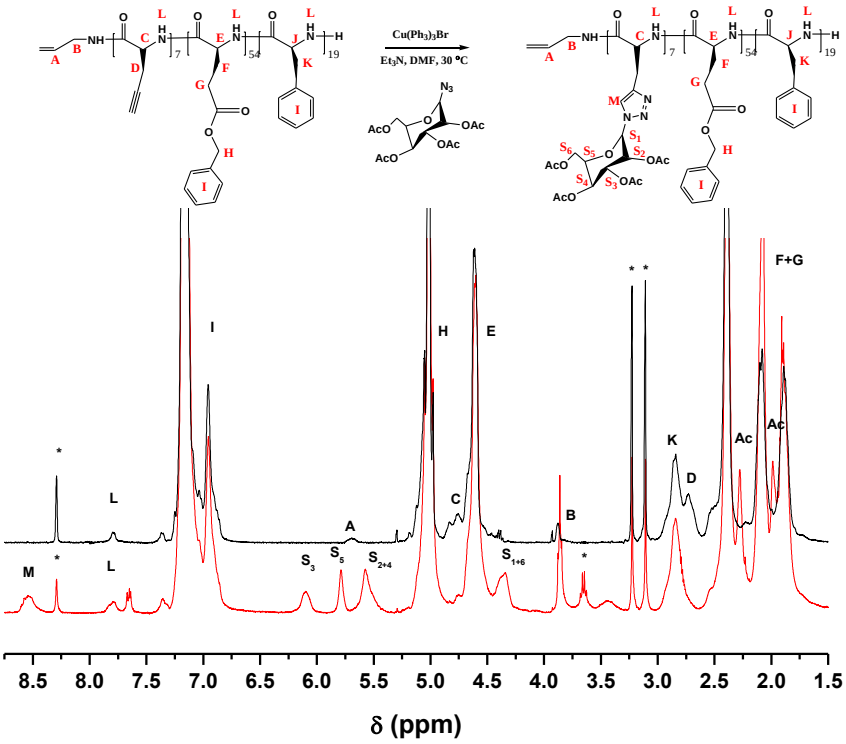

Figure 4. 6 ^{1}H-NMR spectra (TFA-d, 400 MHz) of PGL_7-*b*-$PBLG_{56}$-*b*-PPA_{19} (**3**, black) and GalAc7-*b*-$PBLG_{56}$-*b*-PPA_{19} (**5**, red). The * signals are due to DMF.

Table 4. 1 Polypeptide block copolypeptides

Polymer[(a)]	$[I]_0/[M_1]_0/[M_2]_0$	M_w[(b)] (g/mol)	Đ
$PBLG_{60}$-*b*-PPA_{20}	1:60:20	16600	1.07
$PZLL_{59}$-*b*-PPA_{24}	1:60:20	20400	1.07
PGL_7-*b*-$PBLG_{56}$-*b*-PPA_{19}	1:7:60:20	17500	1.09

[a]Degree of polymerization was determined by 1H-NMR spectroscopy (TFA-d) by calculating the ratio of the methine proton of the initiator allylamine (5.6 ppm) to the methylene protons of the polypeptide protecting group for PBLG/PZLL (4.9 – 5.2 ppm) and methylene group of PPA (2.7 – 3.0 ppm). [b]Values obtained from multi angle light scattering (MALS) detection.

4.4.2 Solution properties of glycopolypeptides

Ionic surfactants such as the block copolypeptides presented here are sensitive to solution pH. pH may directly impact the solubility and, unlike conventional surfactants, the secondary structure of the glycopolypeptides. The latter was investigated in aqueous solution by circular dichroism (CD) before and after glycosylation. CD measurements of the glycosylated and native block copolypeptides where compared at different pH values to establish the onset of secondary conformations. Figure 4.7 and A1 (see Appendix A) shows the CD spectra of $PLGA_{60}$-*b*-PPA_{20} and (GA_{28}-*r*-$PLGA_{32}$)-*b*-PPA_{20} respectively. When lowering the pH a transition from a random coil, as evident from a negative Cotton effect with a minimum at ca. λ = 198 nm, to an α-helix at pH 6.32 is apparent from the two minima at λ = 208 nm and 222 nm.[42] The transition seems to be solely between random-coil and α-helices as indicated by an isodichroistic point occurring at λ = 204 nm.[43] The native copolypeptide shows a maximum helicity of 35 % near pH 4 after which it precipitates from the solution, as the carboxylic moieties are being protonated.

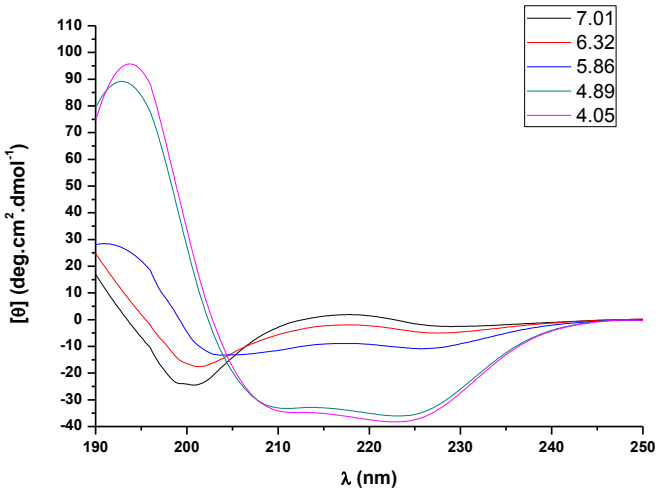

Figure 4. 7 CD spectra of aqueous solutions of $PLGA_{60}$-*b*-PPA_{20} as a function of pH

The CD spectra of the glycosylated (GA_{28}-*r*-$PLGA_{32}$)-*b*-PPA_{20} replicate this trend except for some residual helical conformation still being present at pH 7.10. Glycosylation improves the solubility of the block copolypeptide down to pH 3 with a maximum helicity of 44 %. CD measurements of the triblock copolypeptides PGL_7-*b*-$PLGA_{56}$-*b*-PPA_{19} and GA_7-*b*-$PLGA_{56}$-*b*-PPA_{19} as shown in Figures A2 and A3 display very similar trends before and after glycosylation. Both materials have the sole transition between a random coil and α-helical conformation as indicated by the isodichroistic point at λ = 204 nm. The onset of the transition is in the region of pH 6 irrespective of glycosylation. Furthermore, improved solubility upon glycosylation at lower pH was noticed.

In the case of PLL block copolypeptides, it is known that the PLL block adopts a random coil conformation at low pH while assuming an α-helical conformation at higher pH as the amino groups get deprotonated.[44] CD spectra of PLL_{59}-*b*-PPA_{24} and (LA_{17}-*r*-PLL_{42})-*b*-PPA_{24} (Figure A4 and A5) show exactly this where a transition from random-coil to the α-helical conformation can be seen as indicated by the two minima at λ = 208 nm and 222 nm. Figure 4.8 indicates the calculated helicities for the respective native and glycosylated block copolypeptides.

The helicities were only calculated where no precipitation was evident. The increased solubility over the pH range as a whole is evident for the glycosylated copolypeptides. The inherent electrolytic nature of the two respective amphiphiles means that solubility issues occur at the high and low pH limits, something seemingly well counteracted with the attachment of the carbohydrate moieties.

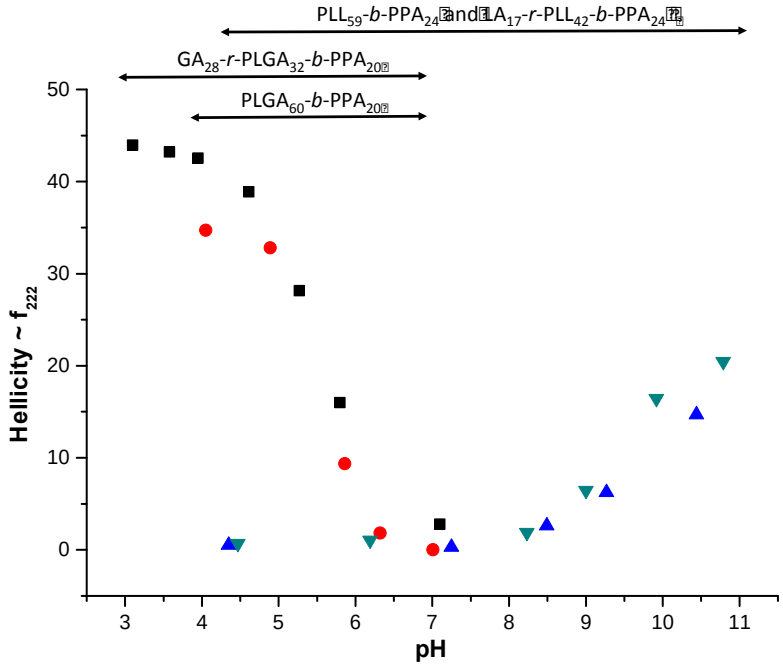

Figure 4. 8 Helicities determined for the block copolypeptides $PLGA_{60}$-*b*-PPA_{20} (●), GA_{28}-*r*-$PLGA_{32}$-*b*-PPA_{20} (■), PLL_{59}-*b*-PPA_{24} (▲) and LA_{17}-*r*-PLL_{42}-*b*-PPA_{24} (▼) as a function of pH. The arrows indicate the solubility range of the block copolypeptides.

A similar trend was observed for the PGL_7-*b*-$PLGA_{56}$-*b*-PPA_{19} and GA_7-*b*-$PLGA_{56}$-*b*-PPA_{19}, where the introduction of only 7 repeat units has a clear influence of the solubility below pH 4 (Figure 4.9).

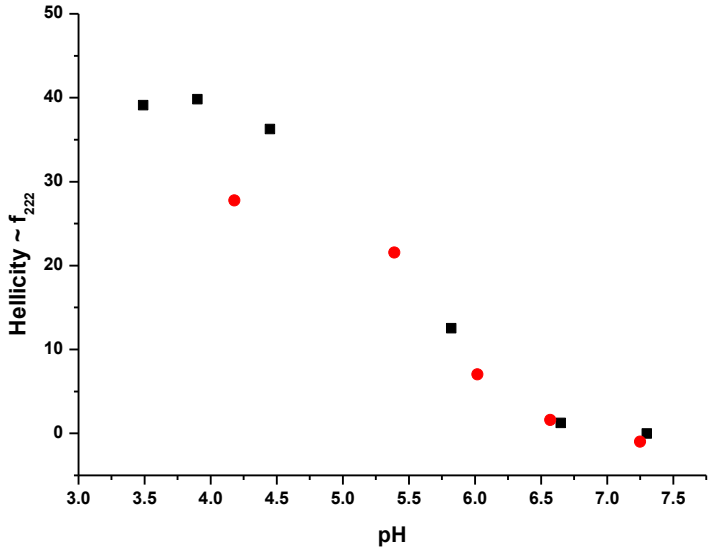

Figure 4. 9 Estimated helicities determined for the native copolypeptide, $PArg_7$-*b*-$PBLG_{56}$-*b*-PPA_{19} (●) and its glycosylated counterpart, Gal_7-*b*-$PLGA_{56}$-*b*-PPA_{19} (■) as a function of pH.

4.4.3 Emulsion Polymerisation

To the best of our knowledge, the stabilization of synthetic latexes by an amphiphilic polypeptide has not been shown yet. For this purpose, the three copolypeptides, GA_{28}-*r*-$PLGA_{32}$-*b*-PPA_{20}, GA_{28}-*r*-$PLGA_{32}$-*b*-PPA_{20} and LA_{17}-*r*-PLL_{42}-*b*-PPA_{24} where utilized as fully amino acid and carbohydrate based macromolecular surfactants in the aqueous emulsion polymerization of styrene. All reactions were performed at 70 °C and initiated *via* the water-soluble initiator potassium persulfate (KPS) at a concentration of 1 wt% with regard to monomer (1 pphm). Monomer contents of 12 and 15 wt%, and block copolymer contents of 2 and 5 wt% with regard to monomer were used. Under the applied conditions the hydrophilic blocks were in a random coil conformation. It was found that all block copolypeptides could readily stabilize the formed polystyrene particles and only in the case where a low concentration of LA_{17}-*r*-PLL_{42}-*b*-PPA_{24} was used (2 pphm) no stable latex was obtained. This implies that the hydrophilic PLGA blocks result in better stabilization, a result we have observed before.[34]

Conversion-time curves for the emulsion polymerization of styrene stabilized by GA_{28}-*r*-$PLGA_{32}$-*b*-PPA_{20} are shown in Figure 4.10. The results (especially at higher stabilizer concentrations) show very short nucleation periods (if any), which suggests that preformed

block copolymer micelles act as seeds for the polymerisation. Furthermore, the results in this figure show an increase in the polymerization rate as the copolypeptide concentration is increased. This result is expected as increasing block copolypeptide concentrations lead to higher particle numbers (N_p), which in turn lead to a higher rates of polymerization, R_p ($R_p \propto N_p$).[45] This argument is supported by the dynamic light scattering (DLS) results shown in Table 4.2, where it is clearly seen that increasing the copolypeptide concentration leads to a decrease in particle diameter.

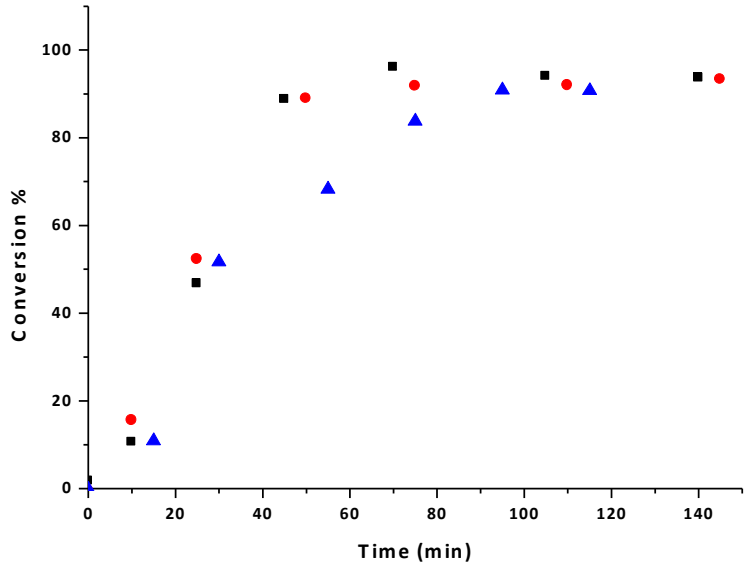

Figure 4. 10 Evolution of monomer conversion with time for the emulsion polymerization of styrene using KPS as initiator (1 wt%) with GA_{28}-r-$PLGA_{32}$-*b*-PPA_{20} as stabilizer. Monomer content of 12 wt% and surfactant content of 5 wt% (■), monomer content of 15 wt% and surfactant content of 5 wt% (●), monomer content of 15 wt% and surfactant content of 2 wt% (▲).

The triblock, GA_7-*b*-$PLGA_{56}$-*b*-PPA_{19}, acted as an effective stabilizer in the emulsion polymerization of styrene. Figure 4.11 shows the conversion-time curves at varying monomer and copolypeptide wt% content and it is evident that no real differentiation can be made regarding the polymerization rates of any of the three curves. Once again DLS showed no significant difference in particle size at increasing monomer content and constant copolypeptides/monomer ratio. A sharp increase in size to 120 nm is however evident after decreasing the copolypeptides content to 2 pphm, as fewer and thus larger particles are prepared (Table 2).

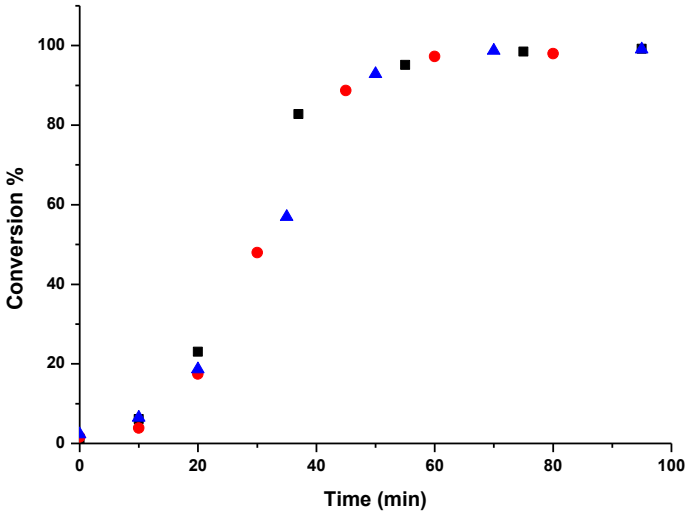

Figure 4. 11 Evolution of monomer conversion with time for the emulsion polymerization of styrene using KPS as initiator (1 wt%), a monomer content of 12 wt% and surfactant content of 5 wt% (■), a monomer content of 15 wt% and surfactant content of 5 wt% (●),a monomer content of 15 wt% and surfactant content of 2 wt% (▲) with GA_7-*b*-$PLGA_{56}$-*b*-PPA_{19} as stabilizer.

LA_{17}-*r*-PLL_{42}-*b*-PPA_{24} was not as effective in stabilizing the polystyrene nanoparticles as its glutamic acid counterparts (Figure 4.12). At low copolypeptide/monomer content (i.e. 2 pphm) it was not possible to prepare a stable latex. At copolypeptides contents of 5 pphm it was however possible to form stable dispersions where the reaction kinetics are very similar to that of GA_{28}-*r*-$PLGA_{32}$-*b*-PPA_{20}. Furthermore, DLS determined the particle sizes to be similar to that stabilized by GA_{28}-*r*-$PLGA_{32}$-*b*-PPA_{20}, concluding that we have comparable particles which in ionic form will be of opposite charge.

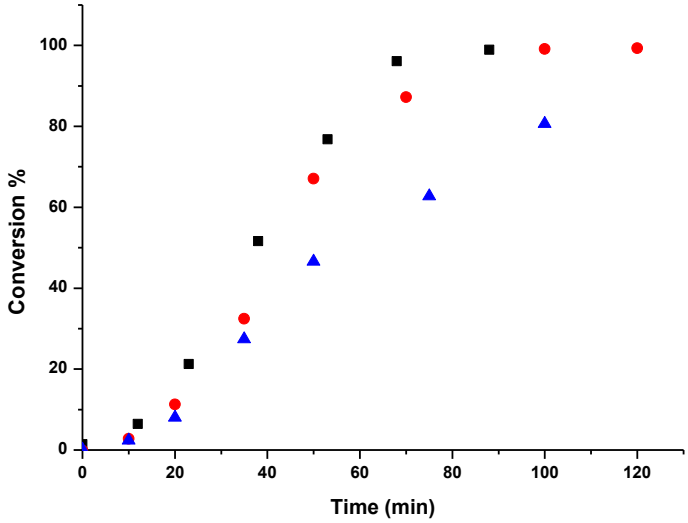

Figure 4. 12 Evolution of monomer conversion with time for the emulsion polymerization of styrene using KPS as initiator (1 wt%), a monomer content of 12 wt% and surfactant content of 5 wt% (■), a monomer content of 15 wt% and surfactant content of 5 wt% (●), a monomer content of 15 wt% and surfactant content of 2 wt% (▲) with LA_{17}-*r*-PLL_{42}-*b*-PPA_{24} as stabilizer.

All particles were further investigated by FE-SEM. The images illustrate the uniformity of the particles in agreement with the low PDIs obtained from DLS (Figure 4.13). Particles sizes (80-100 nm) agree well with sizes obtained by DLS considering the non-hydrated state of the particles surfactant layer in SEM.

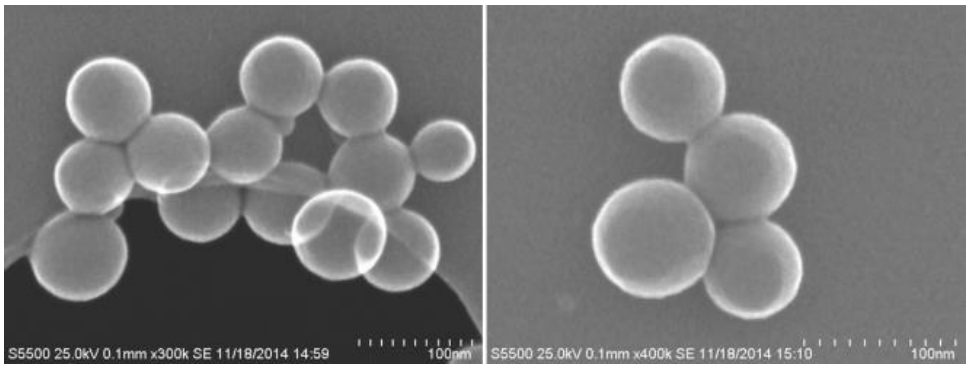

Figure 4. 13 FE-SEM images of polystyrene latex stabilized by GA_{28}-*r*-$PLGA_{32}$-*b*-PPA_{20} (**3)** with a monomer content of 12 wt% and surfactant content of 5 wt% (Table 4.2).

Table 4. 2 Results from the emulsion polymerization of styrene using glycosylated block copolymers as surfactants.

Polymer	monomer content[(a)] (Wt%)	[polymer][(b)] (pphm)	D_z[(c)] (nm)	PDI[(d)]
GA_{28}-*r*-$PLGA_{32}$-*b*-PPA_{20}	12	5	114	0.08
GA_{28}-*r*-$PLGA_{32}$-*b*-PPA_{20}	15	5	118	0.09
GA_{28}-*r*-$PLGA_{32}$)*b*-PPA_{20}	15	2	140	0.03
GA_{7}-*b*-$PLGA_{56}$-*b*-PPA_{19}	12	5	98	0.03
GA_{7}-*b*-$PLGA_{56}$-*b*-PPA_{19}	15	5	106	0.05
GA_{7}-*b*-$PLGA_{56}$-*b*-PPA_{19}	15	2	120	0.05
LA_{17}-*r*-PLL_{42}-*b*-PPA_{24}	12	5	112	0.02
LA_{17}-*r*-PLL_{42}-*b*-PPA_{24}	15	5	115	0.02
LA_{17}-*r*-PLL_{42}-*b*-PPA_{24}	15	2	n.a.	n.a.

(a) solid content = mass polymer/mass dispersion. (b) 1 pphm = 1 g block copolymer/100 g monomer. (c) Z-average particle diameter from Dynamic Light Scatering (DLS). (d) Polydispersity Index of particle size distribution from cumulants DLS analysis.

4.5 Conclusions

Block copolymers consisting of poly(L-phenyl alanine) and partially glycosylated poly(L-glutamic acid) and poly(L-lysine), respectively, were synthesized via sequential NCA polymerization and subsequent polymer glycosylation. The resulting amphiphilic block copolypeptides were found to be efficient stabilizers in the emulsion polymerization of styrene offering a facile method for the synthesis of polystyrene nanoparticles. This signifies an example of functional polymer additives fully based on renewable building blocks in materials applications.

4.6 References

1. Biermann, U.; Bornscheuer, U.; Meier, M. A. R.; Metzger, J. O.; Schäfer, H. J. *Angewandte Chemie International Edition* **2011,** 50, (17), 3854-3871.

2. Coates, G. W.; Hillmyer, M. A. *Macromolecules* **2009,** 42, (21), 7987-7989.

3. Seniha Guner, F.; Yagci, Y.; Tuncer Erciyes, A. *Progress in Polymer Science* **2006,** 31, (7), 633-670.

4. de Geus, M.; van der Meulen, I.; Goderis, B.; van Hecke, K.; Dorschu, M.; van der Werff, H.; Koning, C. E.; Heise, A. *Polymer Chemistry* **2010,** 1, (4), 525-533.

5. Noordover, B. A. J.; van Staalduinen, V. G.; Duchateau, R.; Koning, C. E.; van, B.; Mak, M.; Heise, A.; Frissen, A. E.; van Haveren, J. *Biomacromolecules* **2006,** 7, (12), 3406-3416.

6. Martello, M. T.; Hillmyer, M. A. *Macromolecules* **2011,** 44, (21), 8537-8545.

7. Stempfle, F.; Ritter, B. S.; Mulhaupt, R.; Mecking, S. Green Chemistry 2014, 16, (4), 2008-2014.

8. Hadjichristidis, N.; Iatrou, H.; Pitsikalis, M.; Sakellariou, G. Chem. Rev. (Washington, DC, U. S.) 2009, 109, (11), 5528-5578.

9. Deming, T. J. *Nature* **1997,** 390, (6658), 386.

10. Habraken, G. J. M.; Heise, A.; Thornton, P. D. *Macromolecular Rapid Communications* **2012,** 33, (4), 272-286.

11. Habraken, G. J. M.; Wilsens, K. H. R. M.; Koning, C. E.; Heise, A. *Polymer Chemistry* **2011,** 2, (6), 1322-1330.

12. Wang, J.; Lu, H.; Kamat, R.; Pingali, S. V.; Urban, V. S.; Cheng, J.; Lin, Y. *Journal of the American Chemical Society* **2011,** 133, (33), 12906-12909.

13. Appelhans, D.; Komber, H.; Kirchner, R.; Seidel, J.; Huang, C.-F.; Voigt, D.; Kuckling, D.; Chang, F.-C.; Voit, B. *Macromolecular Rapid Communications* **2005,** 26, (8), 586-591.

14. Sulistio, A.; Widjaya, A.; Blencowe, A.; Zhang, X.; Qiao, G. *Chemical Communications* **2011,** 47, (4), 1151-1153.

15. Byrne, M.; Thornton, P. D.; Cryan, S.-A.; Heise, A. *Polymer Chemistry* **2012,** 3, (10), 2825-2831.

16. Sulistio, A.; Blencowe, A.; Widjaya, A.; Zhang, X.; Qiao, G. *Polymer Chemistry* **2012,** 3, (1), 224-234.

17. Borase, T.; Iacono, M.; Ali, S. I.; Thornton, P. D.; Heise, A. *Polymer Chemistry* **2012,** 3, (5), 1267-1275.

18. Kar, M.; Vijayakumar, P. S.; Prasad, B. L. V.; Gupta, S. S. *Langmuir* **2010,** 26, (8), 5772-5781.

19. Balamurugan, S. S.; Soto-Cantu, E.; Cueto, R.; Russo, P. S. *Macromolecules* **2010,** 43, (1), 62-70.

20. Deming, T. J. *Wiley Interdisciplinary Reviews: Nanomedicine and Nanobiotechnology* **2014,** 6, (3), 283-297.

21. Huang, J.; Bonduelle, C.; Thevenot, J.; Lecommandoux, S.; Heise, A. *Journal of the American Chemical Society* **2012,** 134, (1), 119-122.

22. Bonduelle, C.; Huang, J.; Ibarboure, E.; Heise, A.; Lecommandoux, S. *Chemical Communications* **2012,** 48, (67), 8353-8355.

23. Ho, C. C.; Kondo, T.; Muramatsu, N.; Ohshima, H. *Journal of Colloid and Interface Science* **1996,** 178, (2), 442-445.

24. Saito, M.; Ogasawara, M.; Chikuni, K.; Shimizu, M. *Bioscience, Biotechnology, and Biochemistry* **1995,** 59, (3), 388-392.

25. Enser, M.; Bloomberg, G. B.; Brock, C.; Clark, D. C. *International Journal of Biological Macromolecules* **1990,** 12, (2), 118-124.

26. Dexter, A. F.; Middelberg, A. P. J. *Industrial & Engineering Chemistry Research* **2008,** 47, (17), 6391-6398.

27. Saito, M.; Masashi, O.; Koichi, C.; Makoto, S. *Bioscience, Biotechnology, and Biochemistry* **1995,** 59, (3), 388-392.

28. Gudina, E. J.; Rangarajan, V.; Sen, R.; Rodrigues, L. R. *Trends in Pharmacological Sciences* **2013,** 34, (12), 667-675.

29. Jarrod, A. H.; Connie, B. C.; Sara, M. G.; Zhibo, L.; Thomas, G. M.; Timothy, J. D. *Nature* **2008,** 455, (7209), 85-88.

30. Habraken, G. J. M.; Peeters, M.; Dietz, C. H. J. T.; Koning, C. E.; Heise, A. *Polymer Chemistry* **2010,** 1, (4), 514-524.

31. Sun, J.; Chen, X.; Deng, C.; Yu, H.; Xie, Z.; Jing, X. *Langmuir* **2007,** 23, (16), 8308-8315.

32. Maier, M. A.; Yannopoulos, C. G.; Mohamed, N.; Roland, A.; Fritz, H.; Mohan, V.; Just, G.; Manoharan, M. *Bioconjugate Chemistry* **2003,** 14, (1), 18-29.

33. Mildner, R.; Menzel, H. *Journal of Polymer Science Part A: Polymer Chemistry* **2013,** 51, (18), 3925-3931.

34. Jacobs, J.; Byrne, A.; Gathergood, N.; Keyes, T. E.; Heuts, J. P. A.; Heise, A. *Macromolecules* **2014,** 47, (21), 7303-7310.

35. Yip, J.; Duhamel, J.; Qiu, X. P.; Winnik, F. M. *Canadian Journal of Chemistry* **2011,** 89, (2), 163-172.

36. Morrow, J. A.; Segall, M. L.; Lund-Katz, S.; Phillips, M. C.; Knapp, M.; Rupp, B.; Weisgraber, K. H. *Biochemistry* **2000,** 39, (38), 11657-11666.

37. Killops, K. L.; Rodriguez, C. G.; Lundberg, P.; Hawker, C. J.; Lynd, N. A. *Polymer Chemistry* **2015,** 6, (9), 1431-1435.

38. Munoz-Bonilla, A.; Heuts, J. P. A.; Fernandez-Garcia, M. *Soft Matter* **2011,** 7, (6), 2493-2499.

39. Munoz-Bonilla, A.; van Herk, A. M.; Heuts, J. P. A. *Macromolecules* **2010,** 43, (6), 2721-2731.

40. Munoz-Bonilla, A.; Ali, S. I.; del Campo, A.; Fernandez-Garcia, M.; van Herk, A. M.; Heuts, J. P. A. *Macromolecules* **2011,** 44, (11), 4282-4290.

41. Huang, J.; Habraken, G.; Audouin, F.; Heise, A. *Macromolecules* **2010,** 43, (14), 6050-6057.

42. Kukula, H.; Schlaad, H.; Antonietti, M.; Forster, S. *Journal of the American Chemical Society* **2002,** 124, (8), 1658-1663.

43. Greenfield, N. J.; Fasman, G. D. *Biochemistry* **1969,** 8, (10), 4108-4116.

44. Vorobjev, Y. N.; Scheraga, H. A.; Honig, B. *The Journal of Physical Chemistry* **1995,** 99, (18), 7180-7187.

45. van Herk, A.; Heuts, H., Emulsion Polymerization. In *Encyclopedia of Polymer Science and Technology*, John Wiley & Sons, Inc.: 2009.

Chapter 5

Core cross-linked polypeptide nanoparticles through the miniemulsion polymerization of UV responsive NCAs.

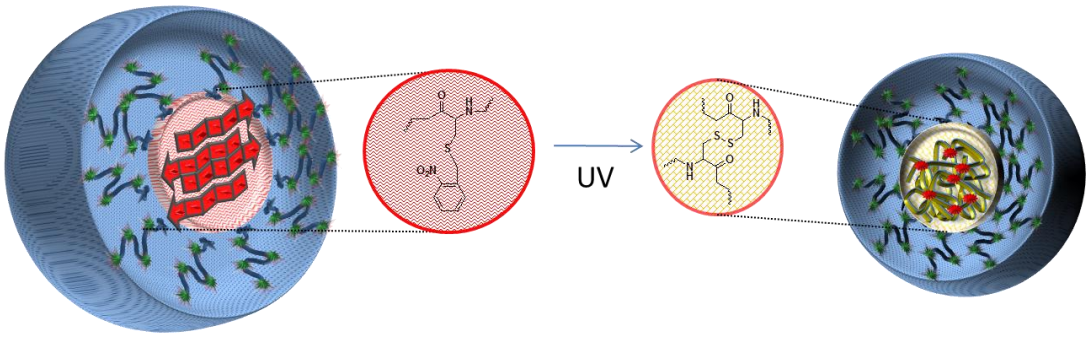

This work has been done in collaboration with Dr J.P.A. Heuts and M. Moradi from Eindhoven University of Technology (TU/e), The Netherlands.

5.1 Introduction

The design of smart carriers in the sub-micron range allows for unique characteristics which lead to changes in the mechanical, electrical and optical properties of materials. This evolution of controlled design has touted nanotechnology as the next revolution in many industries including agriculture, food industry, cosmetics and medicine.[1-6]

Nanoparticle delivery systems with the ability to encapsulate and controllably release bioactive compounds is a sought after trait that has received increased interest due to the broad range of possible applications. One such application area is in the (site-specific) delivery of active pharmaceutical ingredients such as vaccines, genes, drugs and other biomolecules in the (bio)medical field.[7-9] Currently, polymeric nanoparticles based on natural polymers such as chitosan or gelatine, or aliphatic polyesters such as poly(glycolic acid) (PGA) and poly(lactic acid) (PLA) as well as their copolymers i.e., poly(D,L-lactide-coglycolide) (PLGA) are the most widely utilized drug delivery systems.[7, 10-12] Both natural polymers and PLGA have advantages and drawbacks, which makes them more or less suited for certain application areas. For example, natural polymers usually have a good biocompatibility. However, obtaining reproducible sample quality from natural sources can be challenging. PLGA can be produced reproducibly but is hydrophobic in nature, which makes loading of hydrophilic drugs challenging.[13, 14]

For a product to be applicable in nano-particular drug delivery it is necessary to conform to a number of requirements. Generally these materials should be biocompatible, have a tuneable degradation profile, produce only harmless degradation products, allow encapsulation of active ingredients and involve a scalable process that does not require harsh processing conditions, while maintaining a high long-term colloidal stability. Also desirable is the availability of functional groups that allow the surface modification for example to enhance circulation half-life (e.g. through PEGylation) or attachment of active/targeting biomolecules such as proteins, glycans or antibodies (specifically for pharmaceutical applications).[7, 9, 15-17]

It is within these boundaries that polypeptides could play such a vital role. Over the last number of years researchers have developed functional materials based on amino acids by a technique called N-carboxyanhydride (NCA) ring-opening polymerisation (ROP). In this process amino acids are converted into a reactive NCA, which can then be polymerised in a ring-opening polymerisation to yield synthetic polypeptides.[18] This technique permits the

synthesis of functional polypeptides with controlled molecular weight, molecular architecture and composition.[19, 20]

Studies have shown that synthetic polypeptides from NCA polymerisation are versatile materials for the loading and release of small drugs and genetic therapeutics, respectively.[21, 22] For example, star shaped polypeptides with improved siRNA and pDNA loading, cargo protection and transfection characteristics were reported.[23-26] Moreover, the functionalities of the amino acids building blocks (e.g. amines and carboxylic acid moieties) allow for facile chemical modification and bioconjugation of the polypeptides.[27] Suitably, polypeptides are emerging as perfect candidates in therapeutic platforms and hold high potential as next generation biodegradable nanoparticles if a suitable processing methodology could be developed. [28]

Several strategies are available towards functional biodegradable nanoparticles. This would typically be dependent on the type of material used which varies from proteins, polysaccharides and biodegradable synthetic polymers. The protocols for nanoparticle preparation of these materials include the dispersion of preformed polymers, polymerization of monomer and ionic gelation methods.[29] Nanoparticles derived from PGA, PLA, PLGA, poly-cyanoacrylate (PCA) and polycaprolactone (PCL) are all typically prepared by the dispersion of preformed polymers. This can be achieved in several ways such as solvent evaporation, solvent displacement, nanoprecipitation and salting out.[30-32]

NPs that are prepared from monomers are polymerized to form in aqueous solution and this has been reported for the synthesis of PCA type NPs.[33, 34] This method of preparation would typically involve mini-, micro-, and emulsion polymerization techniques resulting in nanoparticles, nanospheres or nanocapsules.[6, 35] In brief, the synthesis is carried out in water using only the monomer, initiator and surfactant molecules. The active component can be dissolved or dispersed in the monomer solution followed by emulsification of the mixture to form an oil/water (o/w) emulsion using appropriate surfactant/emulsifying agents. The polymerisation occurs in micelles formed by the surfactants, which act as the seeding templates for the nanoparticles. After formation of a stable emulsion the organic solvent is evaporated resulting in the active compound being entrapped, encapsulated or attached to the nanoparticle matrix. This technology is widely used in industry in the formation of polymer latexes by radical polymerisation.

We have recently shown that it is also possible to use glycosylated block copolypeptides as macromolecular surfactants in the emulsion polymerization of styrene, a methodology we feel is readily applicable to other systems.[36] It is by using the latter approach that we have proposed to prepare polypeptide based nanoparticles. Applying an emulsion polymerisation approach to synthesize these nanoparticles would open exciting new possibilities for the design of biocompatible carriers. The inherent difficulties associated with this approach are due to the instability of NCAs in the presence of moisture as well as the hydrophobic nature of the monomer when in the protected form. Here we report that by tailoring the emulsification conditions, the NCA ROP under emulsion polymerisation conditions is indeed possible and permits the synthesis of nanoparticles fully based on amino acids in a scalable process.

5.2 Experimental

5.2.1 Materials

All chemicals were purchased from Sigma-Aldrich and used as received unless otherwise noted. ε-Benzyloxycarbonyl-L-lysine and DL-phenylalanine were supplied by Bachem. Anhydrous dichloromethyane (DCM), ethyl acetate, tetrahydrofuran (THF) and heptane were used directly from the bottle under an inert and dry atmosphere. ε-Benzyloxycarbonyl-L-lysine (ZLL), Phenyl alanine (PA) and S-(o-nitrobenzyl)-L-cysteine (NBC) NCA was synthesised following literature procedures.[37-39]

5.2.2 Synthesis of block copolypeptides $PZLL_{47}$-*b*-PPA_{10}

The NCA monomer of ZLL (3.0 g, 9.8 mmol) was dissolved in 20 mL anhydrous DMF and transferred to a Schlenk tube. The solution was degassed *via* three successive freeze-pump-thaw cycles and kept under vacuum. The reaction flask was immersed in a 0 °C water bath and a solution of 15 μL allylamine in 1 mL anhydrous DMF ($[M]_0/[I]_0 = 35$) was injected through a rubber septum with a syringe. The reaction was left to stir until the ZLL NCA had been completely consumed as monitored by ATR-FTIR spectroscopy. The polypeptide was further chain extended *via* the introduction of phenyl alanine NCA (0.38 g, 2.0 mmol, $[M]_0/[I]_0 = 10$) dissolved in 5 mL DMF. After full monomer conversion monitored via ATR FTIR spectroscopy the polymer was precipitated into an excess of diethyl ether, filtered and dried under vacuum. Isolated yield: 2.3 g.

5.2.3 Block copolypeptide deprotection

A general procedure was used for the deprotection of the PZLL pendant groups. $PZLL_{47}$-*b*-PPA_{10} (2.0 g, 6.8 mmol ZLL repeat units) was dissolved in trifluoroacetic acid (15 mL). 3.5 mL of HBr solution (33 wt.% in acetic acid; 3-fold excess with respect to the ZLL repeat units) was added slowly to the reaction at 0 °C. After 2 h, the solution was added to 300 mL diethyl ether and the precipitate washed three times with 50 mL diethyl ether. The product was dialyzed against distilled deionized (DDI) water using Spectra/Por dialysis membranes (MWCO, 3.5 kDa) for 72 h at room temperature. The product PLL_{47}-*b*-PPA_{10} was lyophilized and isolated as a white powder. Isolated yield: 0.93 g.

5.2.4 Glycosylation of PLL_{47}-*b*-PPA_{10}

A general procedure for 1-Ethyl-3-[3-dimethylaminopropyl]carbodiimide hydrochloride (EDC)/*N*-hydroxysulfosuccinimide (Sulfo-NHS) coupling was employed to attach lactobionic acid to the lysine residues of the amphiphilic copolypeptide. Lactobionic acid (LA) (0.43 g, 1.2 mmol, 0.2 eq w.r.t the lysine repeat units), EDC (0.23 g, 1.2 mmol, 1 eq w.r.t. LA) and sulfo-NHS (26 mg, 0.1 mmol, 0.1 eq w.r.t. EDC) were dissolved in 3 mL 10 mM MES buffer (pH 4.7) and stirred for 20 minutes. The latter was added to a solution of PLL_{47}-*b*-PPA_{10} (0.9 g, 0.12 mmol) in 7 mL of DDI water. The reaction mixture was stirred overnight. The resulting product was purified *via* dialysis against DDI water using Spectra/Por dialysis membranes (MWCO, 3.5 kDa) for 72 h at room temperature. The product was subsequently lyophilized and isolated as a white powder. Isolated yield: 1.2 g.

5.2.5 Preparation of polypeptide latex via mini-emulsion polymerization

The polypeptide NPs where prepared *via* the miniemulsion polymerization of *N*-carboxyanhydrides stabilized in an aqueous environment with glycosylated amphiphilic copolypeptides. The copolypeptide, (LA_{12}-r-PLL_{35})-*b*-PPA_{10} (80 mg, 6.8 x 10^{-6} mol), was dissolved in 8 mL of 2-(*N*-morpholino)ethanesulfonic acid (MES) buffer (pH 4.5, 0.1 M) and the solution cooled in an ice bath for 5 min under magnetic stir. The NBC NCA (190 mg, 0.7 mmol) was dissolved in 1.5 mL DCM and introduced into the aqueous system dropwise via syringe while under heavy stir (Turrax homogenizer). The reaction mixture was left under heavy stir using a T 10 basic ULTRA-TURRAX® homogenizer for 5 min, while being kept in the ice bath. Triethylamine (7 uL) was subsequently added to the reaction to initiate the

reaction and left under magnetic stir for 5 hours at room temperature. The reaction mixture was then subjected to high vacuum rotary evaporation to remove the organic solvent, DCM. The resulting latex was dialyzed against DDI for 24 hours using Spectra/Por dialysis membranes (MWCO, 3.5 kDa).

5.2.6 Methods

Nuclear magnetic resonance (NMR) spectra were recorded on a Bruker Avance 400 (400 MHz) in DMSO-d6 and $CDCl_3$ as solvents. All chemical shifts are reported in parts per million (ppm) with tetramethylsilane (TMS) as an internal reference. Attenuated Total Reflection (ATR) FTIR measurements were performed on a Perkin-Elmer Spectrum 100 instrument. Spectra were obtained from 4 scans with a resolution of 2 cm^{-1} in the spectral region of 650 – 4000 cm^{-1}. A background measurement was taken before the sample was loaded onto the ATR for measurement. Samples could be characterized in the liquid state without prior sample preparation. Size Exclusion Chromatography (SEC) was performed on an Agilent 1200 system in conjunction with two PSS GRAM analytical (8 x 300 and 8 x 100, 10 μ) columns, a Wyatt Dawn Heleos 8 multi angle light scattering (MALS) detector and Wyatt Optilab rEX differential refractive index (DRI) detector with a 658 nm light source. The eluent was DMF containing 0.1 M LiBr at a flow rate of 1 mL/min. The column temperature was set to 40 °C with the MALS detector at 35 °C and the DRI detector at 40 °C. Molar masses and dispersities were calculated from the MALS signal by the Astra software (Wyatt) using the refractive index increment (d*n*/d*c*) as calculated relative to the ratio of the homopolymer. The dn/dc values used for the polymers were experimentally determined or as found in literature.[40, 41] All samples for SEC analysis were filtered through a 0.45 mm PTFE filter (13 mm, PP housing, Whatman) prior to injection. Dynamic light scattering (DLS) experiments were performed at 25°C on a Malvern NanoZS (Malvern Instruments, Malvern UK) which uses a detection angle of 173°, and a 3 mW He-Ne laser operating at a wavelength of 633 nm. Cryogenic transmission electron microscopy (cryo-TEM) measurements were performed on an FEI Tecnai 20, type Sphera TEM instrument equipped with a LaB_6 filament operating at 200 kV. Images were recorded with a bottom-mounted Gatan CCD camera. The sample vitrification procedure was carried out using an automated vitrification robot (FEI Vitrobot Mark III). A 3 μL sample was applied on a Quantifoil grid (R 2/2, Quantifoil Micro Tools GmbH; freshly glow-discharged just prior to use), excess liquid was blotted away, and the formed thin film was shot into melting ethane. The grid

containing vitrified film was immediately transferred to a cryoholder (Gatan 626) and observed at −170 °C.

5.3 Results and discussion

Working towards fully biodegradable nanoparticles from the styrene system described in Chapter 4, the question was whether it is possible to replace the synthetic styrene core with a polypeptide based alternative. In a 1998 patent Makino *et al.* disclosed the synthesis of solid poly-α-amino acid particles *via* an oil-in-water emulsion consisting of water, water immiscible organic solvent and NCA monomer in the presence of an emulsifier, polyoxyethylene sorbitane monolaurate (Tween 20) and triethylamine.[42] Initial attempts of recreating their results by simply replacing the emulsifier with a polypeptides based one where all unsuccessful. The major constraints faced with a classical emulsion polymerisation approach were the initial introduction of the NCA monomer into an aqueous environment without pre-maturely initiating the monomer solution as well as the monomer transport into the growing particles. Under these conditions it was repeatedly observed that the monomer precipitated from solution resulting in a heterogeneous mixture of hydrophobic polypeptide and water.

It was envisioned that the normal diffusion based transport mechanism of monomer in an emulsion polymerization system would not suffice as this could lead to early initiation of the monomer and/or possibly no diffusion of the bulky monomer towards the stabilized polypeptide particles. It was thus decided to change the synthetic approach and rather utilize a miniemulsion polymerization, in which the monomer is encapsulated into preformed micelles. These subsequently act as particles seeds in the polymerisation process. Miniemulsions are produced by the introduction of a high shear force typically provided by a sonicator or mechanical homogenizer. The emulsion droplets are broken up into sub-micron particles stabilized by surfactant and/or co-stabilizer molecules. Effective stabilization of the droplets is necessary to ensure predominant droplet nucleation. While the surfactant retards coalescence of droplets, the costabilizer inhibits Ostwald ripening, a phenomena where the monomer diffuses from smaller droplets to larger ones, resulting in creaming of the latex. Due to the hydrophobicity of the NCA monomer along with the relatively low chance of diffusion from the bulky molecule it was expected that a costabilizer was unnecessary allowing the design of a system whereby ultimately we would obtain fully amino acid and carbohydrate based nanoparticles.

5.3.1. Synthesis of the glycosylated block copolypeptides

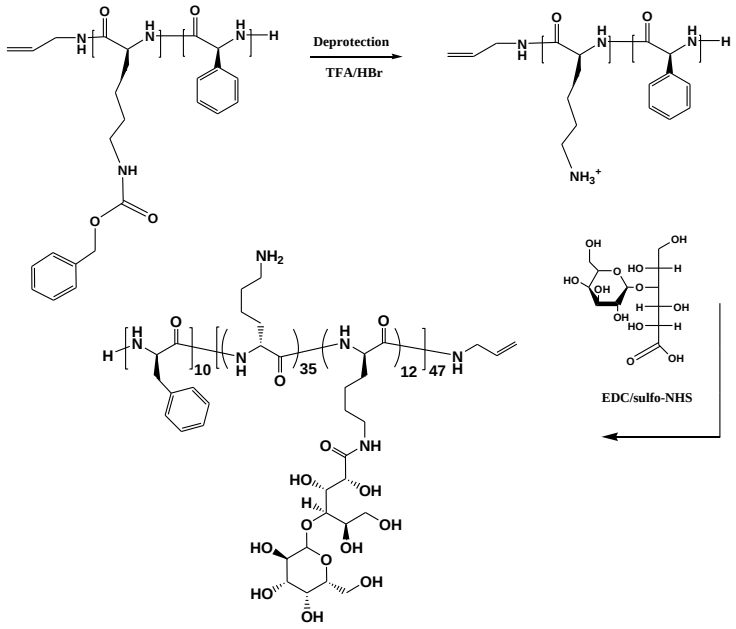

Scheme 5. 1 General strategy towards the glycosylated block copolypeptide, (LA_{12}-*r*-PLL_{35})-*b*-PPA_{10}.

The emulsification was tailored to proceed under acidic conditions so as to ensure that the NCA would remain stable once dispersed in the aqueous phase. Under these conditions, poly(L-lysine) (PLL) would be most suitable for the hydrophilic block as the amino moieties could be protonated ensuring a random coil formation to further enhance the solubility of the amphiphile. Moreover, it was necessary that the hydrophobic block would not be hydrolysed as this would inadvertently affect the hydrophilic-lipophilic balance.[43] Therefore, poly(phenylalanine) (PPA) was chosen to be incorporated inside the core of the nanoparticle and amphiphilic copolypeptides to be used as macromolecular surfactants were prepared in a similar fashion as reported before.[36]. Sun *et al.* have shown that PLL-*b*-PPA copolypeptides of c.a. 10 PPA repeat units readily self-assemble into giant vesicles and theoretically paving the way towards templated designs.[38] Based on these results, it was thought to be a promising system for the stabilization of particles and the formation of a stable emulsion.

The option of glycosylating the block copolypeptides was primarily to increase the hydrophilicity of the copolypeptides as reported in previous work where it lead to improved water solubility over a broad pH range. Accordingly, we prepared the amphiphilic copolypeptides, (LA_{12}-*r*-PLL_{35})-*b*-PPA_{10} (Scheme 5.1) and further characterised with ^{1}H-NMR spectroscopy and SEC. ^{1}H-NMR (DMSO-d6, ^{1}H-NMR not shown) was used to

quantify the repeat units of the PZLL of the PPA backbone by referencing the methylene protons of the two polypeptide segments (5.1 and 2.9 ppm respectively) to that of the single allylic methine proton from the initiator (5.65 ppm). The degree of glycosylation was quantified by referencing the protons from the galactose moiety (Figure 5.1, **$S_{1\text{-}11}$**) to that of the methylene protons on the PLL backbone (Figure 5.1, **C**). Furthermore, a narrow and monomodal distribution is evident from the SEC trace (Figure 5.2) highlighting the successful synthesis of the block copolypeptide.

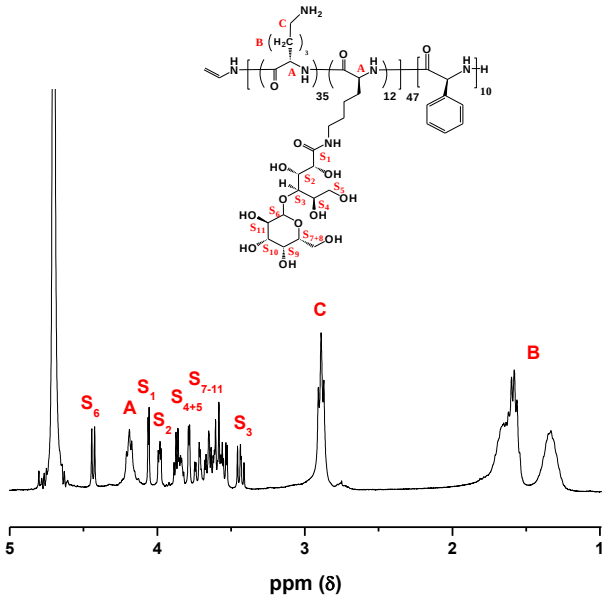

Figure 5. 1 ^{1}H-NMR spectra (D_2O, 400 MHz) of (LA_{12}-*r*-PLL_{35})-*b*-PPA_{10}.

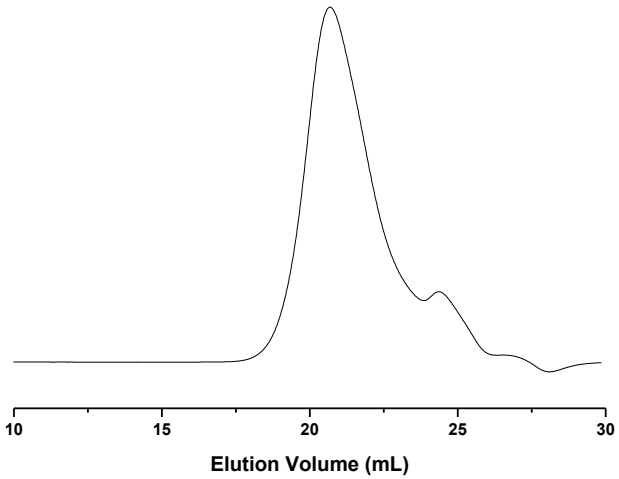

Figure 5. 2 SEC trace of the $PZLL_{47}$-*b*-PPA_{10} copolypeptide.

5.3.2. Polypeptide NP synthesis

The experimental procedure for the synthesis of the polypeptide NPs involved solubilizing the electrolytic surfactants into an amine free MES buffer (pH 4.5) and cooling the solution down. The monomer chosen was a photoresponsive S-(o-nitrobenzyl)-L-cysteine (NBC) NCA, which would allow for post polymerization crosslinking the particle core thereby increasing the particle stability (see Scheme 5.2).

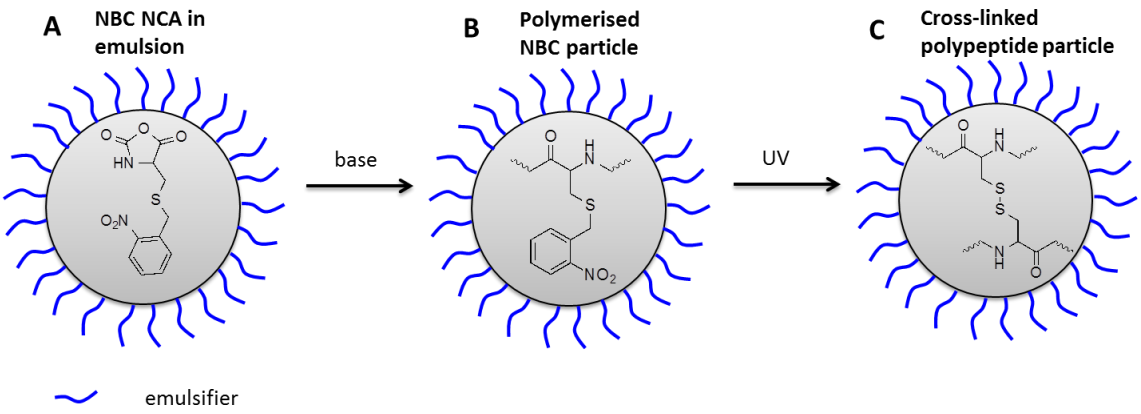

Scheme 5. 2 Cartoon showing the generalized reaction scheme for the synthesis of the PNBC NP before and after UV radiation, leading to a core cross-linked polypeptide NP.

It is understood that the NCA ROP follows two reaction mechanisms, a controlled normal amine mechanism (NAM) and the other, an uncontrolled base catalysed reaction (activated monomer mechanism, AMM).[20, 44, 45] Both mechanisms were utilized in this process to compare the slower controlled propagation of the NAM against that of the fast and uncontrolled AMM.

For the NAM and AMM type reactions, the copolypeptide and MES buffer solution was cooled down in an ice bath prior to the introduction of the monomer, after which the reaction was left to proceed at room temperature while stirring magnetically.To promote the NAM, a nucleophilic initiator, hexylamine, was introduced to a separate DCM solution containing the NCA monomer just prior emulsification. The latter was achieved *via* dropwise addition of the monomer/initiator reaction mixture into the surfactant solution while under heavy mechanical stir (utilizing a high powered homogenizer).

Typically, conversion during NCA ROP polymerization is measured with ATR-FTIR spectroscopy by following the disappearance of the initial NCAs anhydride peaks (1850 and

1790 cm^{-1}). The current system does not allow for this method and consequently the progress of the reaction was visually monitored by bubbling the evolving CO_2 through an attached vial. After no CO_2 was produced anymore, the reaction was left to stir for another hour. Sample purification involved removing the MES buffer as well as the water-immiscible organic solvent. This involved dialysis to obtain a solution with neutral pH while removing DCM under vacuum (care was taken to do this progressively to not rupture the particles).

In all our attempts, we could not isolate a single distribution of products (even after purification attempts) and ultimately found that this procedure resulted in a multimodal distribution of particles sizes (see figure 5.3). DLS characterization during the initial stages of the reaction showed a monomodal distribution of particles, only to grow in disparity as the reaction progressed. It was therefore speculated that the mechanism was too slow and phase separation occurred, resulting in a distribution of particles.

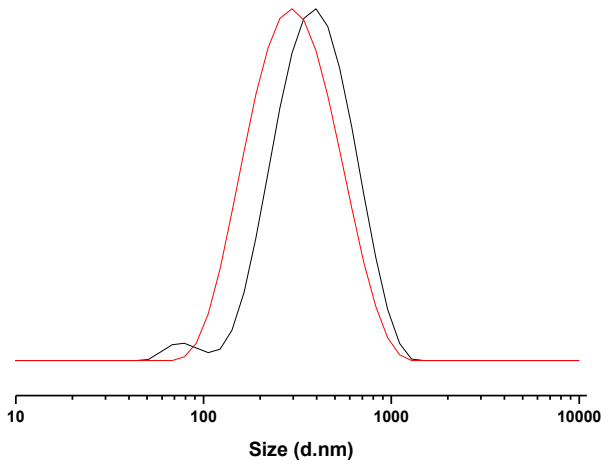

Figure 5. 3 Dynamic light scattering traces of the intensity distributions directly after emulsification of the NCA/DCM solution (red) as well as after completion of the reaction (black), using hexylamine as the initiator.

Cryogenic TEM was utilized to obtain a clearer image of the particles in their hydrated state which resulted in some very interesting images regarding the morphology of the particles. Figure 5.4 depicts the heterogeneity we obtained when using the hexylamine initiator where a subsequent distribution of particle sizes and morphologies was observed. What was obtained could most accurately be described as ‘jellyfish’ like structures. It was found that the particle morphology strived towards this jellyfish like deformation, the extent of which is seemingly

size dependent as it is only noticeable above a threshold size. It should be noted that in all three of these images, the latex has only been dialysed and that DCM is still present. This makes the structure more pronounced, revealing the level of intricacy present. In image B the three main morphologies generally encountered with this preparation method can be seen in one slide. The smaller particles were attributed to particles of mainly DCM with little to no polymer present.

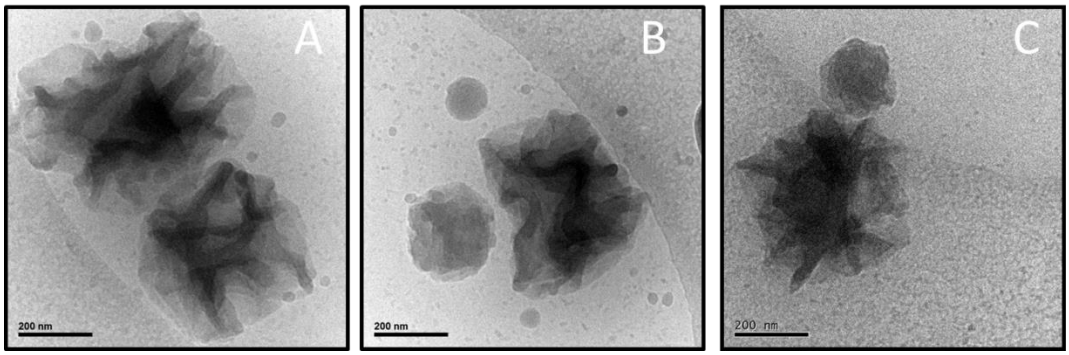

Figure 5. 4 Cryo-TEM images of the PNBC nanoparticles initiated *via* hexylamine, showing a distribution of different morphologies dependent on the particle size.

It was hypothesized that the specific characteristics of the hexylamine initiation (AMM) might be responsible for the size distribution and non-uniform shape of the particles. Typically this polymerisation is slow, which might open the door for various mechanical and chemical influences affecting the particles formation over the reaction time. Modeling the approach on the clasical radical emulsion polymerisation, which is a very fast process, it was decided to try and exploit the activated monomer mechanism in an attempted to 'capture' the particles directly after applying the high shear force. This is necessary as the monomer droplets are not thermodynamically stable. In contrast to the previous approach, the initiator was only added after the formation of a stable DCM/monomer emulsion. This was achieved via dropwise addition of the monomer solution into the surfactant/MES buffer mixture while under heavy mechanical stir. That means that only after preparing the stabilized emulsion was the initiator (triethylamine) added to the reaction mixture. The basic nature of TEA leads to proton abstraction from the nitrogen atom of the monomer resulting in an anion NCA, the result of which is fast and uncontrolled propagation, a characteristic of the AMM.

Figure 5.5 shows the DLS traces directly before and after the introduction of the initiator as well as the progression of the particle distributions as a function of time. We see in all cases a single distribution, which is consistent right through the reaction with minimal change in the

particle size as the reaction proceeds to completion. This would seem to indicate that the initial droplets formed using the homogeniser acts as seeds for the growing particles which are effectively stabilized by the glycosylated copolypeptides. Table 5.1 represents a summary of the characterization results from DLS.

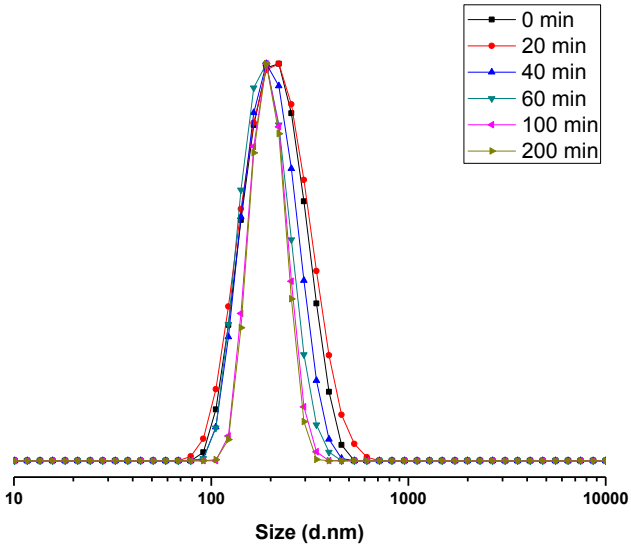

Figure 5. 5 Dynamic light scattering traces of the normalized intensity distributions of the polypeptide nanoparticles as a function of time after the addition of the initiator, triethylamine.

The images in figure 5.6 show the particles synthesized after purification (no DCM present), using TEA as initiator. Image A is a snapshot of what the majority of particles looked like while images B and C show the close-up. The difference in densities throughout the particles is quite evident with what looks like a collection of collapsed tunnels. It is known that poly(L-cysteine) exclusively assume β-sheet confirmations, where this has been shown to be true for PNBC homopolymer as well.[39, 44] It was therefore argued that these regions of higher (density) could be attributed to the secondary structure of the polypeptide. This is a characteristic which becomes more pronounced with larger particles, possibly due to more monomer being encapsulated in particles resulting in an increase in the repeating units and subsequently cumulating the effect of the β-sheet formation.

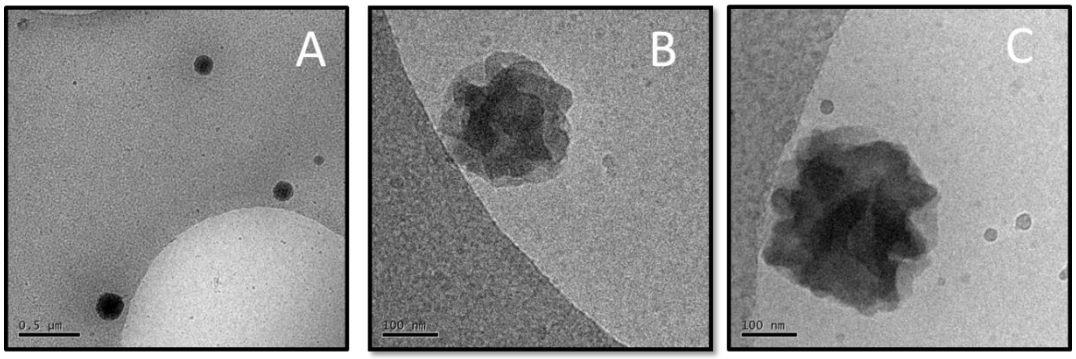

Figure 5. 6 Cryo-TEM images of the PNBC nanoparticles initiated *via* triethylamine, resulting in a monomodal distribution of UV reactive nanoparticles.

Future work would involve influencing particle size and increasing control of the distribution of products, characteristics we expect to be dependent on how the emulsion is prepared at the start of the reaction. This would of course be directly correlated to the amount of surfactant present to act as particle stabilizer as well as the effectiveness of the high shear dispersion method used initially where it can be assumed that a better dispersion tool would lead to a narrower distribution of products.

Figure 5.7 shows a monomodal particle distribution after purification with decrease in diameter as well as narrower distribution when compared to the NP directly after synthesis (see Table 5.2). The significant decrease in the PDI after purification is most likely due to the removal of dispersed DCM outside the NPs. It is expected that some heterogeneous phase separation will occur as propagation proceeds due to the insolubility of the polypeptide, PNBC in DCM.

Table 5. 1 Summary of the DLS characterization data for the polypeptide nanoparticles as a function of time after the addition of the initiator, triethylamine.

Reaction time (min)	Temp (°C)	Z-Ave (d.nm)	PDI	Peak Area (percent)
0	25	195	0.10	100
20	25	200	0.16	100
40	25	205	0.21	100
60	25	204	0.24	100
100	25	200	0.19	100
200	25	202	0.20	100

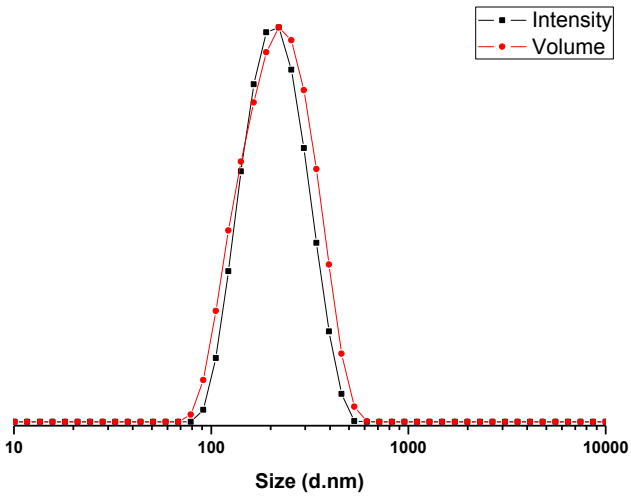

Figure 5. 7 Dynamic light scattering traces of the intensity and volume distributions of the polypeptide nanoparticles after purification.

In a subsequent procedure we aimed to prepared stable, cross-linked particles by subjecting the polypeptide latex to UV light. This was done to cleave the UV labile o-nitrobenzyl groups inside the core of the polypeptide NPs (Scheme 5.2 C). It was expected that this would result in the formation of disulfide bridges leading to denser particles. Upon UV irradiation, DLS confirmed a significant decrease in particle size of 20 nm, that is from 196 nm to 176 nm (Figure 5.8 and Table 5.2).

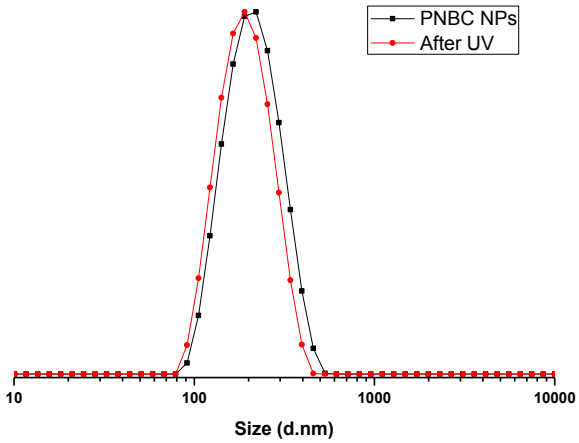

Figure 5. 8 Dynamic light scattering traces the intensity distributions before (black) and after (red) exposure to a UV source, resulting in a decrease of the particle diameter.

Complimentary to the DLS results, Cryo-TEM images show a clear change in morphology after being subjected to UV radiation (Figure 5.9). The decrease in particle diameter as the core is cross-linked is quite clear and subsequently leads to a seemingly denser and more compact particle.

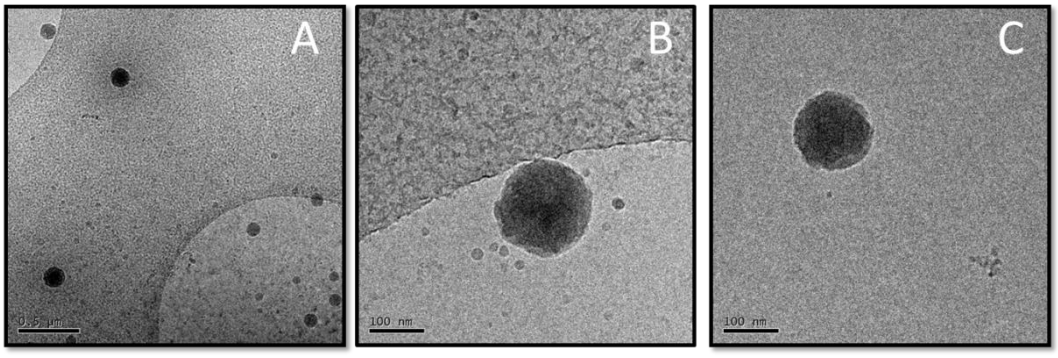

Figure 5. 9 Cryo-TEM images of the PNBC nanoparticles after exposure to UV light. A sharp decrease in size was observed leading to a denser, more compact cross-linked nanoparticle.

Table 5. 2 Summary of the DLS characterization data for the polypeptide nanoparticles after purification and exposure to UV.

Polypeptide NP	**Temp (°C)**	**Z-Ave (d.nm)**	**PDI**	**Peak Area (percent)**
PNBC NP (with DCM)	25	202	0.20	100
PNBC NP (Purified)	25	196	0.11	100
PNBC NP after UV exposure	25	176	0.12	100

5.4 Conclusion

Glycosylated block copolypeptides have been shown to be effective stabilizers in the preparation of fully amino acid and sugar based nanoparticles. A UV responsive NCA, S-(o-nitrobenzyl)-L-cysteine (NBC), was successfully polymerized by a mini-emulsion polymerization process in aqueous conditions to prepare narrowly distributed, PNBC nanoparticles. Furthermore, it was shown that propagation kinetics as determined by the type of initiator and thus the type of propagation mechanism plays a crucial part in ensuring a monomodal distribution of products.

5.5 References

1. DeRosa, M. C.; Monreal, C.; Schnitzer, M.; Walsh, R.; Sultan, Y. *Nat Nano* **2010,** 5, (2), 91-91.

2. Huang, Q.; Yu, H.; Ru, Q. *Journal of Food Science* **2009,** 75, (1), R50-R57.

3. Raj, S.; Jose, S.; Sumod, U. S.; Sabitha, M. *Journal of Pharmacy & Bioallied Sciences* **2012,** 4, (3), 186-193.

4. Bakhru, S. H.; Furtado, S.; Morello, A. P.; Mathiowitz, E. *Advanced Drug Delivery Reviews* **2013,** 65, (6), 811-821.

5. Ezhilarasi, P. N.; Karthik, P.; Chhanwal, N.; Anandharamakrishnan, C. *Food and Bioprocess Technology* **2012,** 6, (3), 628-647.

6. Sultana, S.; Khan, M. R.; Kumar, M.; Kumar, S.; Ali, M. *Journal of Drug Targeting* **2013,** 21, (2), 107-125.

7. Elsabahy, M.; Wooley, K. L. *Chemical Society Reviews* **2012,** 41, (7), 2545-2561.

8. Shokeen, M.; Pressly, E. D.; Hagooly, A.; Zheleznyak, A.; Ramos, N.; Fiamengo, A. L.; Welch, M. J.; Hawker, C. J.; Anderson, C. J. *ACS Nano* **2011,** 5, (2), 738-747.

9. Kamaly, N.; Xiao, Z.; Valencia, P. M.; Radovic-Moreno, A. F.; Farokhzad, O. C. *Chemical Society Reviews* **2012,** 41, (7), 2971-3010.

10. Lai, P.; Daear, W.; Lobenberg, R.; Prenner, E. J. *Colloids and Surfaces B: Biointerfaces* **2014,** 118, (0), 154-163.

11. Danhier, F.; Ansorena, E.; Silva, J. M.; Coco, R.; Le Breton, A.; Preat, V. *Journal of Controlled Release* **2012,** 161, (2), 505-522.

12. Fornaguera, C.; Dols-Perez, A.; Caldero, G.; Garcia-Celma, M. J.; Camarasa, J.; Solans, C. *Journal of Controlled Release* **2015,** 211, (0), 134-143.

13. Peltonen, L.; Aitta, J.; Hyvonen, S.; Karjalainen, M.; Hirvonen, J. *AAPS PharmSciTech* **2004,** 5, (1), 115-120.

14. Bilati, U.; Allemann, E.; Doelker, E. *AAPS PharmSciTech* **2005,** 6, (4), E594-E604.

15. Hudak, J. E.; Bertozzi, Carolyn R. *Chemistry & Biology* **2014,** 21, (1), 16-37.

16. Rösler, A.; Vandermeulen, G. W. M.; Klok, H.-A. *Advanced Drug Delivery Reviews* **2012,** 64, Supplement, (0), 270-279.

17. Duncan, R.; Vicent, M. J. *Advanced Drug Delivery Reviews* **2013,** 65, (1), 60-70.

18. Hadjichristidis, N.; Iatrou, H.; Pitsikalis, M.; Sakellariou, G. *Chemical Reviews* **2009,** 109, (11), 5528-5578.

19. Huang, J.; Heise, A. *Chemical Society Reviews* **2013,** 42, (17), 7373-7390.

20. Hadjichristidis, N.; Iatrou, H.; Pitsikalis, M.; Sakellariou, G. *Chem. Rev. (Washington, DC, U. S.)* **2009,** 109, (11), 5528-5578.

21. Wu, H. M.; Pan, S. R.; Chen, M. W.; Wu, Y.; Wang, C.; Wen, Y. T.; Zeng, X.; Wu, C. B. *Biomaterials* **2011,** 32, (6), 1619-1634.

22. Liu, D.-L.; Chang, X.; Dong, C.-M. *Chemical Communications* **2013,** 49, (12), 1229-1231.

23. Byrne, M.; Victory, D.; Hibbitts, A.; Lanigan, M.; Heise, A.; Cryan, S.-A. *Biomaterials Science* **2013,** 1, (12), 1223-1234.

24. Guo, Z.; Tian, H.; Lin, L.; Chen, J.; He, C.; Tang, Z.; Chen, X. *Macromolecular Bioscience* **2014,** 14, (10), 1406-1414.

25. Fu, C.; Lin, L.; Shi, H.; Zheng, D.; Wang, W.; Gao, S.; Zhao, Y.; Tian, H.; Zhu, X.; Chen, X. *Biomaterials* **2012,** 33, (18), 4589-4596.

26. Chen, J.; Tian, H.; Guo, Z.; Xia, J.; Kano, A.; Maruyama, A.; Jing, X.; Chen, X. *Macromolecular Bioscience* **2009,** 9, (12), 1247-1253.

27. Bonduelle, C.; Lecommandoux, S. *Biomacromolecules* **2013,** 14, (9), 2973-2983.

28. Hehir, S.; Cameron, N. R. *Polymer International* **2014,** 63, (6), 943-954.

29. Mahapatro, A.; Singh, D. *Journal of Nanobiotechnology* **2011,** 9, (1), 55.

30. Vrignaud, S.; Benoit, J.-P.; Saulnier, P. *Biomaterials* **2011,** 32, (33), 8593-8604.

31. Pinto Reis, C.; Neufeld, R. J.; Ribeiro, A. n. J.; Veiga, F. *Nanomedicine: Nanotechnology, Biology and Medicine* **2006,** 2, (1), 8-21.

32. Kumari, A.; Yadav, S. K.; Yadav, S. C. *Colloids and Surfaces B: Biointerfaces* **2010,** 75, (1), 1-18.

33. Landfester, K.; Mailander, V. *Expert Opinion on Drug Delivery* **2013,** 10, (5), 593-609.

34. Duan, J.; Liu, M.; Zhang, Y.; Zhao, J.; Pan, Y.; Yang, X. *Journal of Nanoparticle Research C7 - 761* **2012,** 14, (4), 1-9.

35. Rao, J. P.; Geckeler, K. E. *Progress in Polymer Science* **2011,** 36, (7), 887-913.

36. Jacobs, J.; Gathergood, N.; Heuts, J. P. A.; Heise, A. *Polymer Chemistry* **2015,** 6, (25), 4634-4640.

37. Habraken, G. J. M.; Peeters, M.; Dietz, C. H. J. T.; Koning, C. E.; Heise, A. *Polymer Chemistry* **2010,** 1, (4), 514-524.

38. Sun, J.; Chen, X.; Deng, C.; Yu, H.; Xie, Z.; Jing, X. *Langmuir* **2007,** 23, (16), 8308-8315.

39. Liu, G.; Dong, C.-M. *Biomacromolecules* **2012,** 13, (5), 1573-1583.

40. Deming, T. J. *Nature* **1997,** 390, (6658), 386.

41. Yip, J.; Duhamel, J.; Qiu, X. P.; Winnik, F. M. *Canadian Journal of Chemistry* **2011,** 89, (2), 163-172.

42. Makino, K.; Fukuhara, S.; Kuroda, K.; Hayashi, T., Poly-alpha-amino acid particles, emulsions containing the same and process for preparing the same. Google Patents: 1998.

43. Lin, I. J.; Friend, J. P.; Zimmels, Y. *Journal of Colloid and Interface Science* **1973,** 45, (2), 378-385.

44. Kricheldorf, H. R. *Angew. Chem., Int. Ed.* **2006,** 45, (35), 5752-5784.

45. Cheng, J.; Deming, T., Synthesis of Polypeptides by Ring-Opening Polymerization of alpha-Amino Acid N-Carboxyanhydrides. In *Peptide-Based Materials*, Springer Berlin Heidelberg: 2012; Vol. 310, pp 1-26.

Chapter 6

6.1 Conclusions and future outlook

The aim of this PhD was to expand the reach of synthetic polypeptide based materials with potential utilization in existing technologies as green alternatives. Specifically, we wanted to incorporate polypeptides in the synthesis of nanoparticles as fully biocompatible and biodegradable surfactants or emulsifiers.

In Chapter 2 we demonstrated the versatility of combining reversible addition-fragmentation chain transfer (RAFT) mediated polymerization and the ring-opening polymerization (ROP) of *N*-carboxyanhydrides (NCAs) in the synthesis of polypeptide-polymer hybrids. Key to this successful approach was an end-group engineering strategy that prevents the simultaneous presence of amino and CTA groups. We devised two such strategies, which are simple and highly efficient, i.e. the aminoethanol CTA removal with in-situ thiolactone formation for PBA and simultaneous aminolysis/thiol-ene reaction with hydroxyl ethylacrylate for PS and PNIPAM. The combination of these two polymerization techniques have shown to be effective in synthesizing a wide range of hybrid conjugates only limited by the compatibility of the RAFT CTA and monomer while the presented end-capping strategies allow the introduction of a range of functional end-groups.

In the third chapter we apply our strategy in preparing well-defined polymer-polypeptide conjugates and illustrate the versatile nature of these hybrid conjugates as well as potential applications. In this approach, hybrid block copolymers consisting of poly(styrene) and poly(amino acid) segments were synthesized via the combination of RAFT and NCA polymerization. The polypeptide segments were glycosolated with galactose moieties using traditional coupling chemistry. The resulting amphiphilic block copolymers were found to be efficient stabilizers in the emulsion polymerization of styrene offering a facile method for the synthesis of fluorescent glycosylated polystyrene nanoparticles. The availability of the galactose units introduced through the glycopolymer surfactant at the nanoparticles surface for selective binding was successfully demonstrated by lectin binding experiments and binding to Chinese hamster ovary (CHO) cells. This approach provided a straightforward route to highly fluorescent nanoparticles with selective binding properties for imaging applications avoiding particle post-modification.

The fourth chapter was a step towards greener surfactants, where the aim was utilize fully amino acid based stabilizers in synthetic emulsion systems. Block copolymers consisting of poly(L-phenyl alanine) and partially glycosylated poly(L-glutamic acid) and poly(L-lysine), respectively, were synthesized via sequential NCA polymerization and subsequent polymer glycosylation. The resulting amphiphilic block copolypeptides were found to be efficient stabilizers in the emulsion polymerization of styrene offering a facile method for the synthesis of polystyrene nanoparticles. This signifies an example of functional polymer additives fully based on renewable building blocks in materials applications.

The last part of the work is a culmination of the knowledge gained right through the PhD study. Chapter 5 is the answer to a question which initiated this whole study – "Is it possible to prepare solid nanoparticles consisting entirely of amino acid based building block?" This has been partly answered as we have shown that glycosylated block copolypeptides are effective stabilizers in the preparation of fully amino acid and sugar based nanoparticles. A UV responsive NCA, S-(o-nitrobenzyl)-L-cysteine (NBC), was successfully polymerized by a mini-emulsion polymerization process in aqueous conditions to prepare narrowly distributed, PNBC nanoparticles. Furthermore, it was shown that propagation kinetics as determined by the type of initiator and thus the type of propagation mechanism plays a crucial part in ensuring a monomodal distribution of products.

The future outlook of this work can only be described as positive, particularly the work done in chapter 5. Here, the emphasis should be on the expansion of knowledge regarding the synthesis of these polypeptide nanoparticles. These materials hold high potential as a next generation nanoparticle platform with real world applications if the processing methodology can be further developed and refined.

Furthermore, with the immense array of synthetic tools available it is possible to introduce novelty and "smart" features to these materials. This opens a path for these polypeptide NPs as next generation carrier systems with vast potential in functionalizability to readily enable loading with multiple classes of active agents, allow chemical modification, bio-conjugation or diagnostic labelling.

Appendix A

CD spectroscopy data (see Chapter 4)

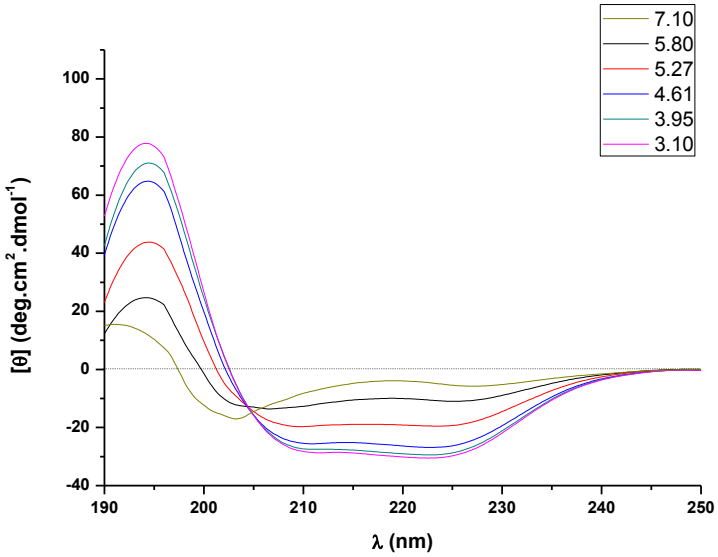

Figure A. 1 CD spectra of aqueous solutions of GA_{28}-*r*-$PLGA_{32}$-*b*-PPA_{20} as a function of pH.

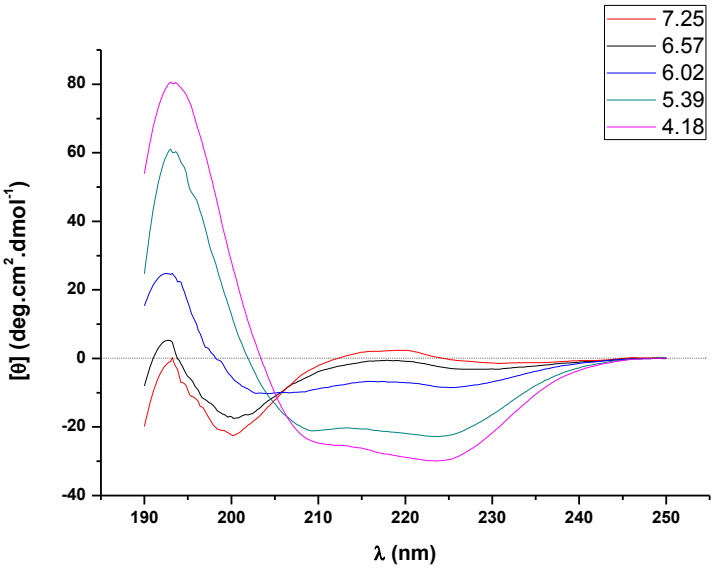

Figure A. 2 CD spectra of aqueous solutions of PGL_7-*b*-$PBLG_{56}$-*b*-PPA_{19} as a function of pH.

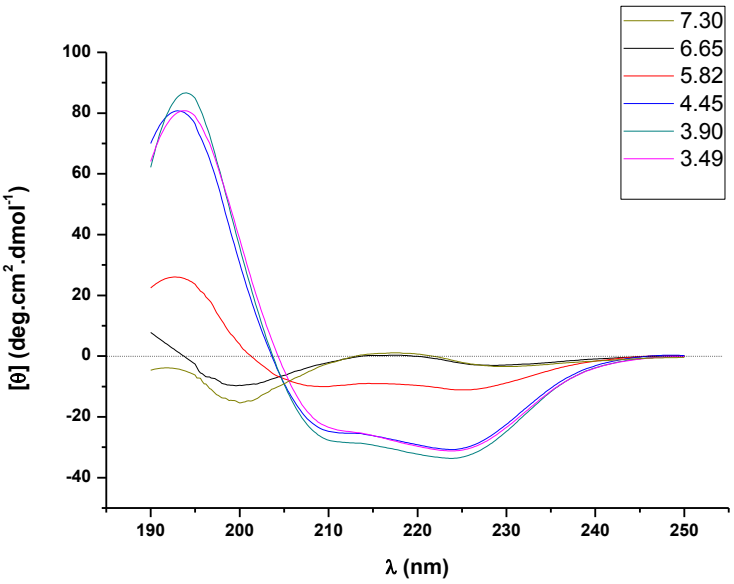

Figure A. 3 CD spectra of aqueous solutions of Gal_7-*b*-$PBLG_{56}$-*b*-PPA_{19} as a function of pH.

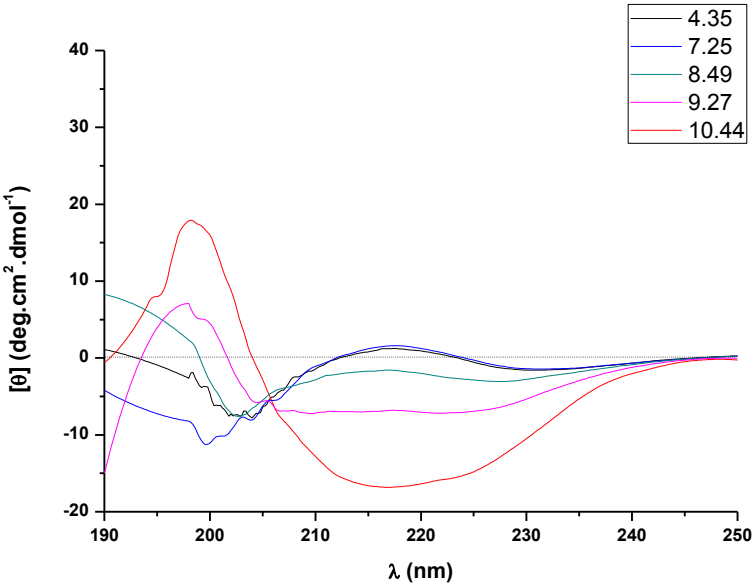

Figure A. 4 CD spectra of aqueous solutions of PLL_{59}-*b*-PPA_{24} as a function of pH.

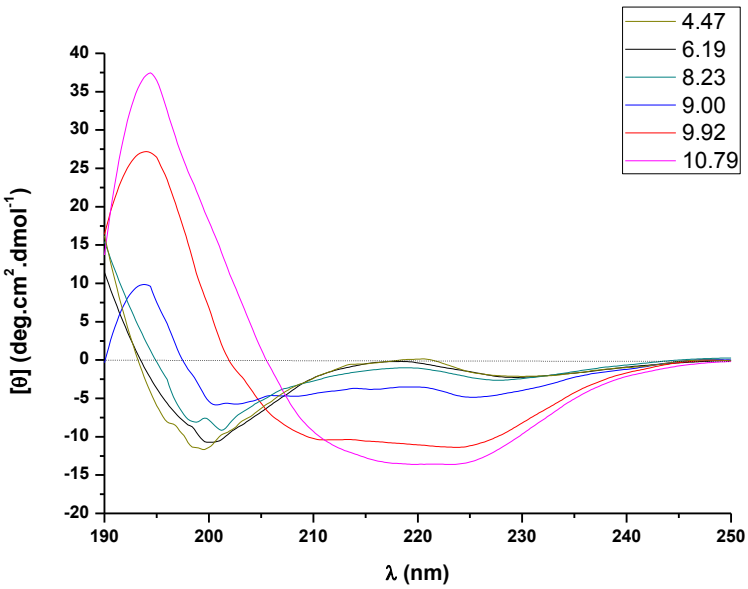

Figure A. 5 CD spectra of aqueous solutions of LA_{17}-r-PLL_{42}-*b*-PPA_{24} as a function of pH.